1-1-2011

Processing parameters and chamber length impact on detached die and attached die resin injection pultrusion

Dinesh Raj Palikhel
University of Mississippi

PROCESSING PARAMETERS AND CHAMBER LENGTHS IMPACT ON DETACHED DIE AND ATTACHED DIE RESIN INJECTION PULTRUSION

A Thesis

Submitted to the Graduate School

in partial fulfillment of the requirements for the

Degree of Master of Science in Engineering Science

The University of Mississippi

Dinesh Raj Palikhel

May, 2011

ABSTRACT

Injection pultrusion is an efficient and highly automated continuous process for high-quality, low-cost, high-volume manufacturing of composites. The main objective of this study is to analyze "attached die configuration" and "detached die configuration" for the better injection pultrusion process. In this work the impact of various processing parameters on complete wet out of composite parts is investigated in the attached die and detached die injection pultrusion with various chamber length considerations. The various processing parameters considered are pull speed, fiber volume fraction, resin viscosity, injection port location and compression ratio. 3-D finite volume technique is used to simulate the liquid resin flow through the fiber reinforcement in the injection pultrusion process. The purpose of the present work is to investigate the resin injection pressure needed to achieve complete wet-out, the corresponding maximum pressure inside the resin injection chamber and to predict the resin flow front by varying the length of injection chamber for different processing parameters.

ACKNOWLEDGMENTS

I express my hearty thanks to Dr. Jeffrey A. Roux for guiding me throughout my study and thesis work in the University of Mississippi in accomplishing my Master of Science Degree. He has always been the best teacher and source of inspiration throughout my course of study at the University and shall remain all my life. Dr. Rajendran M. Arunachalam, Chairman of Mechanical Engineering Department has always been a great support for confidence and knowledge. I would like to thank Dr. James P. Chambers, Interim Director of NCPA, for always supporting me with my work at NCPA and other works. I am very grateful to the committee members Dr. Rajendran M. Arunachalam, and Dr. Jagdish P. Sharma for their guidance and suggestions in this work. I would also like to thank Mrs. Janet McBride, Senior Secretary of Mechanical Engineering for supporting me.

TABLE OF CONTENTS

LIST OF TABLES

LIST OF FIGURES

LIST OF ABBREVATION AND SYMBOLS

x……	Axial coordinate, in the longitudinal direction of fiber, m
y……	Vertical coordinate, in the transverse (height) direction of fiber, m
z……	Coordinate along the width dimension, m
x_{IS} …….	Injection slot location
L_{IC}…….	Tapered length, m (Fig. 2-3)
L_D…….	Exit length, m (Fig. 2-3)
L_T…….	Total length, m (Fig. 2-3)
K_{11}……	Permeability in x (axial) direction, m^2
K_{22}……	Permeability in y (transverse) direction, m^2
K_{33}……	Permeability in z (transverse) direction, m^2
P……...	Pressure, Pa
φ ……..	Porosity
U……...	Fiber velocity in x (axial) direction, m/s
V……...	Fiber velocity in y (transverse) direction, m/s
u……	Resin velocity in x (axial) direction, m/s
v……	Resin velocity in y (transverse) direction, m/s
w……...	Resin velocity in z (transverse) direction, m/s
μ……	Viscosity of liquid resin, Pa.s
V_{f0}……..	Fiber volume fraction of the finished product
V_f……	Local fiber volume fraction, $V_f(x)$
ρ…….	Density of the liquid resin, kg/m^3
$F_{i,j,k}$…….	Fill factor for a specific control volume

CHAPTER 1
INTRODUCTION

1.1 Composite Materials and its Manufacturing

Composite materials are the engineered materials formed by the artificial combination of two or more materials differing in form or composition in macroscale so as to attain the properties that the individual components by themselves cannot attain. The constituents retain their characteristics, that is, they do not dissolve or merge completely into one another although they act in concert. Normally, the components can be physically identified and exhibit an interface between one another. An example is a lightweight structural composite that is obtained by embedding continuous carbon fibers in one or more orientations in a polymer resin matrix. The fibers provide the strength and stiffness, while the polymer serves as the binder.

Composites have many applications which can be generally summarized as structural applications, electronic applications, thermal applications, electrochemical applications, environmental applications and biomedical applications. Aerospace application of composites is exotic due to their high specific strength and stiffness and the ability to shape and tailor their structures to produce aerodynamically efficient structures. Composite materials have many advantages such as lighter weight, higher performance and corrosion resistance and also offer two more advantages; the part count can be significantly reduced, and bonding the structure using resins or adhesives can significantly reduce the assembly time and cost.

Some methods for manufacturing composite materials consists of extrusion, injection molding, open molding, autoclave, compression molding, filament winding, resin film infusion

(RFI), reinforced reaction injection molding (RRIM), thermoplastic molding, resin transfer molding (RTM), structural reaction molding (SRIM), and pultrusion. Selection of a manufacturing process depends on the application need. The criteria for selecting a process depend on the production rate, strength, cost, and shape and size requirement of the part.

One of the major cost factors in the manufacturing of polymer composites is the high cost of fabrication. The composite industry will continue striving forward to cope with the requirements for superb mechanical properties and the need for economical manufacturing methods. The manufacturing side is changing rapidly. Manufacturing costs can be reduced by improving present processes, increasing processing speeds and reducing off-spec product through tighter process control. To take advantage of the benefits of composite materials a significant investment in sophisticated computer-based design tools is necessary. Extensive mechanization in the design and manufacture process is important for the rapid design iterations and design integration. Design-to-cost techniques are particularly suitable for composite production. A cost-effective product in composite materials can only outcome from a program which interactively considers the performance criteria, design, technology, materials and manufacturing techniques which are available.

1.2 Pultrusion Process

Pultrusion is a composite manufacturing method used to manufacture fiber-reinforced polymeric composite materials. It is a continuous, cost-effective method for manufacturing composite structural components with constant cross sections. Pultrusion manufacturing involves heat transfer, phase transition, combination between the temperature, concentration, and flow fields. A composite manufactured from pultrusion consists of a resin that binds the composite together; reinforcing materials; a surfacing cover to improve the composite surface

appearance, chemical resistance and weather resistance; and a variety of auxiliary materials such as color, accelerators, and internal release agents. The reinforcement is commonly fiberglass and a common resin is polyester resin. Higher modulus polyester (e.g. nylon) and high density fibers (e.g. polyethylene) have also been used to enhance the versatility of the products. Epoxy resin and vinyl esters are also used for high temperature and corrosion applications.

The components of a pultrusion machine are creel, resin wet-out station, forming dies, heated metal die, puller mechanism, and cutoff saw as shown in the Fig. 1-1 [1]. The pultrusion process consists of pulling a number of continuous rovings and/or mats from a creel through a resin bath or impregnator. Then the fiber/resin system is pulled through a performing fixture where excess resin is removed and the part is partially shaped and then into the heated die where the wetted fiber bundles cure producing the final part. With electric cartridge heaters, the pultursion die is heated, and the resin in the fiber/resin system cures as it passes through the heated die. After curing, the profile laminate is pulled from die via reciprocating clamps and finally cut to the desired length with a synchronized cut-off saw. Various selections of solid and hollow profiles can be pultruded, and the process can be customized to fit specific applications.

The impregnation of resin in the fiber reinforcement is a very important physical phenomenon that occurs during the pultrusion composite manufacturing process. There are two basic methods of impregnation of resin. Figures 1-1 and 1-2 show the “open bath” and “resin injection” (closed bath) wet-out methods respectively.

The open bath system is a conventional pultrusion process in which the wet-out of the reinforcement is carried out by allowing it to immerse in and go through an open resin bath before it goes into the pultrusion die. There are many drawbacks in open bath system. The use of open resin bath leads to environmental concerns in the form of volatile organic compound

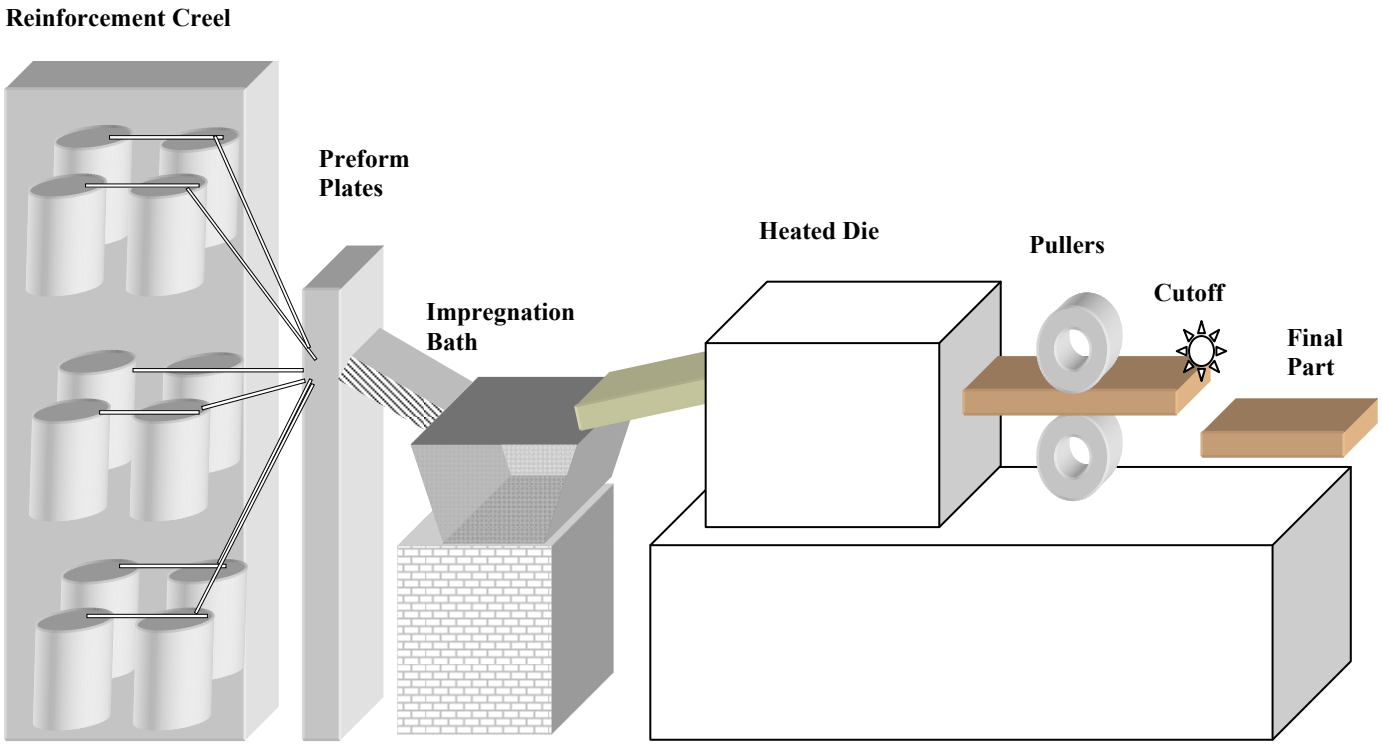

Figure 1-1. Schematic of Open Bath Pultrusion [1].

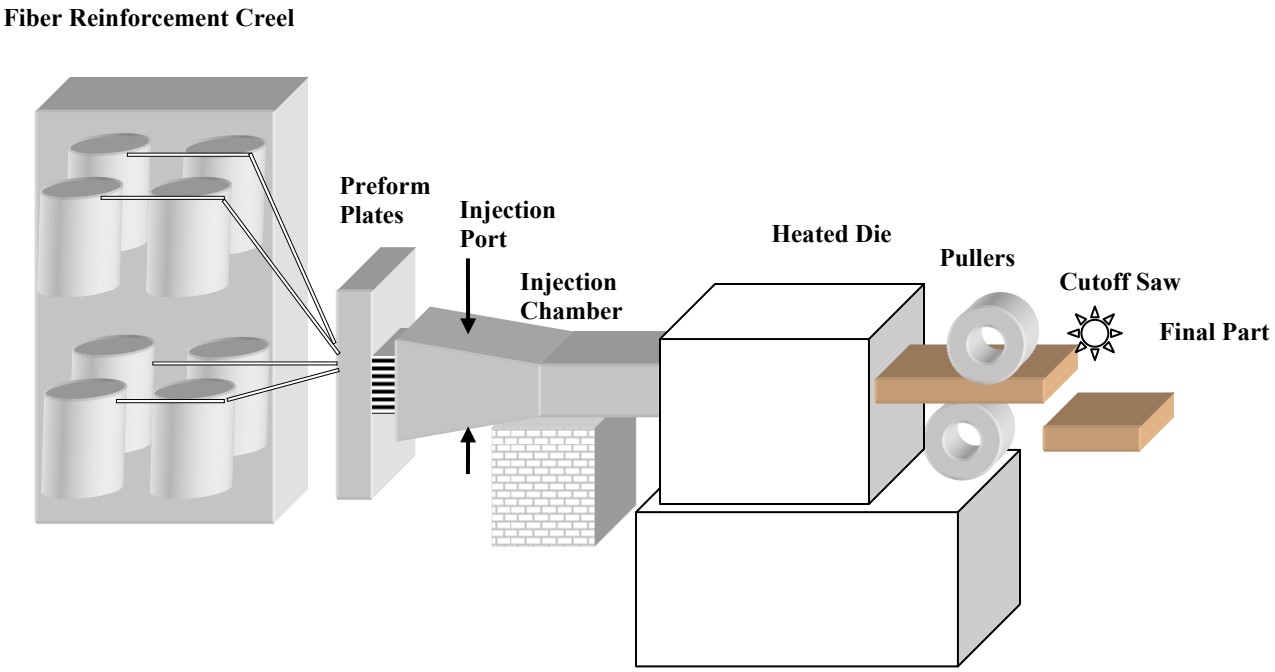

Figure 1-2. Schematic of Resin Injection Pultrusion (Attached Die Configuration) [1].

(VOC) emissions, and also resin wastage. Emission of volatile compounds to the atmosphere is very harmful to the workers. Due to short potlives of some resins at the elevated temperatures required to achieve optimum fiber wet-out only a restricted range of matrix formulations can be used. Tailored fabric orientations, when pulled through a bath, can undergo significant fiber distortion resulting in poor fiber alignments in the final part. Resin with higher or lower viscosity may not be coated with the reinforcement properly. These drawbacks can be overcomed by the injection pultrusion process. In this system, the resin is forced to flow into the reinforcement under an injection pressure.

Pultrusion was initially popular in the electrical and recreation markets, its use and popularity has spread to the corrosion, construction, automotive and aerospace markets as well. With the rapid growth of pultusion, raw material suppliers, processors, equipment suppliers and the academic community seem to be making steady progress to develop new materials, processing technologies, testing procedures and modeling techniques to further quantify, qualify and develop the science of pultrusion.

1.3 Injection Pultrusion Process

Injection pultrusion is an efficient process for high-quality, low-cost, high-volume manufacturing of fiber reinforced polymer matrix composites with relatively simple and constant cross sections. It is a highly automated and efficient continuous process. It is a modification of resin impregnation process; the resin is directly injected into the injection chamber in which resin is forced to flow into the interstices of the fiber system. In the process, resin is injected through top and/or bottom injection ports into the injection chamber and complete fiber wet-out is achieved there. Fibers are cured as they are pulled through the multizone heated die cavity. The cured product leaving the die is cut by a saw and sent for postcuring or finishing treatment.

The principal advantage of the resin injection pultrusion process is that it limits the release of volatile resin components and reaction products. An addition advantage of this process for laboratory or research and development pultruders is that it enables a rapid resin change without removal and cleaning of all the resin bath components. With the use of the injection die method, emission of volatile organic compounds (VOC) can be essentially eliminated or greatly reduced. A complete wet-out of the fibers with resin is also achieved leading to void contents as low as 1-5% [2]. In the resin injection process the resin mixing-to-curing time is much shorter than the conventional pultrusion, fast reaction resin systems can be used, which can increase the production speed significantly. Complete wet-out of the reinforcement fibers in the resin injection chamber is essential for producing good quality pultruded parts. Injection pressure is an important criterion to be designed and controlled properly in this process. Low injection pressure may result in the poor wet-out of the reinforcement and excessive pressure may result in resin flow out of the die entrance. The quality of a pultruded composite depends very much on achieving complete wet-out of the fiber reinforcement at the lowest resin injection pressure possible.

The injection pultrusion process has developed to a constructive extent, and efforts to develop tools for model-based design and optimization of this process are ongoing. Composite process modeling and model-based predictive control can be used to achieve greater performance of the injection pultrusion process. Process models can be used to overcome the limitations imposed by the lack of adequate sensors to monitor the key processing variables. This also saves significant sums of money spent on industrial design of the injection pultrusion process which involves costly trial and error procedure. For example large quantity of pressure sensors are required for the hit and trial method to predict optimum injection pressure for different operating

conditions. The models can also be used in a predictive control strategy which provides the ability to view the forecasted behaviors of the process. So, model based design and improvement is desirable and necessary. Overall, simulation models are very useful and can be effectively used to design the injection pultrusion process and to improve productivity and reduce cost.

1.4 Previous Work

Significant research work has been done on experimental and numerical analyses of the injection pultrusion process. These consist of the research at University of Mississippi [1,3,4,5,6], Washington University [7,8,9], University of Minnesota [2], Ohio State University [10,11]. Table 1.1 summarizes the important features of the work done by the researchers and the prospect of the present work.

Liu [12] developed 2-D and 3-D finite element/nodal volume techniques to simulate the resin flow through the reinforcement during the injection pultrusion process. He investigated the effect of process and model parameters on the resin flow process. He suggested that constant injection pressure employed should be significantly larger than that required to maintain the quasi-steady-state for the good flow pattern in injection pultrusion process. Liu [13] also developed transient and iterative finite element/nodal volume methods to predict the steady-state flow fronts and numerical performance from these models was investigated for pull speed, injection pressure and variation of permeability.

Kommu, Khomami and Kardos [14] developed a computer simulation model of injection pultrusion process using finite element/control volume and finite difference techniques. The equation of continuity and conservation of momentum were solved in 2-D using a Galerkin FE/CV technique. The energy and chemical species balance equations were solved in 3-D,

where streamline upwind Petrov-Galerkin (SUPG) or streamline upwind (SU) FE/CV were used to discretize the equations in two dimensions while finite differences had been used in the third dimension. Using the simulation model, the effect of fiber pull speed, reinforcement anisotropy, and taper of the die were studied. It was shown that the simulation model could be effectively used to design the die geometry as well as to improve the operation conditions.

Srinivasagupta et.al. [7] developed a rigorous model-based design algorithm and using a validated 3D dynamic processing model, developed integrated procedure for model-based design incorporating economic, controllability, environmental, and quality objectives. Using a response surface methodology with iterative meshing they developed a multiobjective optimization algorithm to determine improved equipment specifications (die dimensions, puller ratings) and processing condition parameters (heating zone temperatures, resin injection pressure). This research gave the initiative for the integration of design and control for a complex multiphase process using a single dynamic physical model.

Srinivasagupta et.al. [8] examined the operational characteristics of the injected pultrusion process using a bench-scale unit. The steady state and dynamics of the processing model from their previous work was validated using experimental data from the bench scale unit with the primary measurements of temperature and pressure profiles, and cure, as well as secondary measurements of pull force and part exit temperature. The relationship of the primary controlled variable (degree of cure at die exit) to the secondary measurement (pull force) was established through process modeling and experimentation.

Mustafa, Khomami and Kardos [9] developed a 3-D flow simulation model for injection pultrusion process and it was used to demonstrate the effect of fiber pull speed, reinforcement anisotropy, and taper of the die on the product quality. A simple pulling-force model was

developed and integrated with the simulation model. It was shown that the simulation model could be used to design the die geometry (i.e., die length, location of the injection port, shape of the injection section) and to improve the operating conditions (injection pressure, fiber pull speed, wall temperature) for a given product. To account for the tapering of the injection chamber, the source term is crucial in the conservation pressure equation for correct injection pressure assessment but they omitted the source term in the pressure equation in their analysis.

Rahetakar and Roux [4] developed a 2-D finite volume method to predict resin pressure field, resin velocity field and resin moving flow front location. They modeled and analyzed the slot injection port system developed from the 2-D model. Jeswani and Roux [1] developed a 3-D finite volume technique to simulate the flow of resin through the fiber reinforcement (E-glass rovings) in the injection pultrusion process. The numerical model developed was used to predict the impact of geometric and process parameters on wetout, pressure field, resin velocity field, and location of the liquid resin flow front. They predicted the impact of the tapering of walls of the injection chamber on the minimum injection pressure necessary to achieve complete wetout. They studied two injection chamber configurations (a) attached die (Fig. 1-2) and (b) detached die (Fig. 1-3) configurations and predicted the minimum injection pressure necessary to attain complete wetout, location of the liquid resin flow front, and the pressure field. Their work showed that the resin injection chamber exit pressures can reach dangerously high levels.

Ranga and Roux [6] used 3-D finite volume technique to simulate the resin flow through the fiber reinforcement in the injection pultrusion process. They considered attached die configuration and modeled the impact of the tapering of walls of the injection chamber on the minimum injection pressure necessary to achieve complete wetout by varying the length of the injection chamber and the processing parameters. Their work showed that high compression

ratios and short injection chamber lengths are desirable to achieve complete wet-out at reasonable resin injection pressures, chamber exit pressures, and with high pull speeds, high resin viscosity, and high fiber volume fractions.

1.5 Present Work

The goal of the present work is to investigate the resin injection pressure needed to achieve complete wetout, the corresponding maximum pressure inside the resin injection chamber and to predict the resin flow front by varying the length of injection chamber for different processing parameters in the "detached die configuration" of the resin injection pultrusion process. The various processing parameters considered are pull speed, fiber volume fraction, resin viscosity, injection port location and compression ratio. The present work focuses on finding the minimum injection pressure required for various injection chamber lengths to achieve complete wetout for the detached die configuration. In this work an improvement of the design of the injection chamber is anticipated with a detached die configuration as compared to the attached die configuration.

Various numerical formulations, laws and models are used to create 3-D numerical modeling of the injection pultrusion process. Dracy's law of flow through porous media is used to simulate resin flow through a fiber matrix. The Krozeny-Carmen model, Gebart's model and Gutowski's model are used to predict the permeability of the fiber matrix. The pressure equation is obtained by substituting the equations from Darcy's law into the continuity equation. The governing pressure equation is descretized, and the pressure field is obtained by using the line-by-line TDMA (tridiagonal matrix algorithm) technique. After solving for the pressure field, the velocity field is obtained by finite differentiation of Darcy's equations.

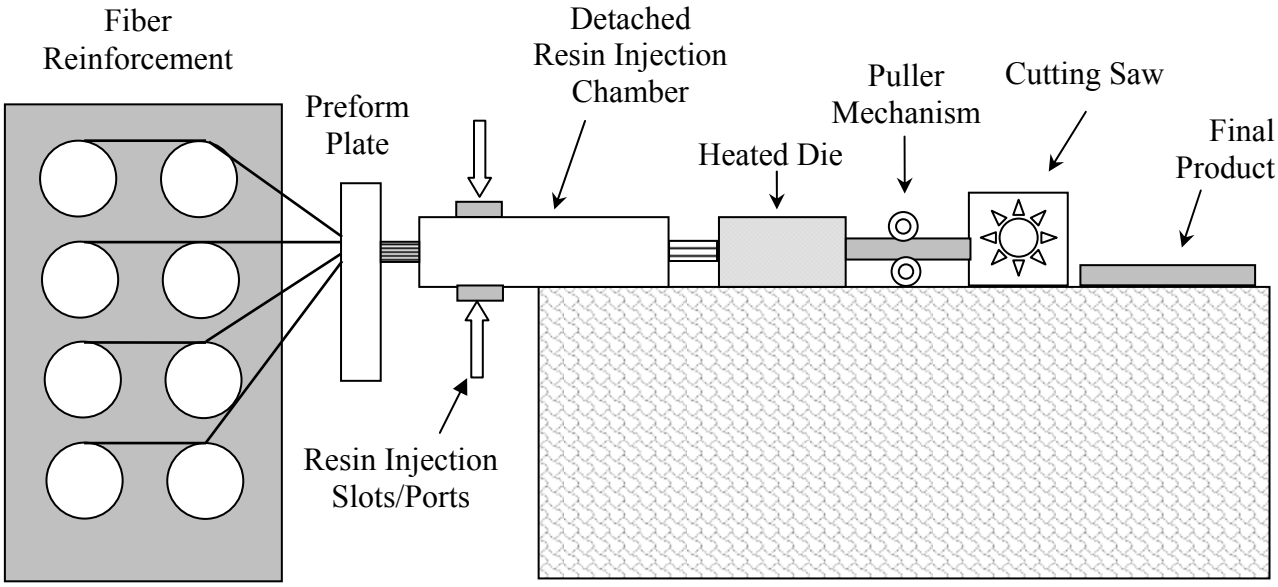

Figure 1-3. Schematic of Detached Resin Injection Pultrusion [1].

In this work, using the numerical model, the analysis will be conducted to predict the impact of variation of injection chamber length and the processing parameters on the minimum resin injection pressure required to achieve complete wetout along with the corresponding maximum resin pressure attained inside the injection chamber for the detached die configuration. In this work, successful manufacturing conditions correspond to minimum injection pressures to achieve complete reinforcement wet-out of not more than 0.41 MPa (60 Psi) and a corresponding maximum allowable internal chamber pressure of not more than 1.72 MPa (250 Psi). A broader range of operating conditions is anticipated in this work than that found in the previous works [2, 6]. Table 1-1 illustrates the key features of current model compared with key previous models developed by other researchers. None of the previous researchers have analyzed the impact of varying the length of the tapered resin injection chamber coupled with processing parameters on the "detached die configuration" for the resin wetout process. Next, Chapter 2 contains a detailed physical statement of problem for the present study.

Table 1-1. Comparison of Present Work with Previous Work.

Features \ Research		[12,13]	[14]	[7,8]	[9]	[1]	[6]	Palikhel (Present Work)
Model		3D	2D/3D	3D	2D,3D	3D	3D	3D
Numerical Method		FE/NV	FE/CV	FE/CV	FE/CV	FVM	FVM	FVM
Viscosity Variation	A*	No	No	No	Yes	Yes	Yes	Yes
	D*	No	No	No	No	Yes	No	Yes
Fiber Volume Fraction Variation	A*	No	No	Yes	Yes	Yes	Yes	Yes
	D*	No	No	No	No	Yes	No	Yes
Fiber Pull Speed Variation	A*	No	Yes	Yes	Yes	Yes	Yes	Yes
	D*	No	No	No	No	Yes	No	Yes
Taper Allowed in Injection Chamber	A*	No	Yes	Yes	Yes	Yes	Yes	Yes
	D*	No	No	No	No	Yes	No	Yes
Injection Chamber Length Variation	A*	No	No	No	No	No	Yes	Yes
	D*	No	No	No	No	No	No	Yes

FE = Finite Element
NV = Nodal Volume
CV = Control Volume
FVM = Finite Volume Method

A* = Attached Die Configuration
D* = Detached Die Configuration

CHAPTER 2

STATEMENT OF THE PROBLEM

2.1 Definition of Problem

The objective of the present work is to investigate and improve the performance of the detached die resin injection pultrusion process as a function of the processing parameters and various chamber lengths. An important objective of this work is to investigate the impact of the resin chamber lengths and processing parameters on the minimum injection pressure required for the complete wet-out process, the injection chamber exit pressure, and the resin flow front location in the detached die injection pultrusion process. The processing parameters considered are fiber volume fraction, pull speed, viscosity, injection port location and compression ratio.

The effect of injection pressure on the wet-out process is a very important aspect in the pultrusion process as the wetout of the fiber reinforcement affects the quality of the final composite. For a quality product with good mechanical properties complete wetout is mandatory. Wetout can be achieved with different injection pressures, design and processing configurations; but the main focus here is to determine the successful pressure operating conditions so that the process is economical and efficient and functions within safe injection pressures and safe maximum pressures within the injection chamber.

The compression of the fiber matrix results in a change (increase) of the fiber volume fraction and a resulting decrease in the permeability as the fiber matrix progresses along the longitudinal (x) direction into the tapered resin of the injection chamber. This will impact the wet-out process in the injection pultrusion process; also there is the change of the flow and the

pressure fields of the liquid resin along the longitudinal direction. Thus, the tapered shape of the injection chamber has a strong impact on the wet-out process and the injection pressure required for the complete wetout. In a detached die configuration as seen in Fig. 1-3, a small gap is set between the injection chamber and the heated die inlet. This configuration acts as a pressure release mechanism as the fiber/resin system is subjected to atmospheric pressure at the exit of the injection chamber.

2.2 Description of the Injection Chamber

The regions and the geometry of the injection chamber are illustrated in the Fig. 2-1. The injection chamber is divided into two primary regions: Region I and Region II. In Region I, the injection chamber walls are tapered and the liquid resin injection slots/ports are located here. Region II is of constant cross section. At the end of the injection chamber, the length of 0.005 m (5 mm) of Region II is left as the gap space between the chamber exit and the heated die inlet as shown in Fig. 2-1. Dual injection slots are located on the top and the bottom in Region I. The resin is injected through these slots with an injection pressure which is achieved through a feed pump. Short chamber lengths with different processing parameters and compression ratios are investigated so as to reduce the injection chamber internal pressures and to achieve complete wetout at reduced minimum injection pressures [6]. In this study the total (Region I and Region II) chamber lengths considered are 0.15 m, 0.20 m, and 0.30 m; this was varied by changing the length of Region I, while Region II is set to a constant length of 0.05 m with the last 0.005 m of Region II being the gap between the chamber exit and the heated die entrance.

In this work the injection chamber is detached from the heated die as seen in Fig. 1-3 so that there is a pressure release at the exit of the injection chamber. Lower minimum injection

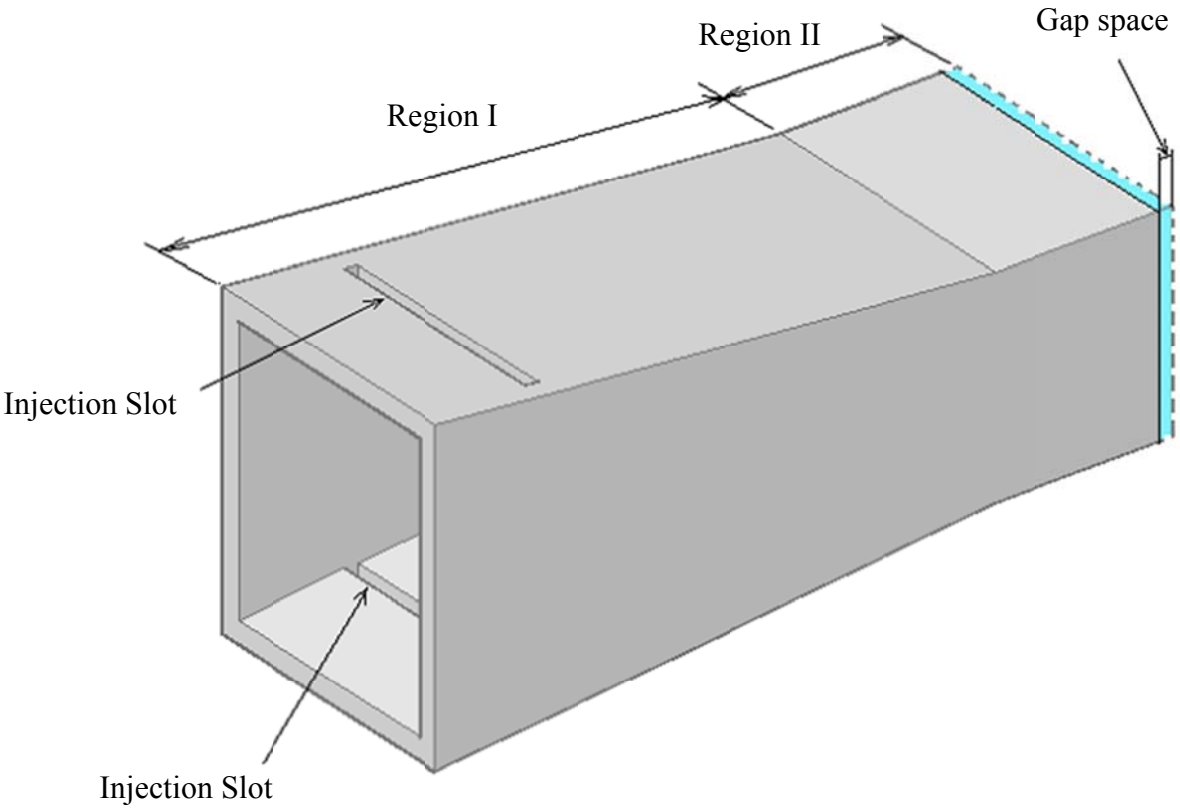

Figure 2-1. Physical Description of Tapered Injection Chamber.

pressure and an associated lower maximum internal chamber pressure are anticipated in the detached die configuration. Fiber reinforcement enters the injection chamber through the Region I where the resin injected through the injection ports impregnates the fibers and the fiber/resin system is compressed along Region I due to the tapered walls. Thus the fiber volume fraction and permeability changes along the length of Region I, whereas these are constant along the length of Region II as its cross-section is uniform. Due to the detached configuration, at the exit of the injection chamber the fiber/resin system is subjected to atmospheric pressure so that the pressure developed internally within the injection chamber is somewhat released as opposed to the attached die configuration as investigated by Ranga [6].

2.3 Computational Domain

A schematic of the computational domain of the injection chamber for the present analysis is shown in Fig. 2-2. This figure illustrates the top and the side views of the injection chamber, axes of the domain, height and width of the front and outflow boundaries, injection slot position (x_{IS}), the taper angle (α), and the lengths of Region I (L_{IC}) and Region II (L_D) considered for the analysis. The slight change in the taper angle α of the injection chamber has a significant impact on the minimum injection pressure required to achieve complete wetout and the associated maximum pressure developed inside the injection chamber.

Here (Fig. 2-2) the total length of the computational domain is represented by L_T whereas L_{IC} and L_D represent the length of Region I and the length of the Region II, respectively. H_{IC} and W_D represent the height and width of the front boundary of the injection chamber in Region I, and H_D and W_D represent the height and width of the exit portion of Region II. Thus, H_D and W_D also represent the thickness and width of the final composite part. A gap space of 0.005 m is

left at the end of Region II of the computational domain between the chamber exit and outflow boundary as shown in Fig. 2-2. Compression ratio, CR, is given by the ratio of the height of the injection chamber at the front boundary in Region I to the height of the injection chamber at the outflow boundary in Region II; CR is given by the following equation

$$CR = H_{IC}/H_D \qquad (2\text{-}1)$$

For the non-tapered injection chamber, H_{IC} and H_D are equal so that the value of CR is equal to 1.0. But in this study the tapered injection chamber is considered so that H_{IC} is always greater than H_D; thus the value of CR is greater than 1.0 and the injection chamber taper angle ($\alpha > 0$) is given by

$$\tan\alpha = \frac{H_D}{2L_{IC}}[CR - 1] \qquad (2\text{-}2)$$

Total lengths of the computational domain of the injection chamber (L_T) considered for this study are 0.15 m, 0.20 m and 0.30 m. Thus the length of Region I (L_{IC}) considered are 0.10 m, 0.15 m and 0.25 m respectively, and the length of Region II (L_D) has a constant value of 0.05 m. The CR values considered are 2.0, 3.0 and 4.0. The value of the nominal part thickness H_D is considered to be 0.00318 m (1/8 inch). Hence the injection chamber lengths and CR values considered for the study yield resulting taper angles as given in Table 2-1.

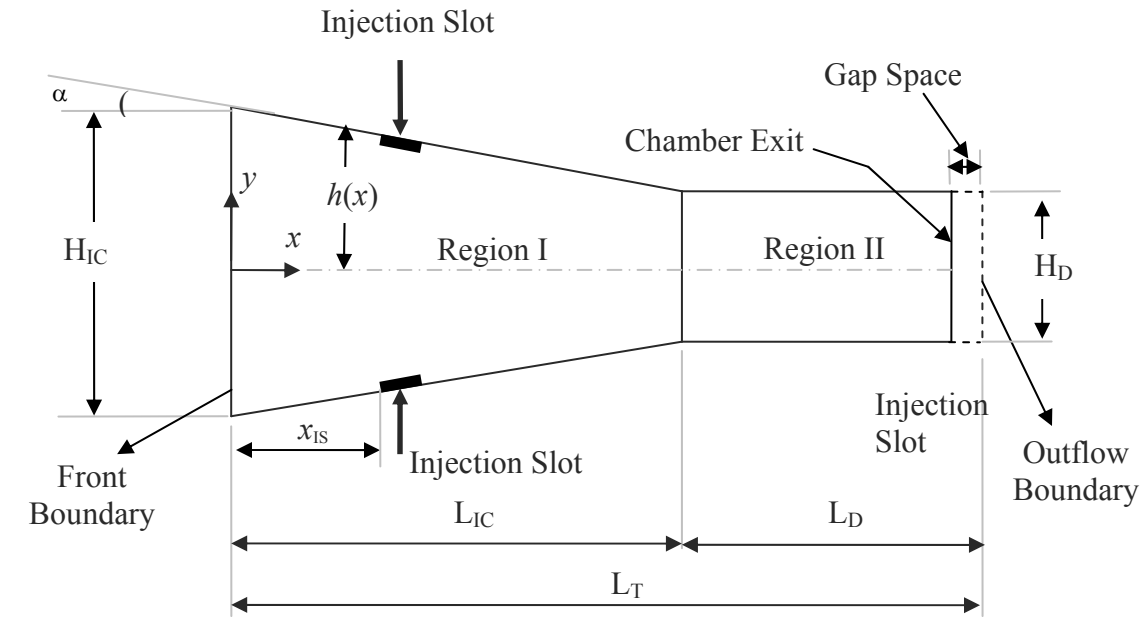

(a) In *xy* Plane (Side View)

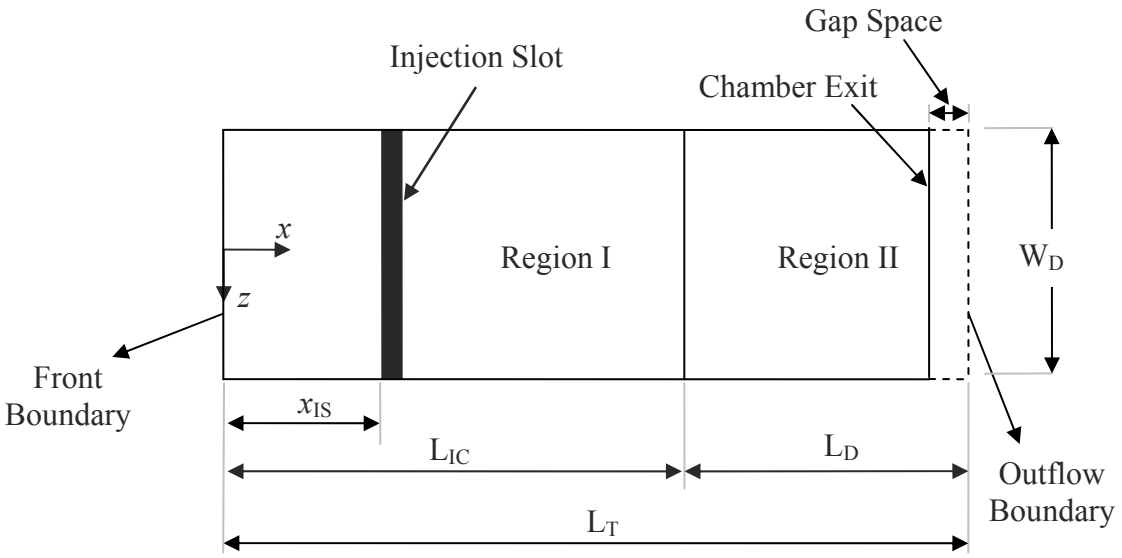

(b) In *xz* Plane (Top View)

Figure 2-2. Sketch of the Computational Domain for the Injection Chamber (Not to Scale) [1].

Table 2-1. CR, Chamber Lengths and Taper Angles*(α) Considered for the Computational Domain.

Length (L_T) / CR	0.15 m	0.20 m	0.30 m
2.0	0.607˚	0.455˚	0.303˚
3.0	1.214˚	0.911˚	0.607˚
4.0	1.821˚	1.366˚	0.911˚

* α is given in degrees (˚)

2.4 Features and Capabilities of Numerical Model

The finite volume method is an important method of discretization for the conservation equations in a flow with the advantages of simplicity and physical interpretations, based on approximation to the conservation laws. This method is used in the numerical model to compute the pressure field, the flow field, and the location of flow front. The computational domain in the analysis is symmetric about the centerline planes. So, only a quarter of the computational domain is modeled. This reduces the modeling time of the domain. This practice also reduces the storage space and runtime of the model by about 75%.

Following are the features/capabilities of the numerical model in this study:

- **Different fiber/resin systems**: Glass or carbon fibers/polyester or epoxy resin
- **Permeability model**: Gutowski's model
- **Different processing parameters**: Pull speed or line speed, fiber volume fraction, and resin viscosity

- **Fiber packing arrangements**: Quadratic and hexagonal arrangement
- **Type of resin injection**: Dual (top and bottom of injection chamber) slot injection configuration.
- **Type of injection chamber configuration**: Attached Die and Detached die Configuration

FORTRAN 90 language is employed in the program for the numerical model and it was executed on a personal computer (Dell Optiplex GX620, Pentium 4, 3.8 GHz, 2 GB RAM). The line-by-line TDMA solver is used in this method which is efficient and fast as compared to the direct (matrix) methods. This program helps the user to input various processing parameters and study their effects on the pultrusion process. On execution of the cases, the output of the program is saved in a data file, and plotting routines are used to visualize the data. The transient solution of the program provides the location of the liquid resin flow front at different time instances until steady state is reached. This program also helps to determine the total simulated time for the flow front to reach steady state.

Having presented the statement of the problem, description of the injection chamber, the computational domain, and the model capabilities in this chapter, the next chapter will provide the analysis with a detailed mathematical description of the governing equations and the solution algorithm.

CHAPTER 3

ANALYSIS

In this work the 3D finite volume method is applied to simulate the flow of liquid resin through the fiber reinforcement in the resin injection pultrusion manufacturing process. In this chapter the permeability model, boundary conditions, details of the governing equations for Region I and II, solution methods, and discretization equations are presented.

3.1 Assumptions

The following assumptions are considered for the mathematical modeling of the resin injection pultrusion process:

- Darcy's law of flow through porous media is applied to simulate the flow of liquid resin through the fiber reinforcement.
- The resin is an incompressible fluid.
- The flow of the liquid resin through the injection chamber is isothermal, so the resin viscosity is constant.
- In Region I of the injection chamber, the cross section varies in the x- direction; thus the fiber volume fraction is a function of x- direction. In Region II the fiber volume fraction is constant as the cross section is constant along the x- direction.
- The numerical model is based on the 3D Cartesian coordinate system.
- The Gutowski permeability model is employed to compute the components of the permeability tensor in the longitudinal and transverse directions. This model predicts the orthotropic permeability behavior.

- The pressure at the inlet and exit to the injection chamber is considered to be at atmospheric pressure (101.325 KPa).

3.2 Mathematical Model

Darcy's law [15] was used to model the flow of the resin through the fibers as it is analogous to the flow through porous media. Darcy's law is used for the flow of fluids in porous media, and it states that the volumetric flow rate (Q) through a specimen is proportional to the cross section area (A), the pressure difference across the specimen (ΔP) and inversely proportional to the length in the stream-wise direction of the specimen (L) and the viscosity (μ)

$$Q = K \frac{A}{\mu} \frac{\Delta P}{L} \tag{3-1}$$

The constant K in the above equation stands for permeability and has units of m^2.

3.2.1 Permeability Models

The easiness with which the liquid resin flows through the fiber matrix determines the extent of permeability. The permeability depicts the resistance to the flow; the higher the permeability the lower is the flow resistance and vice versa. The current numerical study employs the Gutowski permeability model. The resistance to the resin flow in the transverse direction (y and z) is higher than the flow resistance in the longitudinal direction (x) due to the fiber matrix system interference being higher in the transverse direction and also due to the orthotropic nature of the arrangement to the fiber matrix system.

Gutowski et al. [16] have proposed a model in which the permeability in the longitudinal direction is the same as the Kozeny-Carman equation [17] defined by the following expression

$$K_{11} = \frac{R_f{}^2}{4k} \frac{\left(1 - V_f\right)^3}{V_f{}^2} \tag{3-2}$$

but the permeabilities in the transverse direction are given by the following equations

$$K_{22} = K_{33} = \frac{{R_f}^2}{4k'} \frac{\left(\sqrt{\frac{V_a'}{V_f}} - 1 \right)^3}{\left(\frac{V_a'}{V_f} + 1 \right)} \tag{3-3}$$

Where K_{11}, K_{22}, K_{33} are the components of permeability in the x, y, and z directions, respectively, k is the Kozeny constant, R_f is fiber radius, and V_f is the local fiber volume fraction where V_a' and k' are empirical parameters; values for different fiber arrangements are given in Table 3-1.

Table 3-1. Empirical Parameters for Gutowski's model [16]

Fiber Arrangement	V_a'	k'
Quadratic	0.760	0.20
Hexagonal	0.907	0.20

A mean fiber diameters of 30 microns (glass) was determined at the University of Mississippi Composite Materials Research Laboratory (CMRG).

3.2.2 Fiber Volume Fraction and Porosity

The fiber volume fraction (V_{fo}) of the manufactured composite material is defined as the volume fraction of fiber in the final composite. Whereas the fraction of non-fiber volume in the final composite is defined by the porosity, φ. The local fiber volume fraction at different points in the longitudinal coordinate (x) in the injection chamber is expressed as V_f. For Region I the injection chamber is tapered, thus the volume of fiber remains constant but the cross section

decreases continuously along the longitudinal coordinate x, hence the porosity, φ, and local fiber volume fraction, ($V_f(x)$) become functions of the longitudinal coordinate x; the local fiber volume fraction, $V_f(x)$, increases with an increasing x dimension in Region I.

The local fiber volume fraction, $V_f(x)$, is a minimum at the front of the injection chamber. It increases along the axial coordinate, and achieves a maximum value (V_{fo}) at the end of Region I. In the Region II the local fiber volume fraction (V_{fo}) is constant since there is no taper of the walls of the injection chamber in Region II. So the local fiber volume fraction at the end of Region I and along Region II are the same as the fiber volume fraction of the final composite, i.e., $V_f(x) = V_{fo}$ in Region II. The relationship between local porosity $\varphi(x)$ and local fiber volume fraction is $V_f(x)$ given by

$$\varphi(x) = 1 - V_f(x) \tag{3-4}$$

The permeabilities depend on fiber volume faction which in turn is a function of x, thus the permeabilities are also a function of x in Region I. $V_f(x)$ is expressed as

$$V_f(x) = V_{fo}\left(\frac{H_D}{2h(x)}\right) \tag{3-5}$$

where $h(x)$ is shown in Fig. 2-2(a) and also will be defined in Eq. (3-11) in the next section.

3.2.3 Governing Equations for Region I

In Region I of the computational domain, the walls of the injection chamber are tapered so the fiber volume fraction ($V_f(x)$), porosity (φ) and components of the permeability tensor (K_{11}, K_{22}, K_{33}) are not constant but are functions of distance (x) along the longitudinal direction.

The continuity equation for flow of resin through the reinforcement in Region I is expressed by

$$\frac{\partial(u\varphi)}{\partial x}+\frac{\partial(v\varphi)}{\partial y}+\frac{\partial(w\varphi)}{\partial z}=0 \tag{3-6}$$

The components of resin velocity in three coordinate directions, u, v, and w are defined as

$$\begin{aligned} \mathrm{u} &= U-\frac{K_{11}}{\mu\varphi}\frac{\partial P}{\partial x} \\ \mathrm{v} &= V-\frac{K_{22}}{\mu\varphi}\frac{\partial P}{\partial y} \\ \mathrm{w} &= -\frac{K_{33}}{\mu\varphi}\frac{\partial P}{\partial z} \end{aligned} \tag{3-7}$$

where U and V are the velocity components of the fiber reinforcement in the x and y directions respectively; K_{11}, K_{22}, and K_{33} are the components of the permeability tensor, μ is the viscosity of the resin, P is the resin pressure, $-\frac{K_{11}}{\mu\varphi}\frac{\partial P}{\partial x}$, $-\frac{K_{22}}{\mu\varphi}\frac{\partial P}{\partial y}$, and $-\frac{K_{33}}{\mu\varphi}\frac{\partial P}{\partial z}$ are the three components of the liquid resin velocity relative to the reinforcement. The three expressions in Eq. (3-7) are the Darcy momentum equations in x, y and z directions, respectively. Substituting the x, y, z momentum equations (Eq. (3-7)) in the continuity equation, Eq. (3-6), yields

$$\frac{\partial}{\partial x}\left(U\varphi-\frac{K_{11}}{\mu\varphi}\frac{\partial P}{\partial x}\varphi\right)+\frac{\partial}{\partial \mathrm{y}}\left(V\varphi-\frac{K_{22}}{\mu\varphi}\frac{\partial P}{\partial y}\varphi\right)+\frac{\partial}{\partial z}\left(-\frac{K_{33}}{\mu\varphi}\frac{\partial P}{\partial z}\varphi\right)=0 \tag{3-8}$$

On simplifying Eq. (3-8), the pressure equation becomes

$$\frac{\partial}{\partial x}\left(\frac{K_{11}}{\mu}\frac{\partial P}{\partial x}\right)+\frac{\partial}{\partial y}\left(\frac{K_{22}}{\mu}\frac{\partial P}{\partial y}\right)+\frac{\partial}{\partial z}\left(\frac{K_{33}}{\mu}\frac{\partial P}{\partial z}\right)=\frac{\partial(U\varphi)}{\partial x}+\frac{\partial(V\varphi)}{\partial y} \tag{3-9}$$

The relation between fiber velocity in the y-direction (V) in terms of taper angle (α), fiber velocity in x direction (U), and position in the y direction is given by

$$V = -U\left(\frac{y}{h(x)}\right)\tan\alpha \tag{3-10}$$

where the vertical distance y varies according to the relation $-h(x) \le y \le h(x)$ where

$$h(x) = -\left(\frac{H_{IC} - H_D}{2L_{IC}}\right)\left(x - L_{IC}\right) + \frac{H_D}{2} \tag{3-11}$$

Substituting the fiber velocity V from Eq. (3-10) into Eq. (3-9) produces

$$\frac{\partial}{\partial x}\left(\frac{K_{11}}{\mu}\frac{\partial P}{\partial x}\right) + \frac{\partial}{\partial y}\left(\frac{K_{22}}{\mu}\frac{\partial P}{\partial y}\right) + \frac{\partial}{\partial z}\left(\frac{K_{33}}{\mu}\frac{\partial P}{\partial z}\right) = \frac{\partial}{\partial x}\left(U\varphi\right) + \frac{\partial}{\partial y}\left(-U\,\varphi\left(\frac{y}{h(x)}\right)\tan\alpha\right) \tag{3-12}$$

Simplifying Eq (3-12) yields

$$\frac{\partial}{\partial x}\left(\frac{K_{11}}{\mu}\frac{\partial P}{\partial x}\right) + \frac{\partial}{\partial y}\left(\frac{K_{22}}{\mu}\frac{\partial P}{\partial y}\right) + \frac{\partial}{\partial z}\left(\frac{K_{33}}{\mu}\frac{\partial P}{\partial z}\right) = \mathrm{U}\left\{\frac{\partial\varphi}{\partial x} - \frac{\varphi}{h(x)}\tan\alpha\right\} \tag{3-13}$$

Equation (3-13) is the governing pressure equation for Region I. Because of the tapered walls of the injection chamber in Region I, the right hand side in Eq. (3-13) acts like a source for pressure and hence produces a rise in pressure.

3.2.4 Governing Equations for Region II

The continuity equation for flow of resin through the reinforcement is again expressed by the Eq. (3-6). The Region II components of resin velocity in the three coordinate directions, u, v, and w are defined by

$$\begin{aligned} \mathrm{u} &= U - \frac{K_{11}}{\mu\varphi}\frac{\partial P}{\partial x} \\ \mathrm{v} &= -\frac{K_{22}}{\mu\varphi}\frac{\partial P}{\partial y} \\ \mathrm{w} &= -\frac{K_{33}}{\mu\varphi}\frac{\partial P}{\partial z} \end{aligned} \tag{3-14}$$

So, the total resin velocity can be expressed as:

$$\mathbf{u} = \left\{ U - \frac{K_{11}}{\mu\varphi}\frac{\partial P}{\partial x} \quad -\frac{K_{22}}{\mu\varphi}\frac{\partial P}{\partial y} \quad -\frac{K_{33}}{\mu\varphi}\frac{\partial P}{\partial z} \right\}^{\mathrm{T}} \tag{3-15}$$

The governing pressure equation is obtained by substituting the momentum equations, Eq. (3-14) into the continuity equation, Eq. (3-6), which yields

$$\frac{\partial}{\partial x}\left(U\varphi - \frac{K_{11}}{\mu\varphi}\frac{\partial P}{\partial x}\varphi \right) + \frac{\partial}{\partial y}\left(-\frac{K_{22}}{\mu\varphi}\frac{\partial P}{\partial y}\varphi \right) + \frac{\partial}{\partial z}\left(-\frac{K_{33}}{\mu\varphi}\frac{\partial P}{\partial z}\varphi \right) = 0 \tag{3-16}$$

Equation (3-16) further simplifies to,

$$\frac{\partial}{\partial \mathrm{x}}\left(\frac{K_{11}}{\mu}\frac{\partial \mathrm{P}}{\partial \mathrm{x}} \right) + \frac{\partial}{\partial \mathrm{y}}\left(\frac{K_{22}}{\mu}\frac{\partial \mathrm{P}}{\partial \mathrm{y}} \right) + \frac{\partial}{\partial \mathrm{z}}\left(\frac{K_{33}}{\mu}\frac{\partial \mathrm{P}}{\partial \mathrm{z}} \right) = \frac{\partial}{\partial \mathrm{x}}(U\varphi) \tag{3-17}$$

U and φ are constant in Region II, thus the term $\frac{\partial}{\partial x}(U\varphi)$ is zero and Eq. (3-17) simplifies to give the following governing pressure equation for Region II,

$$\frac{\partial}{\partial x}\left(\frac{K_{11}}{\mu}\frac{\partial P}{\partial x} \right) + \frac{\partial}{\partial y}\left(\frac{K_{22}}{\mu}\frac{\partial P}{\partial y} \right) + \frac{\partial}{\partial z}\left(\frac{K_{33}}{\mu}\frac{\partial P}{\partial z} \right) = 0 \tag{3-18}$$

3.2.5 Boundary Conditions:

The governing pressure equations for Region I and Region II (Eq. 3-13 and Eq. 3-18) are second order partial differential equations. So six spatial boundary conditions, two in each coordinate direction are required for solution for the pressure field. In the detached injection chamber configuration, there is a gap between the resin injection chamber and the heated die inlet. At the end of the injection chamber 0.005 m length of the injection chamber is left as the gap and the circumferential surface area of the resin/matrix system in this gap space is subjected to the atmospheric pressure boundary condition between $L_T - 0.005\ \mathrm{m} < x \leq L_T$ (see Eq. (3-19j)

and Eq. (3-19k)). Equations (3-19a) through (3-19k) express the boundary conditions in terms of pressure and velocity.

$P = P_{atm}$ at $x = 0$ (3-19a)

$P = P_{Inj}$ at injection slot (3-19b)

$$\tan\alpha = \frac{-v}{u}$$ at $y = h(x)$ (Region I) (3-19c)

$$\tan\alpha = \frac{v}{u}$$ at $y = -h(x)$ (Region I) (3-19d)

$w = 0$ at $z = W_D/2$ (Region I) (3-19e)

$w = 0$ at $z = -W_D/2$ (Region I) (3-19f)

$v = 0$ at $y = \pm H_D/2$ and $L_{IC} \le x \le L_T - 0.005$ m (Region II) (3-19g)

$w = 0$ at $z = \pm W_D/2$ and $L_{IC} \le x \le L_T - 0.005$ m (Region II) (3-19h)

$u = U$ at $x = L_T$ (3-19i)

$P = P_{atm}$ at $y = \pm H_D/2$ and $L_T - 0.005$ m $< x \le L_T$ (Region II) (3-20j)

$P = P_{atm}$ at $z = \pm W_D/2$ and $L_T - 0.005$ m $< x \le L_T$ (Region II) (3-20k)

At the front of the computational domain (at $x = 0$) dry fiber reinforcement enters the injection chamber and the fluid pressure has been assumed to be one atmosphere (101.3 KPa). At the injection slot, the pressure is at the injection pressure (input to the program).

In Region I and Region II, since a slip boundary condition is used along the chamber walls Eq. (3-19c) through Eq. (3-19j); these are obtained by setting to zero the normal component to the chamber wall of the resin resultant velocity, i.e., no penetration of resin into the wall of the injection chamber. At the exit of the injection chamber, the resin impregnated fibers at the outlet of the injection chamber is assumed to have the velocity in the x-direction equal to the fiber velocity in the x-direction ($u = U$).

In order to solve Eq. (3-13) for Region II and Eq. (3-18) for Region I, all the boundary conditions must be defined in terms of pressure. The resin velocities are substituted into Eq. (3-19c) through Eq. (3-19i) in order to obtain the following boundary conditions in terms of pressure

$$P = P_{atm} \qquad \text{at } x = 0 \qquad (3\text{-}20a)$$

$$P = P_{Inj} \qquad \text{at injection slot} \qquad (3\text{-}20b)$$

$$\frac{K_{11}}{\mu\varphi}\frac{\partial P}{\partial x}\sin\alpha + \frac{K_{22}}{\mu\varphi}\frac{\partial P}{\partial y}\cos\alpha = 0 \qquad \text{at } y = h(x) \quad \text{(Region I)} \qquad (3\text{-}20c)$$

$$\frac{K_{11}}{\mu\varphi}\frac{\partial P}{\partial x}\sin\alpha - \frac{K_{22}}{\mu\varphi}\frac{\partial P}{\partial y}\cos\alpha = 0 \qquad \text{at } y = -h(x) \quad \text{(Region I)} \qquad (3\text{-}20d)$$

$$\frac{\partial P}{\partial z} = 0 \qquad \text{at } z = W_D/2 \quad \text{(Region I)} \qquad (3\text{-}20e)$$

$$\frac{\partial P}{\partial z} = 0 \qquad \text{at } z = -W_D/2 \quad \text{(Region I)} \qquad (3\text{-}20f)$$

$$\frac{\partial P}{\partial y} = 0 \qquad \text{at } y = \pm H_D/2 \text{ and } L_{IC} \le x \le L_T - 0.005 \text{ m} \quad \text{(Region II)} \qquad (3\text{-}20g)$$

$$\frac{\partial P}{\partial z} = 0 \qquad \text{at } z = \pm W_D/2 \text{ and } L_{IC} \le x \le L_T - 0.005 \text{ m} \quad \text{(Region II)} \qquad (3\text{-}20h)$$

$$\frac{\partial P}{\partial x} = 0 \qquad \text{at } x = L_T \qquad (3\text{-}20i)$$

$$P = P_{atm} \qquad \text{at } y = \pm H_D/2 \text{ and } L_T - 0.005 \text{ m} < x \le L_T \quad \text{(Region II)} \qquad (3\text{-}20j)$$

$$P = P_{atm} \qquad \text{at } z = \pm W_D/2 \text{ and } L_T - 0.005 \text{ m} < x \le L_T \quad \text{(Region II)} \qquad (3\text{-}20k)$$

The computational domain is symmetric about the xy and xz-planes. So only a quarter of the computational domain is modeled. Hence the boundary conditions must have to be suitably modified to simulate the resin flow in a quarter of the computational domain. The modified boundary conditions corresponding to the quarter domain are given by

$$P = P_{atm} \qquad \text{at } x = 0 \qquad (3\text{-}21a)$$

$$P = P_{Inj} \qquad \text{at injection port/slot} \qquad (3\text{-}21b)$$

$$\frac{K_{11}}{\mu\phi}\frac{\partial P}{\partial x}\sin\alpha + \frac{K_{22}}{\mu\phi}\frac{\partial P}{\partial y}\cos\alpha = 0 \qquad \text{at } y = h(x) \text{ (Region I)} \qquad (3\text{-}21c)$$

$$\frac{\partial P}{\partial y} = 0 \qquad \text{at } y = 0 \text{ (Region I)} \qquad (3\text{-}21d)$$

$$\frac{K_{11}}{\mu\phi}\frac{\partial P}{\partial x}\sin\beta + \frac{K_{33}}{\mu\phi}\frac{\partial P}{\partial z}\cos\beta = 0 \qquad \text{at } z = W_D/2 \text{ (Region I)} \qquad (3\text{-}21e)$$

$$\frac{\partial P}{\partial z} = 0 \qquad \text{at } z = 0 \text{ (Region I)} \qquad (3\text{-}21f)$$

$$\frac{\partial P}{\partial y} = 0 \qquad \text{at } y = H_D/2 \text{ and } L_{IC} \le x \le L_T - 0.005 \text{ m (Region II)} \qquad (3\text{-}21g)$$

$$P = P_{atm} \qquad \text{at } y = H_D/2 \text{ and } L_T - 0.005 \text{ m} < x \le L_T \text{ (Region II)} \qquad (3\text{-}21h)$$

$$\frac{\partial P}{\partial y} = 0 \qquad \text{at } y = 0 \text{ (Region II)} \qquad (3\text{-}21i)$$

$$\frac{\partial P}{\partial z} = 0 \qquad \text{at } z = W_D/2 \text{ and } L_{IC} \le x \le L_T - 0.005 \text{ m (Region II)} \qquad (3\text{-}21j)$$

$$P = P_{atm} \qquad \text{at z} = W_D/2 \text{ and } L_T - 0.005 \text{ m} < x \le L_T \text{ (Region II)} \qquad (3\text{-}21k)$$

$$\frac{\partial P}{\partial z} = 0 \qquad \text{at } z = 0 \text{ (Region II)} \qquad (3\text{-}21l)$$

$$\frac{\partial P}{\partial x} = 0 \qquad \text{at } x = \text{length of injection chamber} \qquad (3\text{-}21m)$$

3.3 Finite Volume Method

The finite volume method is used in this study to predict the pressure field, the velocity field, and the location and shape of the liquid resin flow front in the computational domain. In this method, the computational domain is divided into touching but non-overlapping finite control

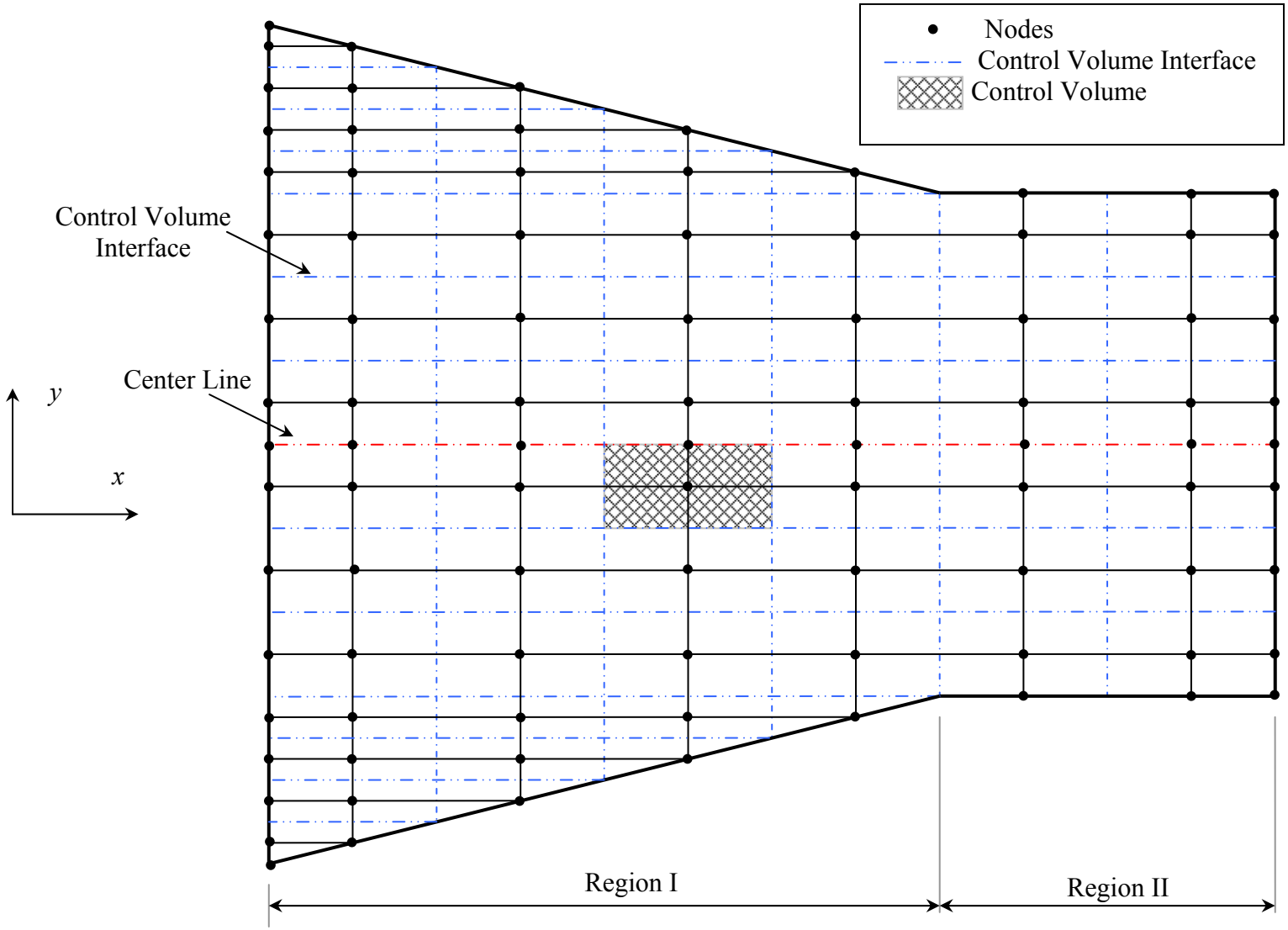

Figure 3-1. Schematic of the Computational Domain with the Grid [1].

volumes (Figure 3-1) which fill the domain, with one computational node associated with each control volume. The finite volume method approximates the partial differential equation over a control volume associated with the grid node. After applying the finite volume approach, discretization equations are obtained by integrating the partial differential equation for each control volume surrounding each grid node. Linear interpolation functions (or piecewise linear profile) expressing the variation of pressure between the grid points are used to evaluate the required integrals.

3.4 Derivation of the Discretization Equation

3.4.1 Derivation of the Discretization Equation for Region I

The general discretization equation for Region I is given by

$$
\begin{aligned}
&P_P\left\{\frac{K_{11}}{\mu}\bigg|_e \frac{\Delta y\,\Delta z}{(\delta x)_e}+\frac{K_{11}}{\mu}\bigg|_w \frac{\Delta y\,\Delta z}{(\delta x)_w}+\frac{K_{22}}{\mu}\bigg|_n \frac{\Delta x\,\Delta z}{(\delta y)_n}+\frac{K_{22}}{\mu}\bigg|_s \frac{\Delta x\,\Delta z}{(\delta y)_s}+\frac{K_{33}}{\mu}\bigg|_t \frac{\Delta x\,\Delta y}{(\delta z)_t}+\frac{K_{33}}{\mu}\bigg|_b \frac{\Delta x\,\Delta y}{(\delta z)_b}\right\}\\
&=P_E\left\{\frac{K_{11}}{\mu}\bigg|_e \frac{\Delta y\,\Delta z}{(\delta x)_e}\right\}+P_W\left\{\frac{K_{11}}{\mu}\bigg|_w \frac{\Delta y\,\Delta z}{(\delta x)_w}\right\}+P_N\left\{\frac{K_{22}}{\mu}\bigg|_n \frac{\Delta x\,\Delta z}{(\delta y)_n}\right\}+P_S\left\{\frac{K_{22}}{\mu}\bigg|_s \frac{\Delta x\,\Delta z}{(\delta y)_s}\right\}+\\
&P_T\left\{\frac{K_{33}}{\mu}\bigg|_t \frac{\Delta x\,\Delta y}{(\delta z)_t}\right\}+P_B\left\{\frac{K_{33}}{\mu}\bigg|_b \frac{\Delta x\,\Delta y}{(\delta z)_b}\right\}-U\left(\left(\varphi_e-\varphi_w\right)\right)\Delta y\,\Delta z+U\frac{tan\alpha_P}{h(x_P)}\varphi_P\Delta x\,\Delta y\,\Delta z
\end{aligned}
\tag{3-22}
$$

This equation has the linear form as

$$a_P P_P = a_E P_E + a_W P_W + a_N P_N + a_S P_S + a_T P_T + a_B P_B + b \tag{3-23}$$

where a_P, a_E, a_W, a_N, a_S, a_T, a_B are the coefficients of the pressures at the given node and its neighboring nodes, respectively. This expresses a relation between a node and its neighbors. The coefficients are defined by the following equations

$$a_E = \frac{K_{11}}{\mu}\bigg|_e \frac{\Delta y\ \Delta z}{(\delta x)_e} \tag{3-24a}$$

$$a_W = \left.\frac{K_{11}}{\mu}\right|_w \frac{\Delta y\,\Delta z}{(\delta x)_w} \tag{3-24b}$$

$$a_N = \left.\frac{K_{22}}{\mu}\right|_n \frac{\Delta x\,\Delta z}{(\delta y)_n} \tag{3-24c}$$

$$a_S = \left.\frac{K_{22}}{\mu}\right|_s \frac{\Delta x\,\Delta z}{(\delta y)_s} \tag{3-24d}$$

$$a_T = \left.\frac{K_{33}}{\mu}\right|_t \frac{\Delta x\,\Delta y}{(\delta z)_t} \tag{3-24e}$$

$$a_B = \left.\frac{K_{33}}{\mu}\right|_b \frac{\Delta x\,\Delta y}{(\delta z)_b} \tag{3-24f}$$

$$a_P = a_E + a_W + a_N + a_S + a_T + a_B \tag{3-24g}$$

$$b = U\frac{\tan\alpha_P}{h(x_P)}\varphi_P \Delta x\,\Delta y\,\Delta z \tag{3-24h}$$

3.4.2 Derivation of the Discretization Equation for Region II

The general pressure discretization equation is

$$\begin{aligned} P_P\ & \left.\frac{K_{11}}{\mu}\right|_e \frac{\Delta y\,\Delta z}{(\delta x)_e} + \left.\frac{K_{11}}{\mu}\right|_w \frac{\Delta y\,\Delta z}{(\delta x)_w} + \left.\frac{K_{22}}{\mu}\right|_n \frac{\Delta x\,\Delta z}{(\delta y)_n} + \left.\frac{K_{22}}{\mu}\right|_s \frac{\Delta x\,\Delta z}{(\delta y)_s} + \left.\frac{K_{33}}{\mu}\right|_t \frac{\Delta x\,\Delta y}{(\delta z)_t} + \left.\frac{K_{33}}{\mu}\right|_b \frac{\Delta x\,\Delta y}{(\delta z)_b} \\ = P_E\ & \left.\frac{K_{11}}{\mu}\right|_e \frac{\Delta y\,\Delta z}{(\delta x)_e} + P_W \left.\frac{K_{11}}{\mu}\right|_w \frac{\Delta y\,\Delta z}{(\delta x)_w} + P_N \left.\frac{K_{22}}{\mu}\right|_n \frac{\Delta x\,\Delta z}{(\delta y)_n} + P_S \left.\frac{K_{22}}{\mu}\right|_s \frac{\Delta x\,\Delta z}{(\delta y)_s} + \\ & P_T \left.\frac{K_{33}}{\mu}\right|_t \frac{\Delta x\,\Delta y}{(\delta z)_t} + P_B \left.\frac{K_{33}}{\mu}\right|_b \frac{\Delta x\,\Delta y}{(\delta z)_b} \end{aligned} \tag{3-25}$$

This equation has the linear form

$$a_P P_P = a_E P_E + a_W P_W + a_N P_N + a_S P_S + a_T P_T + a_B P_B \tag{3-26}$$

where a_P, a_E, a_W, a_N, a_S, a_T, a_B are the coefficients of the pressures at the given node and its neighboring nodes, respectively. Equation (3-26) expresses a relation between a pressure node

and its neighbors. The coefficients are same as described in the Eqs. (3-24). Note since $tan\,\alpha_P = 0$ in Region II the b term (Eq. (3-24h) --- pressure source term) is not there in Region II.

3.5 Solution of the Algebraic Equations by TDMA

The current solution technique employs the line-by-line tridiagonal matrix algorithm (TDMA) to solve the system of discritized equations. Direct methods and iterative methods in general are the two types of methods available to solve the system of equations. Direct methods (that require no iterations) for solving the algebraic equations arising in two or three-dimensional problems are much more complicated and require rather large amounts of computational space and time. Alternatively, iterative methods start from a guessed field of the dependent variable and use the algebraic equations in some manner to obtain a progressively improved field. The progressive repetition of the algorithm leads to a solution that is sufficiently close to the correct solution of the algebraic equations. Additionally, the iterative methods require much smaller additional storage in the computer, and they are especially significant for handling nonlinearities.

Solution by the line-by-line method converges very rapidly because the boundary condition information is transmitted rapidly to the interior of the domain, regardless of how many grid points lie along the line. TDMA is a very powerful and convenient equation solver, and unlike general direct methods (matrix), the TDMA requires computer storage and computer time proportional to N, rather than to N^2 or N^3 [18]; hence the RAM requirement to solve these equations is quite modest.

3.6 Algorithm for time marching scheme:

Fill factor, $F_{i,j,k}$ is defined as the fraction of the control volume occupied by liquid resin at a given time instant relative to the maximum liquid resin the control volume can hold. In the

numerical scheme, $F_{i,j,k}$ is related to the amount of resin in the control volume. For a completely liquid filled control volume, the value of $F_{i,j,k}$ is unity (saturated reinforcement) and is zero (dry reinforcement) if the control volume is empty of liquid. Pressure is computed at a control volume node if the control volume is fully saturated with liquid resin, otherwise atmospheric pressure is assigned to it.

Figure 3-2 illustrates the components of resin velocities at the interface of the control volume. The solid dot is the node and is surrounded by a control volume represented by the dashed line. The fill factors and the porosities of the control volumes are also shown in the figure. The net mass flow rate of liquid resin into and out of the control volume is computed using the following equations.

$$\begin{aligned}\left(NetMass\ Flow\ Rate\right)_{in} = \rho\{ & u_{i-1,j,k}\left(\frac{\phi_{i-1,j,k}+\phi_{i,j,k}}{2}\right)\Delta y\Delta z\left[\frac{u_{i-1,j,k}}{abs(u_{i-1,j,k})}F_{i-1,j,k},\frac{-u_{i-1,j,k}}{abs(u_{i-1,j,k})}F_{i,j,k}\right] \\ & + v_{i,j-1,k}\phi_{i,j,k}\Delta x\Delta z\left[\frac{v_{i,j-1,k}}{abs(v_{i,j-1,k})}F_{i,j-1,k},\frac{-v_{i,j-1,k}}{abs(v_{i,j-1,k})}F_{i,j,k}\right]+ \\ & w_{i,j,k-1}\phi_{i,j,k}\Delta x\Delta y\left[\frac{w_{i,j,k-1}}{abs(w_{i,j,k-1})}F_{i,j,k-1},\frac{-w_{i,j,k-1}}{abs(w_{i,j,k-1})}F_{i,j,k}\right]\}\end{aligned} \quad \text{- (3-27)}$$

$$\begin{aligned}\left(NetMass\ Flow\ Rate\right)_{out} = \rho\{ & u_{i,j,k}\left(\frac{\phi_{i,j,k}+\phi_{i+1,j,k}}{2}\right)\Delta y\Delta z\left[\frac{u_{i,j,k}}{abs(u_{i,j,k})}F_{i,j,k},\frac{-u_{i,j,k}}{abs(u_{i,j,k})}F_{i+1,j,k}\right] \\ & + v_{i,j,k}\phi_{i,j,k}\Delta x\Delta z\left[\frac{v_{i,j,k}}{abs(v_{i,j,k})}F_{i,j,k},\frac{-v_{i,j,k}}{abs(v_{i,j,k})}F_{i,j+1,k}\right]+ \\ & w_{i,j,k}\phi_{i,j,k}\Delta x\Delta y\left[\frac{w_{i,j,k}}{abs(w_{i,j,k})}F_{i,j,k},\frac{-w_{i,j,k}}{abs(w_{i,j,k})}F_{i,j,k+1}\right]\}\end{aligned} \quad \text{- (3-28)}$$

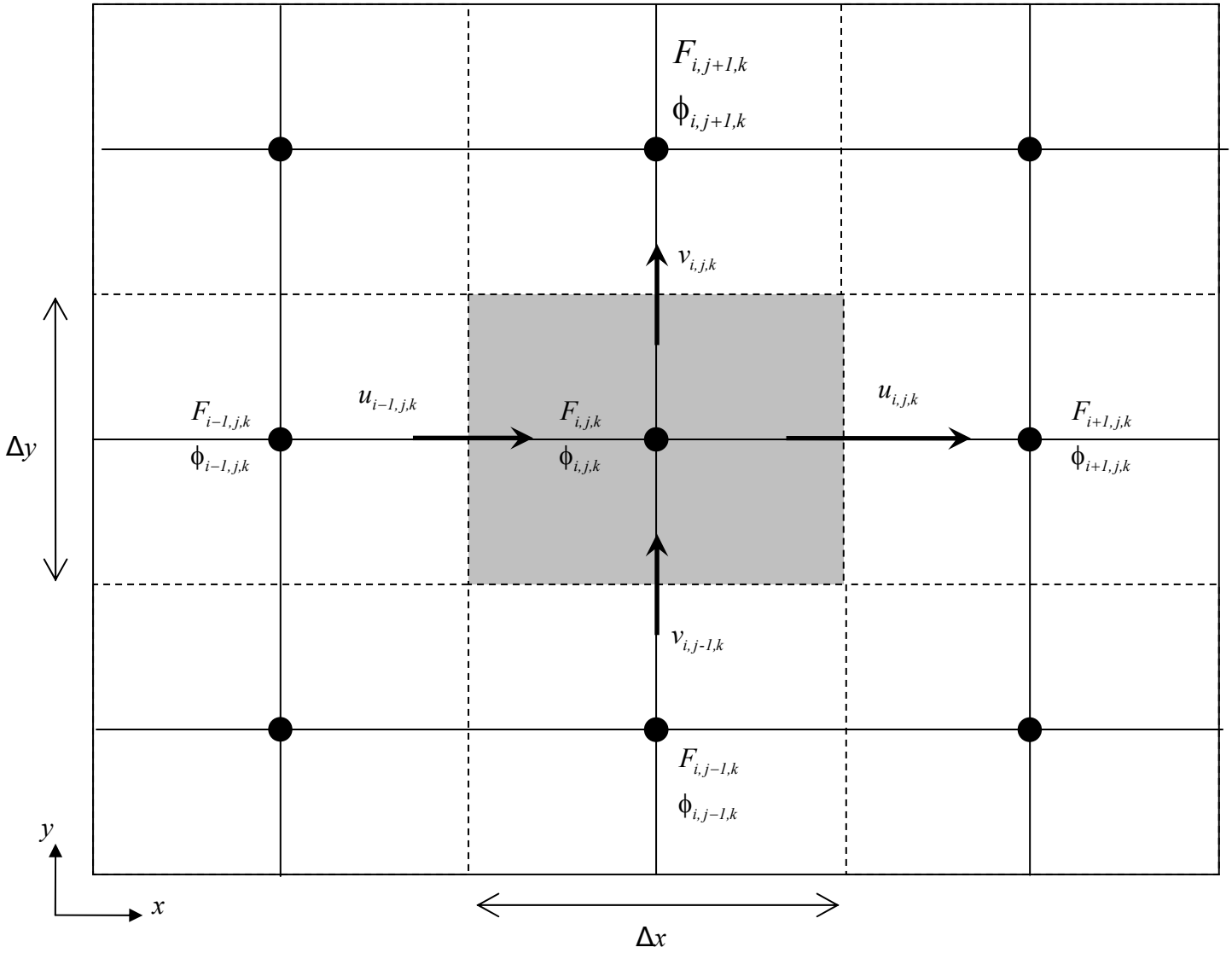

Figure 3-2. Schematic for Net Mass Flow Rate Calculations [1].

The terms $\left(\frac{\phi_{i-1,j,k}+\phi_{i,j,k}}{2}\right)$ and $\left(\frac{\phi_{i,j,k}+\phi_{i+1,j,k}}{2}\right)$ represent the average values of porosity at the interface of a control volume in the longitudinal direction. In the above equations, if the component of resin velocity is positive then the first term in the square bracket is used for computations, and if the velocity component is negative then the second term is used to compute the mass flow rate. Time taken to fill the yet unfilled control volumes is expressed by the following equations.

$$\left(1-F_{i,j,k}\right)\rho\,\Delta x\,\Delta y\,\Delta z\,\phi_{i,j,k}=\left[\left(Mass\ Flow\ Rate\right)_{in}-\left(Mass\ Flow\ Rate\right)_{out}\right]\Delta t \qquad (3\text{-}29)$$

Upon simplifying, Eq. (3-29) yields the time to fill a specific control volume as

$$\Delta t=\frac{\left(1-F_{i,j,k}\right)\rho\,\Delta x\,\Delta y\,\Delta z\,\phi_{i,j,k}}{\left[\left(NetMass\ Flow\ Rate\right)_{in}-\left(NetMass\ Flow\ Rate\right)_{out}\right]} \qquad (3\text{-}30)$$

When the resin flow front approaches steady state, the net flow rate across the interfaces of a control volume approaches zero and so Δt defined by Eq. (3-30) approaches infinity. To avoid this problem and to maintain the numerical stability of the algorithm, the pultruded part is not allowed to travel by more than the length of the nodal control volume in the pull direction during a given time step, i.e.

$$0<\Delta t_{min}<\frac{L_{min}}{U} \qquad (3\text{-}31)$$

where L_{min} is minimum length of the control volume in the pull speed direction and U is the fiber pull speed in the longitudinal direction. This condition is checked at every time step and no more than one control volume is allowed to be newly filled ($F=1$) at that time step. At a given time step, if the calculated value of minimum time step from Eq. (3-30) is greater than as defined by Eq. (3-31), then use the value of minimum time step from Eq. (3-31) is used, otherwise the minimum time step is calculated from Eq. (3-30).

The minimum value of the time step, computed for all of the unfilled control volumes using Eq. (3-30), is the amount of time required to fill the next quickest to fill control volume, which has resin in it but not yet completely filled and yet not overfilling any other control volume. As the flow front is advanced using this minimum time step it is ensured that only one control volume is filled in one time step and no control volume is overfilled as time advances forward.

The fill factors of all unfilled or not completely filled control volumes (where $0 \le F < 1$) are updated at the end of each time step by using the minimum time step determined from Eq. (3-30) or Eq. (3-31) by employing the following equations.

$$\Delta F_{i,j,k} = \left[\left(Mass\ Flow\ Rate \right)_{in} - \left(Mass\ Flow\ Rate \right)_{out} \right] \frac{\Delta t_{min}}{\rho \Delta x \Delta y \Delta z \phi_{i,j,k}} \tag{3-32}$$

$$F_{i,j,k} = F^{o}{}_{i,j,k} + \Delta F_{i,j,k} \tag{3-33}$$

where $\Delta F_{i,j,k}$ is the change in fill factor and $F^{o}{}_{i,j,k}$ is the fill factor at the end of the previous time step.

With the physical description of the problem given in Chapter 2 and the mathematical description and analysis specified in Chapter 3, the following chapter will present the complete results and discussions as determined from the mathematical description given in Chapter 3.

CHAPTER 4

RESULTS AND DISCUSSION

In this chapter, the results obtained from simulating the various cases are presented and discussed. As mentioned in Chapter 2, this work considers the impact of the processing parameters (pull speed (U), fiber volume fraction (V_{fo}) and viscosity (μ)) on the complete fiber reinforcement wet out, on the minimum resin injection pressure to achieve complete wet out, and most importantly on the maximum resin pressure inside the injection chamber. The minimum resin injection pressure to achieve complete wet out and the corresponding maximum resin pressure inside the injection chamber for both the attached configuration and detached configuration are compared for CR values of 2.0, 3.0 and 4.0. The simulations correspond to a composite consisting of fiberglass reinforcement with a phenolic resin system.

Total lengths of the injection chamber (L_T) considered in this study are 0.15 m, 0.20 m and 0.30 m. Dual (one on top and one on bottom (see Fig. 2-2)) injection slots of 0.01 m wide were investigated at two possible axial locations (x_{IS}) which were studied - 40 % or 60 % downstream along the tapered lengths (L_{IC}) for L_T = 0.15 m, 0.20 m and 0.30 m respectively. Simulations are carried out for a variety of processing parameters while other parameters are held fixed at the nominal values – nominal pull speed (line speed) U = 0.0254 m/s (60 in/min), nominal fiber volume fraction, V_{fo} = 0.68, and nominal resin viscosity, μ = 0.75 Pa·s. Thus, the total number of cases considered for each proportional (40 % or 60 %) axial slot location is 63. Tables 4-1 and 4-2 contain the complete result for the cases for the proportional axial slot locations, x_{IS} = 0.40 L_{IC} and x_{IS} = 0.60 L_{IC} respectively. The feasible criteria for acceptable

Table 4-1. Injection Pressure Necessary to Achieve Complete Wet out and Corresponding Maximum Injection Chamber Pressure for Different Processing Parameters for Slot Width = 0.01 m, Part Width = 0.0635 m, Part Thickness = 0.00318 m at a Proportional Slot Location of x_{IS} = 0.40 L_{IC}.

Case	CR	U (m/s)	V_{fo}	μ Pa·s	Injection Pressure (Gauge) (MPa)	Total Length $\mathbf{L_T}$ (m)	Location of x_{IS} (m)	Exit Pressure (Gauge) (MPa) (Attached)	Maximum Chamber Pressure (Gauge) (MPa) (Detached)
A1	2.0	0.0203	0.68	0.75	0.002	0.15	0.04	0.746	0.605
A2	2.0	0.0254	0.68	0.75	0.002	0.15	0.04	0.932	0.756
A3*	2.0	0.0508	0.68	0.75	0.002	0.15	0.04	**1.862**	1.511
A4	2.0	0.0254	0.64	0.75	0.002	0.15	0.04	0.673	0.536
A5	2.0	0.0254	0.72	0.75	0.002	0.15	0.04	1.306	1.100
A6	2.0	0.0254	0.68	0.50	0.002	0.15	0.04	0.622	0.514
A7	2.0	0.0254	0.68	1.00	0.002	0.15	0.04	1.240	1.010
B1	3.0	0.0203	0.68	0.75	0.002	0.15	0.04	0.563	0.510
B2	3.0	0.0254	0.68	0.75	0.002	0.15	0.04	0.705	0.638
B3	3.0	0.0508	0.68	0.75	0.002	0.15	0.04	1.409	1.280
B4	3.0	0.0254	0.64	0.75	0.002	0.15	0.04	0.527	0.470
B5	3.0	0.0254	0.72	0.75	0.002	0.15	0.04	0.952	0.880
B6	3.0	0.0254	0.68	0.50	0.002	0.15	0.04	0.470	0.425
B7	3.0	0.0254	0.68	1.00	0.002	0.15	0.04	0.940	0.850
C1	4.0	0.0203	0.68	0.75	0.002	0.15	0.04	0.442	0.420
C2	4.0	0.0254	0.68	0.75	0.002	0.15	0.04	0.553	0.524
C3	4.0	0.0508	0.68	0.75	0.002	0.15	0.04	1.105	1.050
C4	4.0	0.0254	0.64	0.75	0.002	0.15	0.04	0.421	0.393
C5	4.0	0.0254	0.72	0.75	0.002	0.15	0.04	0.740	0.706
C6	4.0	0.0254	0.68	0.50	0.002	0.15	0.04	0.370	0.350
C7	4.0	0.0254	0.68	1.00	0.002	0.15	0.04	0.737	0.700
D1	2.0	0.0203	0.68	0.75	0.014	0.20	0.06	1.015	0.768
D2	2.0	0.0254	0.68	0.75	0.014	0.20	0.06	1.270	0.961
D3*	2.0	0.0508	0.68	0.75	0.037	0.20	0.06	**2.510**	**1.920**
D4	2.0	0.0254	0.64	0.75	0.014	0.20	0.06	0.924	0.683
D5*	2.0	0.0254	0.72	0.75	0.002	0.20	0.06	**1.744**	1.370
D6	2.0	0.0254	0.68	0.50	0.014	0.20	0.06	0.847	0.640
D7	2.0	0.0254	0.68	1.00	0.021	0.20	0.06	1.672	1.280
E1	3.0	0.0203	0.68	0.75	0.002	0.20	0.06	0.722	0.611
E2	3.0	0.0254	0.68	0.75	0.002	0.20	0.06	0.903	0.764
E3*	3.0	0.0508	0.68	0.75	0.002	0.20	0.06	**1.806**	1.530
E4	3.0	0.0254	0.64	0.75	0.002	0.20	0.06	0.695	0.568
E5	3.0	0.0254	0.72	0.75	0.002	0.20	0.06	1.204	1.040
E6	3.0	0.0254	0.68	0.50	0.002	0.20	0.06	0.602	0.510

Table 4-1. continued

Case	CR	U (m/s)	V_{fo}	μ Pa·s	Injection Pressure (Gauge) (MPa)	Total Length $\mathbf{L_T}$ (m)	Location of x_{IS} (m)	Exit Pressure (Gauge) (MPa) (Attached)	Maximum Chamber Pressure (Gauge) (MPa) (Detached)
E7	3.0	0.0254	0.68	1.00	0.002	0.20	0.06	1.204	1.020
F1	4.0	0.0203	0.68	0.75	0.002	0.20	0.06	0.538	0.477
F2	4.0	0.0254	0.68	0.75	0.002	0.20	0.06	0.672	0.597
F3	4.0	0.0508	0.68	0.75	0.002	0.20	0.06	1.345	1.194
F4	4.0	0.0254	0.64	0.75	0.002	0.20	0.06	0.531	0.453
F5	4.0	0.0254	0.72	0.75	0.002	0.20	0.06	0.877	0.792
F6	4.0	0.0254	0.68	0.50	0.002	0.20	0.06	0.450	0.398
F7	4.0	0.0254	0.68	1.00	0.002	0.20	0.06	0.897	0.796
G1*	2.0	0.0203	0.68	0.75	0.002	0.30	0.10	**1.885**	1.280
G2*	2.0	0.0254	0.68	0.75	0.002	0.30	0.10	**2.356**	1.600
G3*	2.0	0.0508	0.68	0.75	0.007	0.30	0.10	**4.724**	**3.205**
G4	2.0	0.0254	0.64	0.75	0.007	0.30	0.10	1.703	1.124
G5*	2.0	0.0254	0.72	0.75	0.002	0.30	0.10	**3.330**	**2.320**
G6	2.0	0.0254	0.68	0.50	0.002	0.30	0.10	1.571	1.067
G7*	2.0	0.0254	0.68	1.00	0.002	0.30	0.10	**3.148**	**2.134**
H1	3.0	0.0203	0.68	0.75	0.002	0.30	0.10	1.402	1.100
H2*	3.0	0.0254	0.68	0.75	0.002	0.30	0.10	**1.752**	1.378
H3*	3.0	0.0508	0.68	0.75	0.002	0.30	0.10	**3.513**	**2.757**
H4	3.0	0.0254	0.64	0.75	0.002	0.30	0.10	1.310	1.000
H5*	3.0	0.0254	0.72	0.75	0.002	0.30	0.10	**2.372**	**1.912**
H6	3.0	0.0254	0.68	0.50	0.002	0.30	0.10	1.169	0.918
H7*	3.0	0.0254	0.68	1.00	0.002	0.30	0.10	**2.340**	**1.840**
I1	4.0	0.0203	0.68	0.75	0.002	0.30	0.10	1.085	0.911
I2	4.0	0.0254	0.68	0.75	0.002	0.30	0.10	1.358	1.140
I3*	4.0	0.0508	0.68	0.75	0.002	0.30	0.10	**2.718**	**2.280**
I4	4.0	0.0254	0.64	0.75	0.002	0.30	0.10	1.030	0.750
I5*	4.0	0.0254	0.72	0.75	0.002	0.30	0.10	**1.807**	1.550
I6	4.0	0.0254	0.68	0.50	0.002	0.30	0.10	0.904	0.760
I7*	4.0	0.0254	0.68	1.00	0.002	0.30	0.10	**1.811**	1.517

***** Bold font indicates non-acceptable manufacturing solutions, not satisfying the following criteria: injection pressure ≤ 0.42 MPa (60 psi) and corresponding exit pressure (attached configuration) or maximum wall pressure (detached configuration) ≤ 1.72 MPa (250 psi).

Table 4-2. Injection Pressure Necessary to Achieve Complete Wet out and Corresponding Maximum Injection Chamber Pressure for Different Processing Parameters for Slot Width = 0.01 m, Part Width = 0.0635 m, Part Thickness = 0.00318 m at a Proportional Slot Location x_{IS} = 0.60 L_{IC}.

Case	CR	U (m/s)	V_{fo}	μ Pa·s	Injection Pressure (Gauge) (MPa)	Total Length $\mathbf{L_T}$ (m)	Location of x_{IS} (m)	Exit Pressure (Gauge) (MPa) (Attached)	Maximum Chamber Pressure (Gauge) (MPa) (Detached)
A1	2.0	0.0203	0.68	0.75	0.057	0.15	0.06	0.525	0.475
A2	2.0	0.0254	0.68	0.75	0.071	0.15	0.06	0.656	0.570
A3	2.0	0.0508	0.68	0.75	0.147	0.15	0.06	1.347	1.150
A4	2.0	0.0254	0.64	0.75	0.064	0.15	0.06	0.487	0.388
A5	2.0	0.0254	0.72	0.75	0.092	0.15	0.06	0.968	0.827
A6	2.0	0.0254	0.68	0.50	0.064	0.15	0.06	0.471	0.383
A7	2.0	0.0254	0.68	1.00	0.100	0.15	0.06	0.900	0.503
B1	3.0	0.0203	0.68	0.75	0.002	0.15	0.06	0.454	0.415
B2	3.0	0.0254	0.68	0.75	0.002	0.15	0.06	0.570	0.520
B3	3.0	0.0508	0.68	0.75	0.002	0.15	0.06	1.136	1.040
B4	3.0	0.0254	0.64	0.75	0.002	0.15	0.06	0.417	0.367
B5	3.0	0.0254	0.72	0.75	0.002	0.15	0.06	0.784	0.728
B6	3.0	0.0254	0.68	0.50	0.002	0.15	0.06	0.379	0.346
B7	3.0	0.0254	0.68	1.00	0.002	0.15	0.06	0.758	0.691
C1	4.0	0.0203	0.68	0.75	0.002	0.15	0.06	0.380	0.361
C2	4.0	0.0254	0.68	0.75	0.002	0.15	0.06	0.474	0.413
C3	4.0	0.0508	0.68	0.75	0.002	0.15	0.06	0.950	0.904
C4	4.0	0.0254	0.64	0.75	0.002	0.15	0.06	0.355	0.334
C5	4.0	0.0254	0.72	0.75	0.002	0.15	0.06	0.639	0.620
C6	4.0	0.0254	0.68	0.50	0.002	0.15	0.06	0.316	0.302
C7	4.0	0.0254	0.68	1.00	0.002	0.15	0.06	0.632	0.603
D1	2.0	0.0203	0.68	0.75	0.057	0.20	0.09	0.677	0.576
D2	2.0	0.0254	0.68	0.75	0.078	0.20	0.09	0.880	0.715
D3	2.0	0.0508	0.68	0.75	0.147	0.20	0.09	1.700	1.375
D4	2.0	0.0254	0.64	0.75	0.078	0.20	0.09	0.631	0.522
D5	2.0	0.0254	0.72	0.75	0.133	0.20	0.09	1.273	1.030
D6	2.0	0.0254	0.68	0.50	0.050	0.20	0.09	0.583	0.491
D7	2.0	0.0254	0.68	1.00	0.105	0.20	0.09	1.174	0.926
E1	3.0	0.0203	0.68	0.75	0.002	0.20	0.09	0.560	0.475
E2	3.0	0.0254	0.68	0.75	0.002	0.20	0.09	0.700	0.590
E3	3.0	0.0508	0.68	0.75	0.002	0.20	0.09	1.400	1.190
E4	3.0	0.0254	0.64	0.75	0.002	0.20	0.09	0.518	0.434
E5	3.0	0.0254	0.72	0.75	0.002	0.20	0.09	0.953	0.827
E6	3.0	0.0254	0.68	0.50	0.002	0.20	0.09	0.470	0.397

Table 4-2. continued

Case	CR	U (m/s)	V_{fo}	μ Pa·s	Injection Pressure (Gauge) (MPa)	Total Length L_T (m)	Location of x_{IS} (m)	Exit Pressure (Gauge) (MPa) (Attached)	Maximum Chamber Pressure (Gauge) (MPa) (Detached)
E7	3.0	0.0254	0.68	1.00	0.002	0.20	0.09	0.933	0.793
F1	4.0	0.0203	0.68	0.75	0.002	0.20	0.09	0.450	0.400
F2	4.0	0.0254	0.68	0.75	0.002	0.20	0.09	0.561	0.501
F3	4.0	0.0508	0.68	0.75	0.002	0.20	0.09	1.122	1.000
F4	4.0	0.0254	0.64	0.75	0.002	0.20	0.09	0.426	0.375
F5	4.0	0.0254	0.72	0.75	0.002	0.20	0.09	0.743	0.675
F6	4.0	0.0254	0.68	0.50	0.002	0.20	0.09	0.374	0.330
F7	4.0	0.0254	0.68	1.00	0.002	0.20	0.09	0.748	0.670
G1	2.0	0.0203	0.68	0.75	0.064	0.30	0.15	1.380	0.968
G2*	2.0	0.0254	0.68	0.75	0.078	0.30	0.15	**1.727**	1.198
G3*	2.0	0.0508	0.68	0.75	0.133	0.30	0.15	**3.393**	**2.390**
G4	2.0	0.0254	0.64	0.75	0.064	0.30	0.15	1.210	0.801
G5*	2.0	0.0254	0.72	0.75	0.147	0.30	0.15	**2.440**	**1.747**
G6	2.0	0.0254	0.68	0.50	0.050	0.30	0.15	1.150	0.776
G7*	2.0	0.0254	0.68	1.00	0.092	0.30	0.15	**2.263**	0.689
H1	3.0	0.0203	0.68	0.75	0.002	0.30	0.15	1.135	0.890
H2	3.0	0.0254	0.68	0.75	0.002	0.30	0.15	1.420	1.120
H3*	3.0	0.0508	0.68	0.75	0.002	0.30	0.15	**2.840**	**2.230**
H4	3.0	0.0254	0.64	0.75	0.002	0.30	0.15	1.040	0.801
H5*	3.0	0.0254	0.72	0.75	0.002	0.30	0.15	**1.960**	1.581
H6	3.0	0.0254	0.68	0.50	0.002	0.30	0.15	0.947	0.745
H7*	3.0	0.0254	0.68	1.00	0.002	0.30	0.15	**1.900**	1.490
I1	4.0	0.0203	0.68	0.75	0.002	0.30	0.15	0.936	0.786
I2	4.0	0.0254	0.68	0.75	0.002	0.30	0.15	1.171	0.984
I3*	4.0	0.0508	0.68	0.75	0.002	0.30	0.15	**2.342**	**1.960**
I4	4.0	0.0254	0.64	0.75	0.002	0.30	0.15	0.876	0.721
I5	4.0	0.0254	0.72	0.75	0.002	0.30	0.15	1.583	1.356
I6	4.0	0.0254	0.68	0.50	0.002	0.30	0.15	0.781	0.656
I7	4.0	0.0254	0.68	1.00	0.002	0.30	0.15	1.562	1.310

***** Bold font indicates non-acceptable manufacturing solutions, not satisfying the following criteria: injection pressure ≤ 0.42 MPa (60 psi) and corresponding exit pressure (attached configuration) or maximum wall pressure (detached configuration) ≤ 1.72 MPa (250 psi).

manufacturing solutions are: an injection pressure to achieve complete wet out of not greater than 0.42 MPa (60 psi) and a corresponding maximum exit resin pressure (attached configuration) or maximum interior chamber resin pressure (detached configuration) of not greater than 1.72 MPa (250 psi).

It can be seen from the Table 4-1, that for the proportional axial injection slot location x_{IS} = 0.40 L_{IC}, the total number of non-acceptable manufacturing solutions (bolded) is 16 cases for the attached configuration and 8 cases for the detached configuration; in accordance with the table footnote, the unbolded cases satisfy the pressure constraints stated above but the bolded cases do not satisfy the pressure constraints. Similarly from Table 4-2 for the proportional axial injection slot location of x_{IS} = 0.60 L_{IC}, the total number of non-acceptable manufacturing solutions is 8 cases for the attached configuration and 4 cases for the detached configuration. There are more acceptable manufacturing solutions for the proportional axial slot location of x_{IS} = 0.60 L_{IC} than for the x_{IS} = 0.40 L_{IC} location. Also, the general behaviors of the results are the same for both axial proportional locations. Hence, all the discussions are presented for the x_{IS} = 0.60 L_{IC} location with figures given in this chapter; whereas, the figures for the x_{IS} = 0.40 L_{IC} location are not given.

For the attached configuration, the maximum resin pressure is attained at the exit of Region II; whereas, for the detached configuration, the maximum resin pressure is attained inside Region I of the resin injection chamber. Figures 4-1, 4-2 and 4-3 show the resin pressure profiles for the nominal processing parameters (U = 0.0254 m/s, V_{fo} = 0.68, μ = 0.75 Pa.s) for CR = 2.0, 3.0, 4.0; each figure is for a different chamber length (L_T). The chamber wall pressure is an important component for safety considerations; thus only the chamber wall pressure has been shown and discussed throughout this work. Figures 4-1, 4-2 and 4-3 illustrate that the

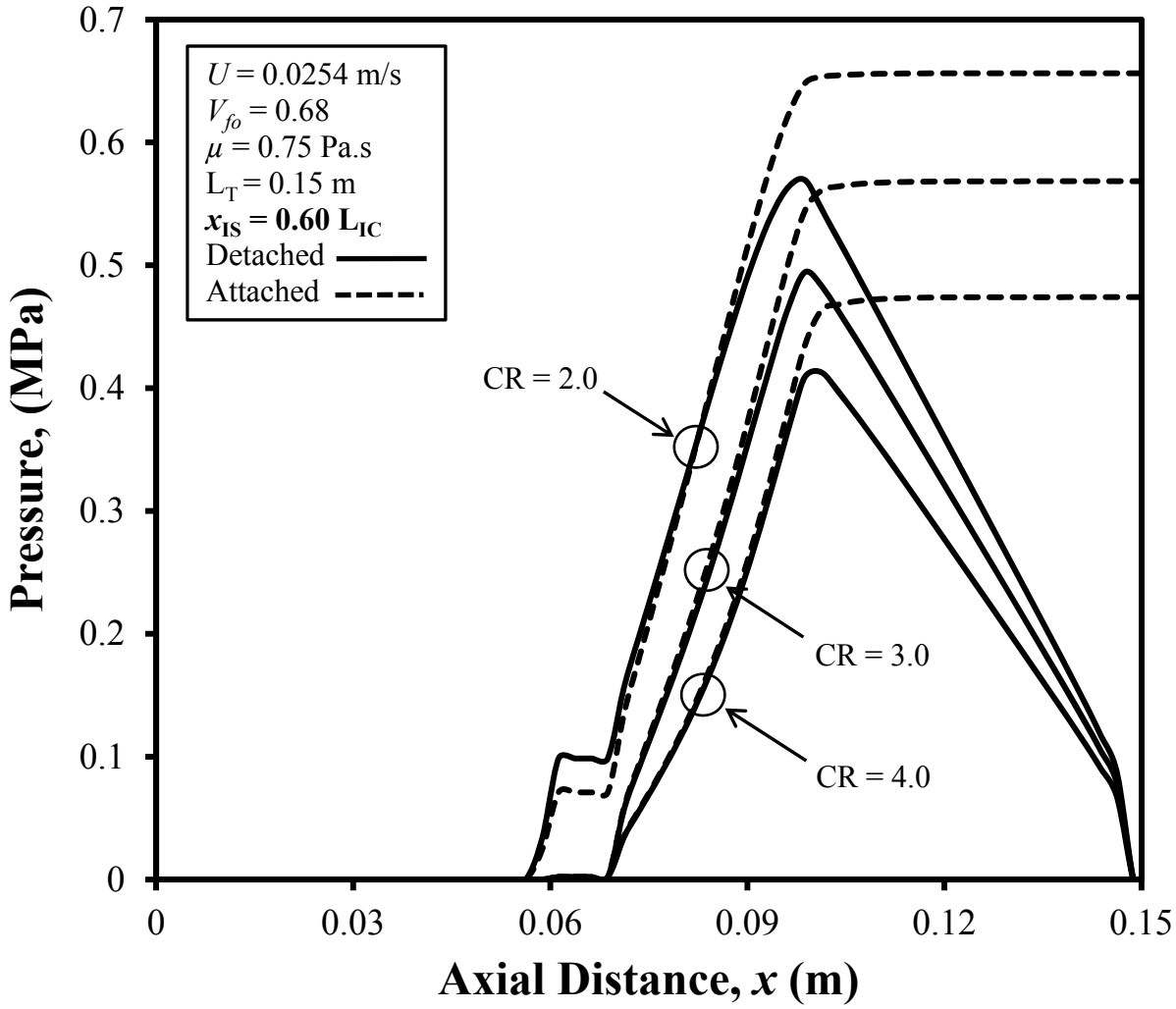

Figure 4-1. Chamber Wall Axial Pressure Profiles for Detached Injection Chamber and Attached Injection Chamber for L_T = 0.15 m for the Nominal Processing Parameters and x_{IS} = 0.60 L_{IC}. (H_D = 0.0635 m, W_D = 0.00318 m)

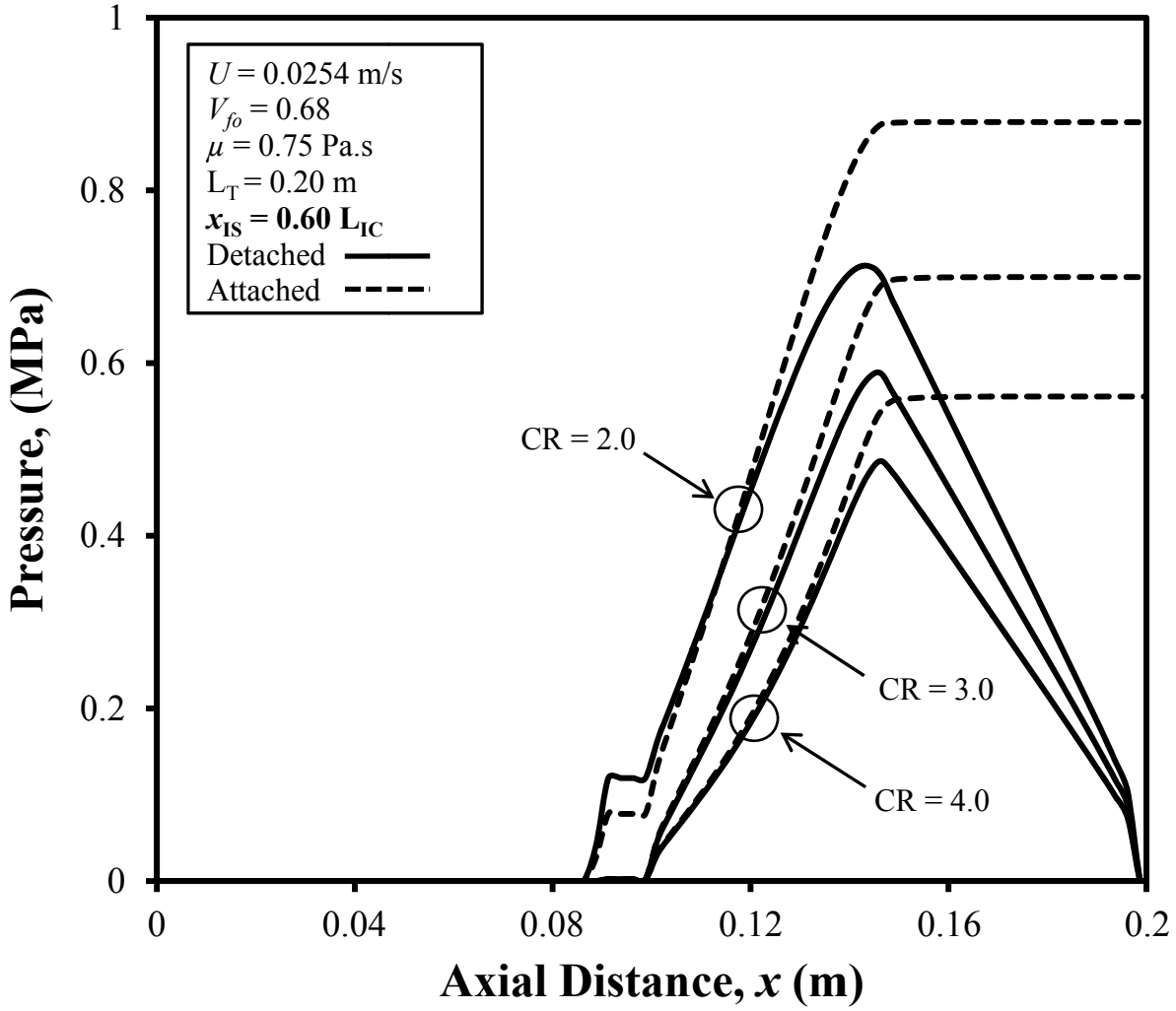

Figure 4-2. Chamber Wall Axial Pressure Profiles for Detached Injection Chamber and Attached Injection Chamber for $L_T = 0.20$ m for the Nominal Processing Parameters and $x_{IS} = 0.60\ L_{IC}$. ($H_D = 0.0635$ m, $W_D = 0.00318$ m)

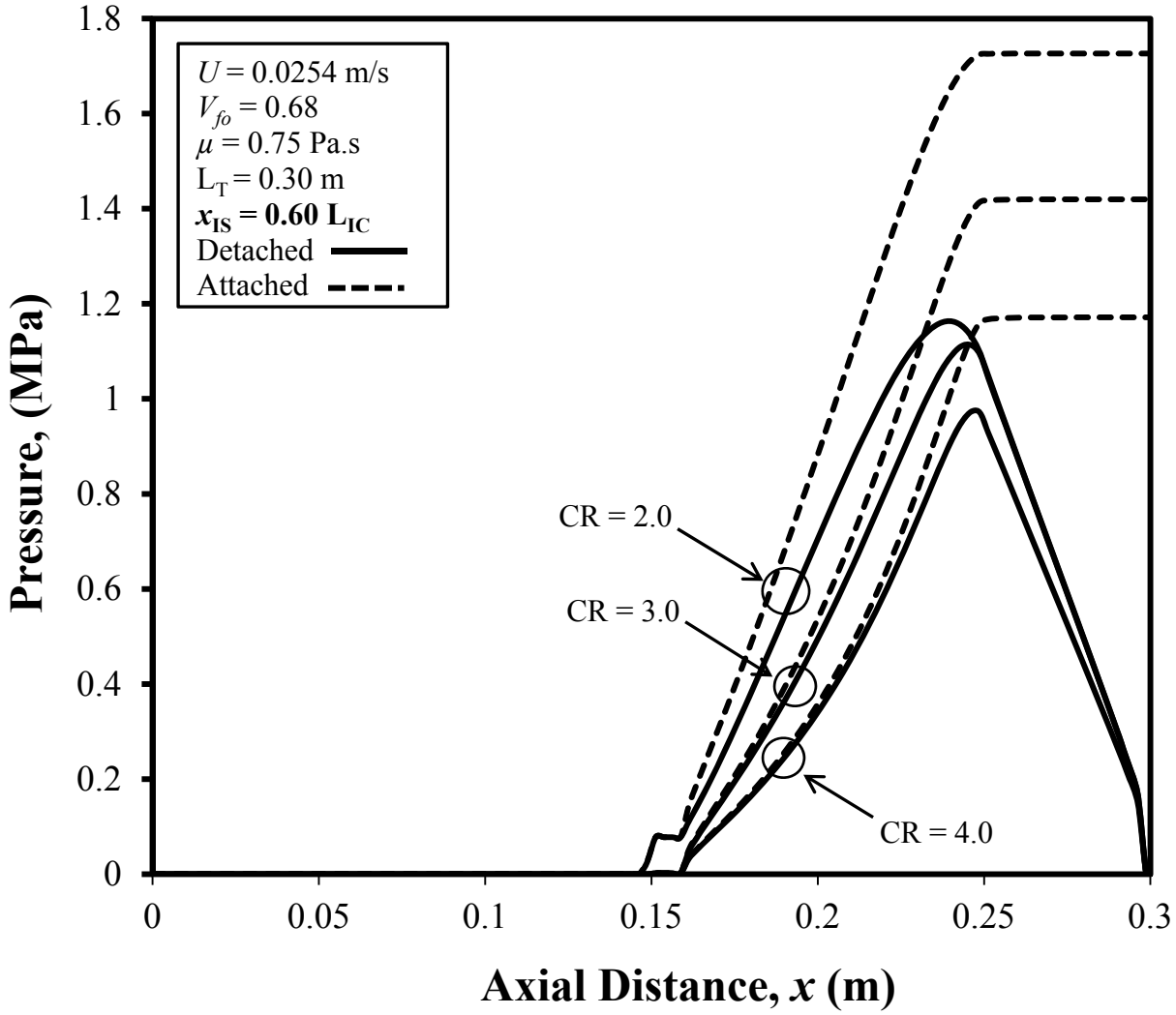

Figure 4-3. Chamber Wall Axial Pressure Profiles for Detached Injection Chamber and Attached Injection Chamber for L_T = 0.30 m for the Nominal Processing Parameters and x_{IS} = 0.60 L_{IC}. (H_D = 0.0635 m, W_D = 0.00318 m).

maximum chamber wall pressure for the detached configuration is always less than the exit pressure for the corresponding attached configuration. For the detached configuration, the injection chamber is separated from the heated pultrusion die (see Figs. 1-2 and 1-3) whereas for the attached configuration the injection chamber is not separated from the entrance to the heated pultrusion die. So the atmospheric pressure boundary condition (Eqs. (3-21h) and (3-21k)) applies to the circumference of the injection chamber exit in the detached configuration and thus there is a resin pressure relief occurring before entering the pultrusion die. Figures 4-1, 4-2 and 4-3 illustrate the pressure profile for the two configurations (attached and detached) and show how the atmospheric pressure boundary condition works in the detached configuration, in comparison to the attached configuration, to yield a lower maximum chamber wall pressure. Hence the maximum chamber wall pressure in the detached configuration is always lower than that in the attached configuration; this shows the detached configuration to be favorable from a safety perspective.

In all the cases for the CR value of 2.0, the minimum injection pressure required for the complete wet out is higher than that required for higher CR values 3.0 and 4.0. This is because the local fiber volume fraction is greater at the injection port location for CR = 2.0 and thus a higher injection pressure is needed to push the resin through the fiber and achieve complete wet out. The injection pressure required for CR values of 3.0 and 4.0 is only slightly greater than atmospheric pressure; for higher CR values (3.0 and 4.0), the larger taper angles (α) result in a lower local fiber volume fraction ($V_f(x)$) than for CR = 2.0. The resistance to the resin flow decreases as the local fiber volume fraction decreases. Hence, for CR values of 3.0 and 4.0, the injection pressure of slightly greater than atmospheric pressure is sufficient for complete fiber

wet out; in other words, essentially pouring the liquid resin into the injection slot will work in the case of CR values of 3.0 or higher.

The maximum resin pressure occurring at the exit of the chamber for the attached configuration or the maximum resin pressure occurring inside the injection chamber for the detached configuration is dependent on: a) the CR value (taper angle, α), b) the injection pressure necessary to achieve complete wet out, and c) the length of the tapered region of the injection chamber over which the compression of the resin takes place. The maximum resin pressure also depends on the axial location at which the resin flow front reaches the centerline. In all the simulation cases, the resin flow front essentially reaches the centerline near the axial location of the injection port; thus this effect is about same for all cases. For the CR values of 3.0 and 4.0, the injection gauge pressure required for the complete wet out is only about 0.002 MPa. Thus for CR values of 3.0 and 4.0, the maximum chamber wall pressure is essentially only a function of the CR value and the injection chamber length (L_T). High maximum chamber wall pressure is always undesirable since as it can damage the injection chamber, and also may cause resin leakage due to the high pressure.

Comparing Figs. 4-1, 4-2, and 4-3 shows that as the length of the injection chamber increases, the maximum chamber wall pressure for the detached configuration and the exit pressure for the attached configuration both increase; this is due to the increased tapered length over which the resin is compressed. The difference (ΔP) between the maximum chamber wall pressure (detached) and the exit pressure (attached) is greater as the injection chamber is made longer. For the CR value of 2.0, the pressure difference between the two configurations is 13 % for the chamber length of 0.15 m (Fig 4-1), 23 % for the chamber length of 0.20 m (Fig. 4-2) and 31 % for the chamber length of 0.30 m (Fig. 4-3). Seen from Fig. 4-1, the maximum pressure for

the detached configuration is decreased by 27 % when CR value is increased from 2.0 (taper angle, $\alpha = 0.607^{\circ}$) to a CR value of 4.0 (taper angle, $\alpha = 1.821^{\circ}$) for the chamber length of 0.15 m; there is nearly the same percentage decrease of the maximum chamber pressure (27.7 %) for the attached configuration. Similarly, for the chamber length of 0.30 m (Fig. 4-3), the maximum chamber pressure decrease for the detached configuration is 18 % and for the attached configuration is 32 % in going from CR = 2.0 to 4.0. This shows that as CR increases, the maximum chamber wall pressure for the detached and attached configurations decreases significantly; thus injection chamber design with higher CR values are desirable. Figures 4-1, 4-2, and 4-3 also demonstrate that as CR increases, the maximum chamber wall pressure difference between the attached and detached configurations decreases.

4.1. Effect of Pull Speed, *U*

Pull speed is an important processing parameter in pultrusion manufacturing to achieve high productivity. For high productivity, high pull speed is always desired without compromising the risk of exceeding the maximum resin injection pressure and maximum resin pressure constraints inside the injection chamber. Thus investigating the effect of the pull speed on minimum resin injection pressure and the associated maximum chamber resin pressure is very important. The simulation cases for the effect of pull speed on the minimum injection pressure to achieve complete wet out and maximum interior chamber pressure are given in Table 4-3. The higher the pull speed, the higher the injection pressure required to achieve complete reinforcement wet out and the higher the corresponding maximum chamber pressure. Higher pull speeds also increase the maximum chamber wall pressure because the resin is more rapidly compressed. For a CR value of 2.0, as the pull speed increases, the injection pressure necessary

Table 4-3. Effect of Pull Speed, *U*, on Minimum Injection Pressure Necessary to Achieve Complete Wet out for Different Processing Parameters for Slot Width = 0.01 m, Part Width = 0.0635 m, Part Thickness = 0.00318 m at a Proportional Slot Location x_{IS} = 0.60 L_{IC}.

Case	CR	***U*** (m/s)	V_{fo}	μ Pa·s	Injection Pressure (Gauge) (MPa)	Total Length $\mathbf{L_T}$ (m)	Location of x_{IS} (m)	Exit Pressure (Gauge) (MPa) (Attached)	Maximum Chamber Pressure (Gauge) (MPa) (Detached)
A1	2.0	0.0203	0.68	0.75	0.057	0.15	0.06	0.525	0.475
A2	2.0	0.0254	0.68	0.75	0.071	0.15	0.06	0.656	0.570
A3	2.0	0.0508	0.68	0.75	0.147	0.15	0.06	1.347	1.150
B1	3.0	0.0203	0.68	0.75	0.002	0.15	0.06	0.454	0.415
B2	3.0	0.0254	0.68	0.75	0.002	0.15	0.06	0.570	0.520
B3	3.0	0.0508	0.68	0.75	0.002	0.15	0.06	1.136	1.040
C1	4.0	0.0203	0.68	0.75	0.002	0.15	0.06	0.380	0.361
C2	4.0	0.0254	0.68	0.75	0.002	0.15	0.06	0.474	0.413
C3	4.0	0.0508	0.68	0.75	0.002	0.15	0.06	0.950	0.904
D1	2.0	0.0203	0.68	0.75	0.057	0.20	0.09	0.677	0.576
D2	2.0	0.0254	0.68	0.75	0.078	0.20	0.09	0.880	0.715
D3	2.0	0.0508	0.68	0.75	0.147	0.20	0.09	1.700	1.375
E1	3.0	0.0203	0.68	0.75	0.002	0.20	0.09	0.560	0.475
E2	3.0	0.0254	0.68	0.75	0.002	0.20	0.09	0.700	0.590
E3	3.0	0.0508	0.68	0.75	0.002	0.20	0.09	1.400	1.190
F1	4.0	0.0203	0.68	0.75	0.002	0.20	0.09	0.450	0.400
F2	4.0	0.0254	0.68	0.75	0.002	0.20	0.09	0.561	0.501
F3	4.0	0.0508	0.68	0.75	0.002	0.20	0.09	1.122	1.000
G1	2.0	0.0203	0.68	0.75	0.064	0.30	0.15	1.380	0.968
G2*	2.0	0.0254	0.68	0.75	0.078	0.30	0.15	**1.727**	1.198
G3*	2.0	0.0508	0.68	0.75	0.133	0.30	0.15	**3.393**	**2.390**
H1	3.0	0.0203	0.68	0.75	0.002	0.30	0.15	1.135	0.890
H2	3.0	0.0254	0.68	0.75	0.002	0.30	0.15	1.420	1.120
H3*	3.0	0.0508	0.68	0.75	0.002	0.30	0.15	**2.840**	**2.230**
I1	4.0	0.0203	0.68	0.75	0.002	0.30	0.15	0.936	0.786
I2	4.0	0.0254	0.68	0.75	0.002	0.30	0.15	1.171	0.984
I3*	4.0	0.0508	0.68	0.75	0.002	0.30	0.15	**2.342**	**1.960**

***** Bold font indicates non-acceptable manufacturing solutions, not satisfying the following criteria: injection pressure ≤ 0.42 MPa (60 psi) and corresponding exit pressure (attached configuration) or maximum wall pressure (detached configuration) ≤ 1.72 MPa (250 psi).

for the complete wet out increases due to the increased sweeping away of the liquid resin at the resin injection slot by the fiber reinforcement. But for CR values of 3.0 and 4.0, the injection pressure necessary for complete wet out has a constant value of about 0.002 MPa (15 psi). This is due to the quite low local fiber volume fraction ($V_f(x)$) at the resin injection slot for these higher CR values which more easily allow the flow of the liquid resin through the fiber reinforcement.

Figures 4-4, 4-5, and 4-6 show the pull speed impact on pressure for CR values of 2.0, 3.0 and 4.0 for chamber lengths of 0.15 m, 0.2 m, and 0.3 m. The injection pressure lines could be discernible only in Fig. 4.4 for CR 2.0 because for the higher CR values the injection pressure values are essentially 0.002 MPa and near zero. The lower horizontal dotted line (0.42 MPa) and the upper horizontal line (1.72 MPa) represent the limits for the acceptable manufacturing solutions for the resin injection pressure and the maximum chamber wall resin pressure respectively. To be an acceptable pultrusion manufacturing solution, both the maximum chamber pressure must be below the 1.72 MPa horizontal line and the minimum injection pressure to achieve complete wet out must be below the 0.42 MPa horizontal line simultaneously. The longer the length of the injection chamber, the higher is the maximum chamber wall pressure. The higher maximum chamber wall pressure is the result of the pressure rise due to the source term in Eq. (3-24h) which occurs as a result of tapering the walls of the injection chamber; the maximum chamber pressure increases as L_T increase due to the longer distance over which the resin is compressed. Because of this, it can be seen in all the Figs. 4-4, 4-5, 4-6 and 4-9 that for the highest pull speed of 0.0508 m/s, the maximum chamber pressure occurs in the non-feasible manufacturing region (1.72 MPa) for large L_T values. As the pull speed increases the maximum chamber pressure also increases due to rapid compressing of the

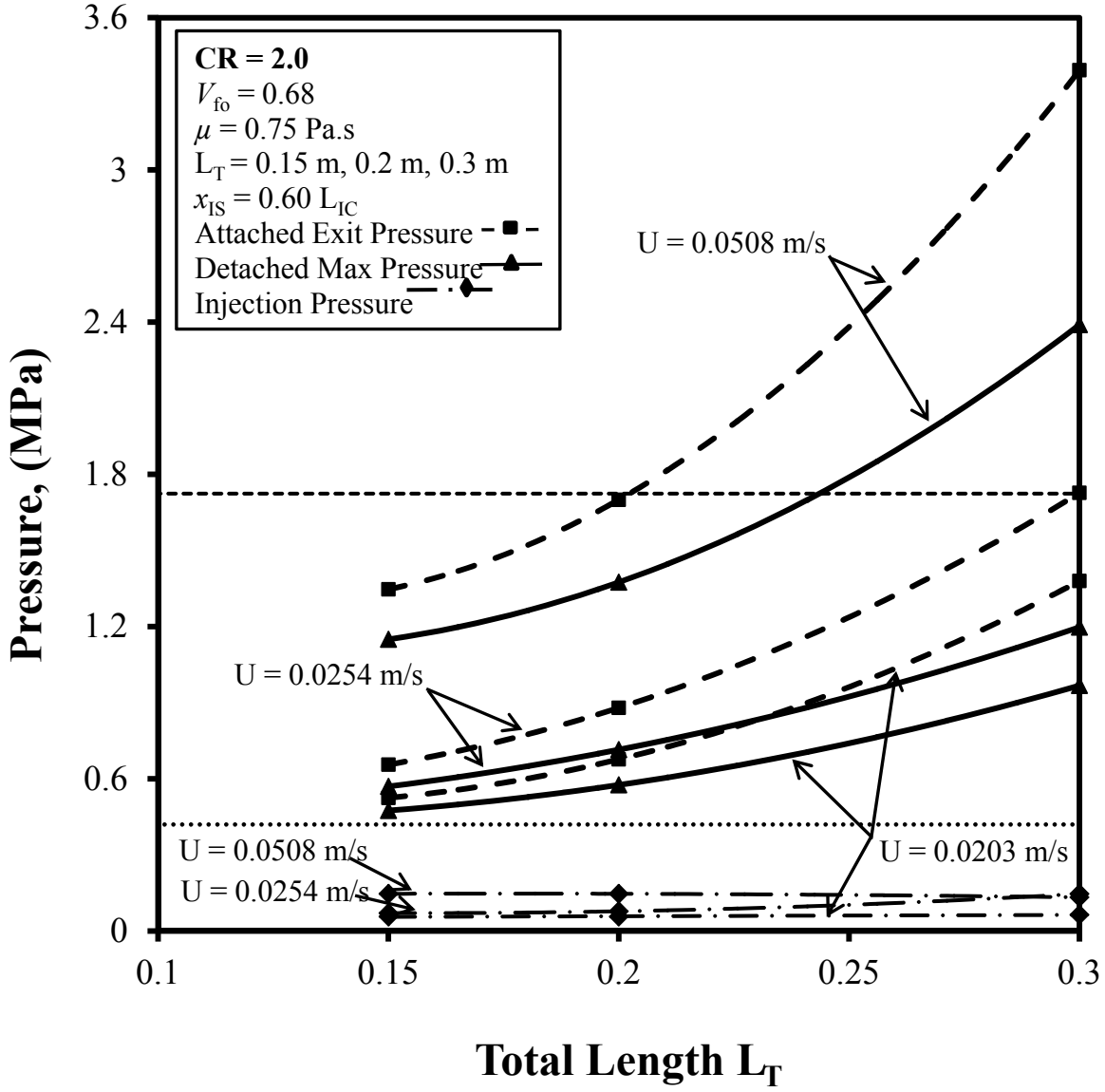

Figure 4-4. Maximum Wall Pressure (———) for Detached Injection Chamber and Exit Wall (Maximum) Pressure (– – –) for Attached Injection Chamber vs. Chamber Length for CR = 2.0 (H_D = 0.0635 m, W_D = 0.00318 m); Minimum Injection Pressure (— · —) to Achieve Complete Wet Out.

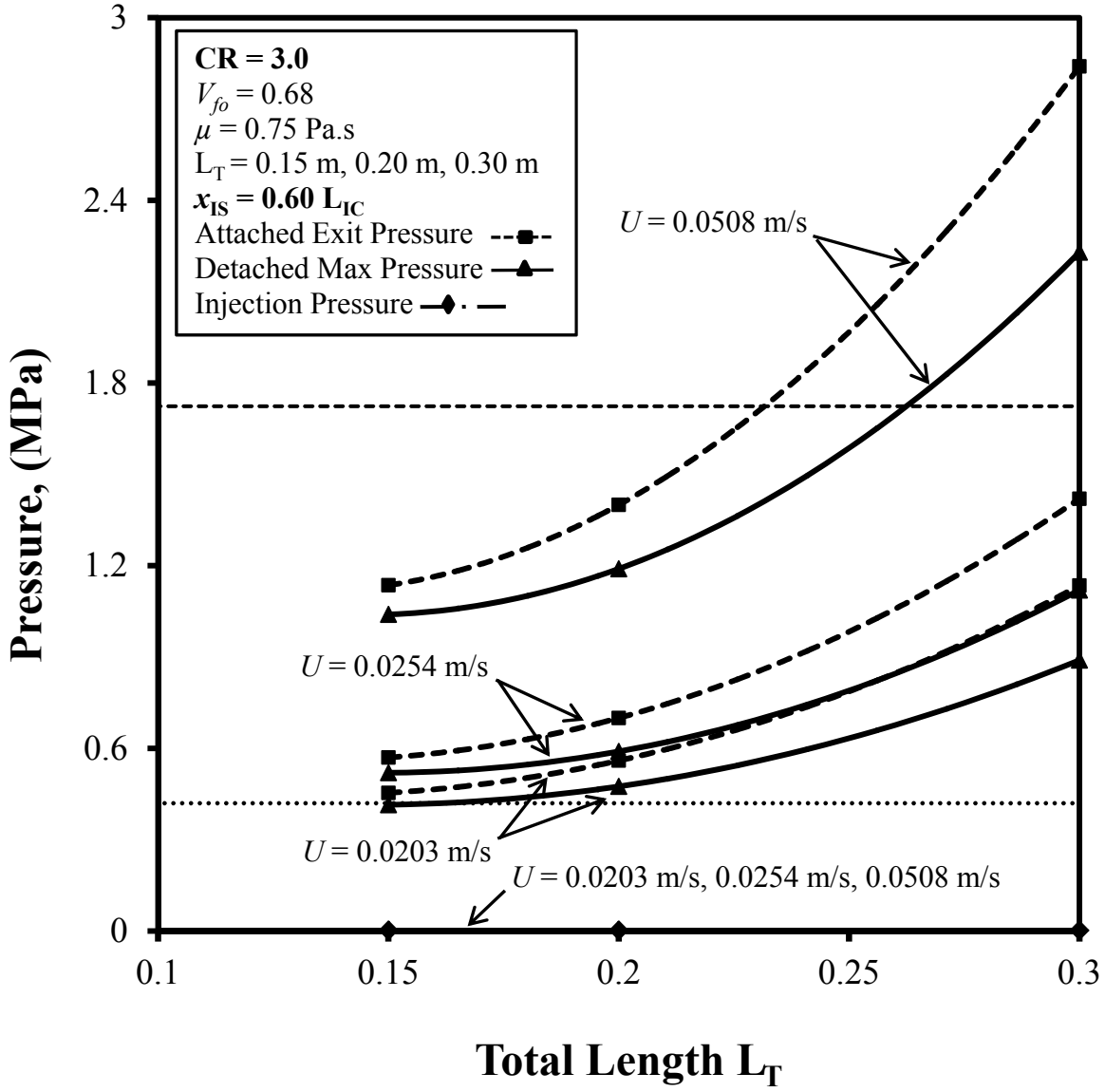

Figure 4-5. Maximum Wall Pressure (———) for Detached Injection Chamber and Exit Wall (Maximum) Pressure (– – –) for Attached Injection Chamber vs. Chamber Length for CR = 3.0, (H_D = 0.0635 m, W_D = 0.00318 m); Minimum Injection Pressure (— · —) to Achieve Complete Wet Out.

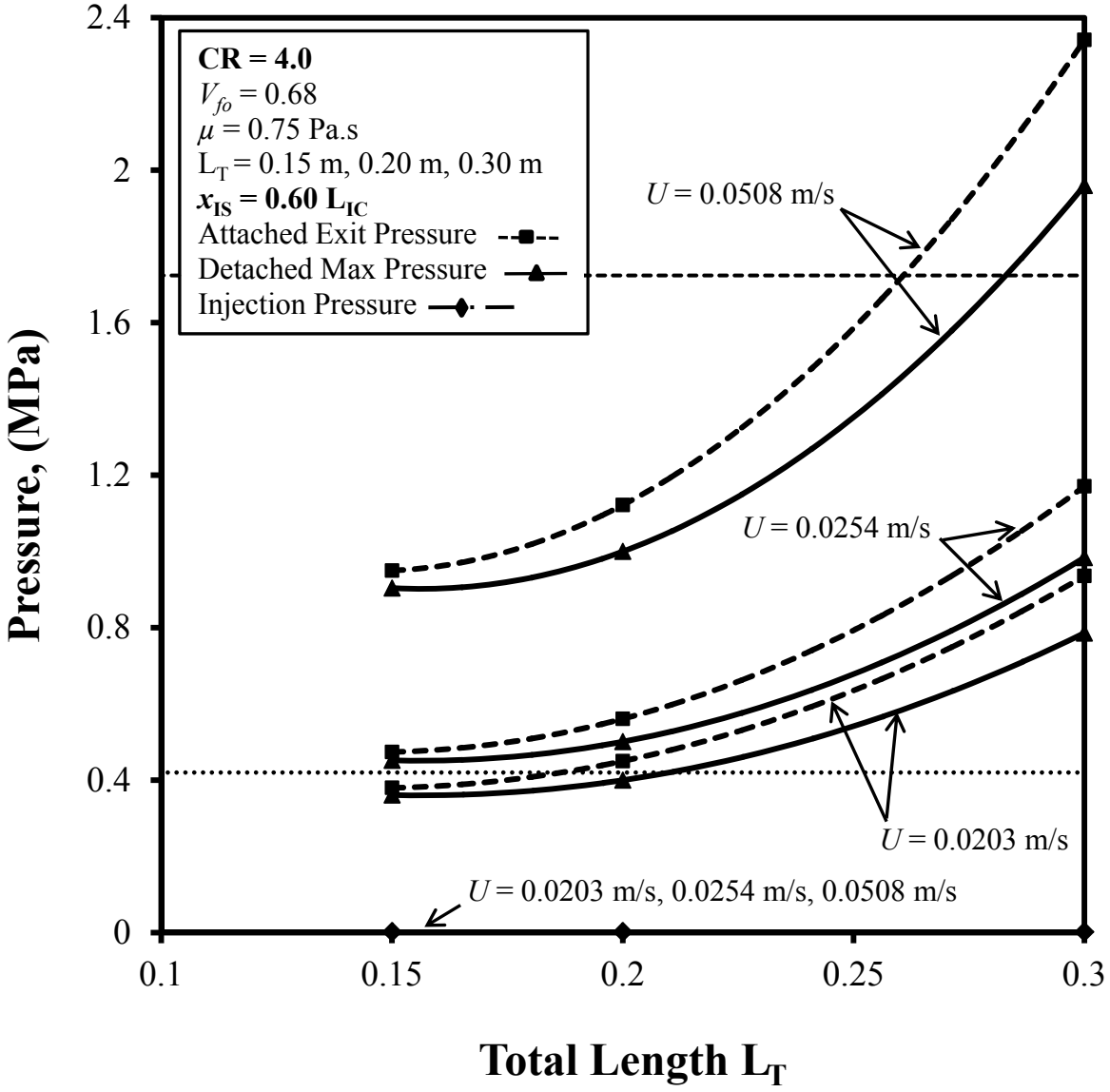

Figure 4-6. Maximum Wall Pressure (——) for Detached Injection Chamber and Exit Wall (Maximum) Pressure (– – –) for Attached Injection Chamber vs. Chamber Length for CR = 4.0, (H_D = 0.0635 m, W_D = 0.00318 m); Minimum Injection Pressure (— · —) to Achieve Complete Wet Out.

liquid resin by the rapid increasing of the local fiber volume fraction along the chamber length. Comparison of the maximum chamber pressure between the attached configuration and detached configuration is illustrated in Figs. 4-4, 4-5, and 4-6. It can be observed that the maximum chamber pressure is always lower for the detached configuration and for the lower pull speed; the maximum chamber pressure difference between the two configurations (attached versus detached) increases as the pull speed increases.

Figures 4-7, 4-8, and 4-9 demonstrate the minimum injection pressure to achieve complete wet out and the corresponding maximum chamber pressure variations for different CR values at specific pull speeds of U = 0.0203 m/s, 0.0254 m/s and 0.0508 m/s respectively. As the CR value increases the maximum chamber pressure also decreases due to the larger taper angle (α) in the source term in Eq. (3-24h). All the attached configuration curves and detached configuration curves show the same qualitative behavior as in Figs. 4-4, 4-5, and 4-6, but the detached configuration curves have greater curvature due to the higher rise in maximum chamber pressure as the injection chamber length increases. For the highest pull speed of 0.0508 m/s (Fig. 4-9), the most favorable combination for the chamber wall pressure is the detached configuration with a CR value of 4.0 and an injection chamber length of 0.15 m.

Figure 4-10 shows the resin flow front profile through the fiber reinforcement for the most favorable case with an injection chamber length of 0.15 m and CR = 4 for the highest pull speed of 0.0508 m/s considered and other nominal processing parameters (V_{fo} = 0.68 and μ = 0.75 Pa·s). The white portion inside the injection chamber is dry fiber and the shaded region is the resin and fiber mixture. The thick dark line corresponds to the flow front of the resin/fiber system and the thin lines show the isopressure contours labeled with pressure values in KPa. The resin flow front and the pressure values for the attached die configuration and the detached die

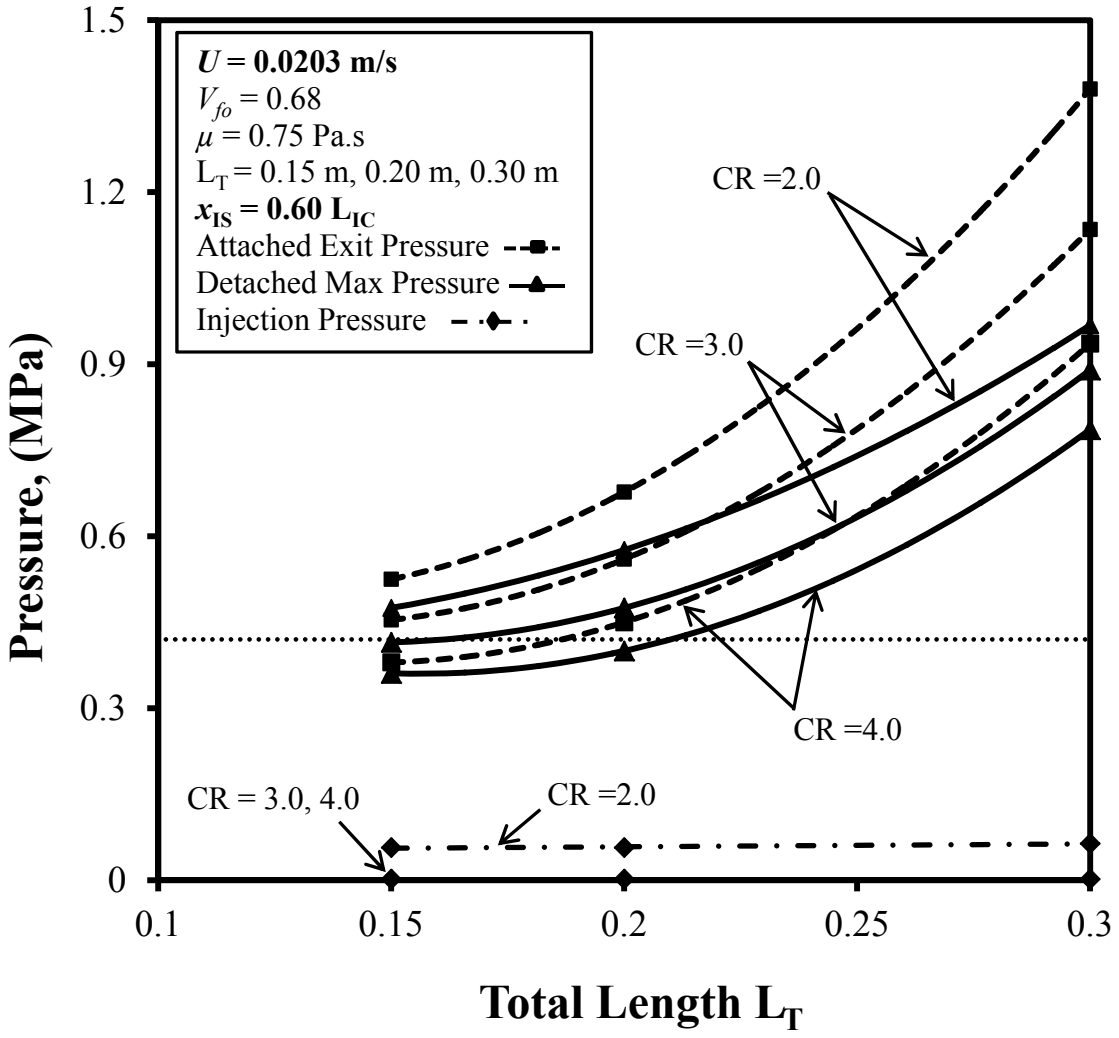

Figure 4-7. Maximum Wall Pressure (——) for Detached Injection Chamber and Exit Wall (Maximum) Pressure (- - -) for Attached Injection Chamber vs. Chamber Length for Various CR, (H_D = 0.0635 m, W_D = 0.00318 m); Minimum Injection Pressure (— · —) to Achieve Complete Wet Out.

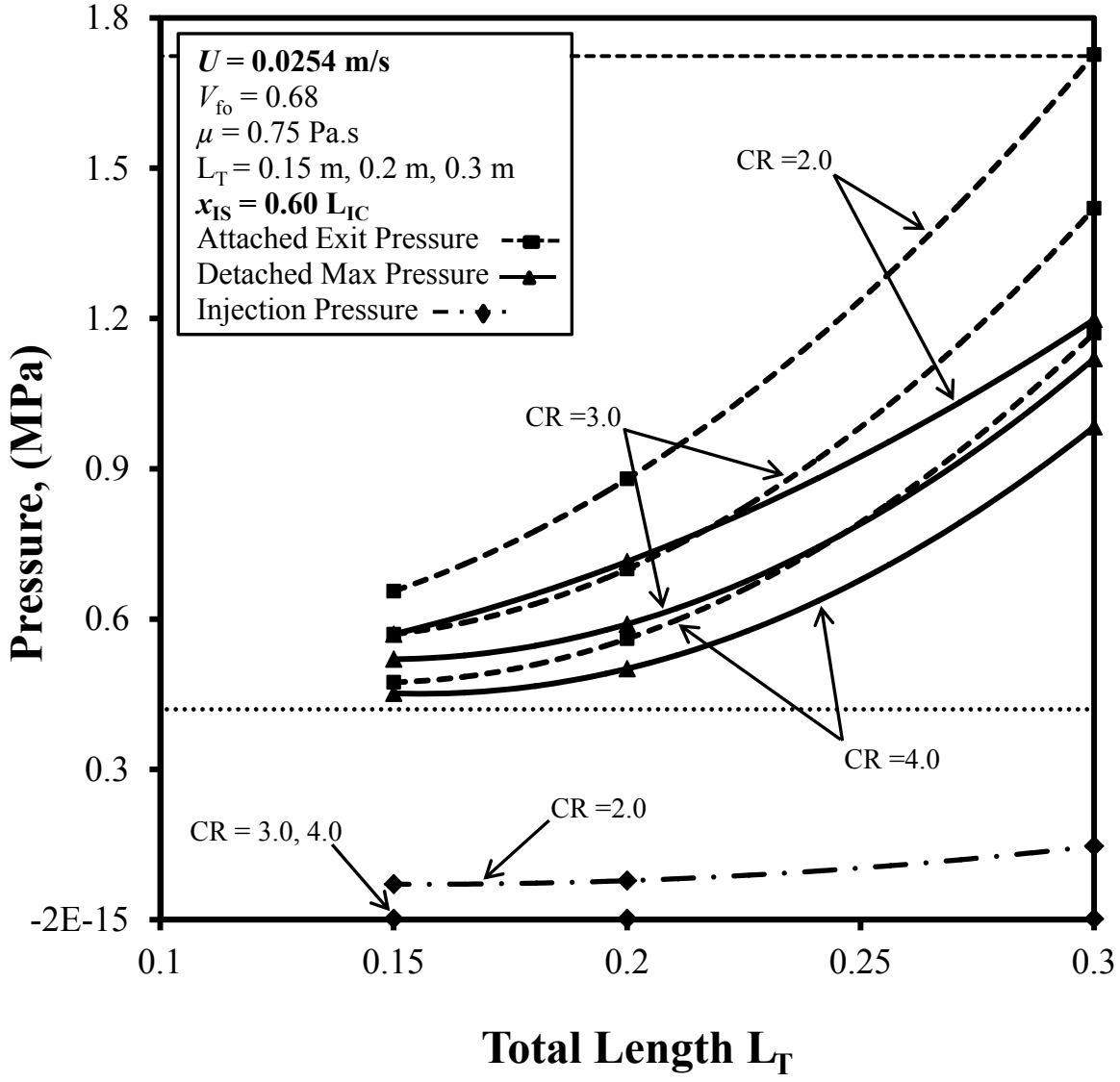

Figure 4-8. Maximum Wall Pressure (——) for Detached Injection Chamber and Exit Wall (Maximum) Pressure (– – –) for Attached Injection Chamber vs. Chamber Length for Various CR, (H_D = 0.0635 m, W_D = 0.00318 m); Minimum Injection Pressure (— · —) to Achieve Complete Wet Out.

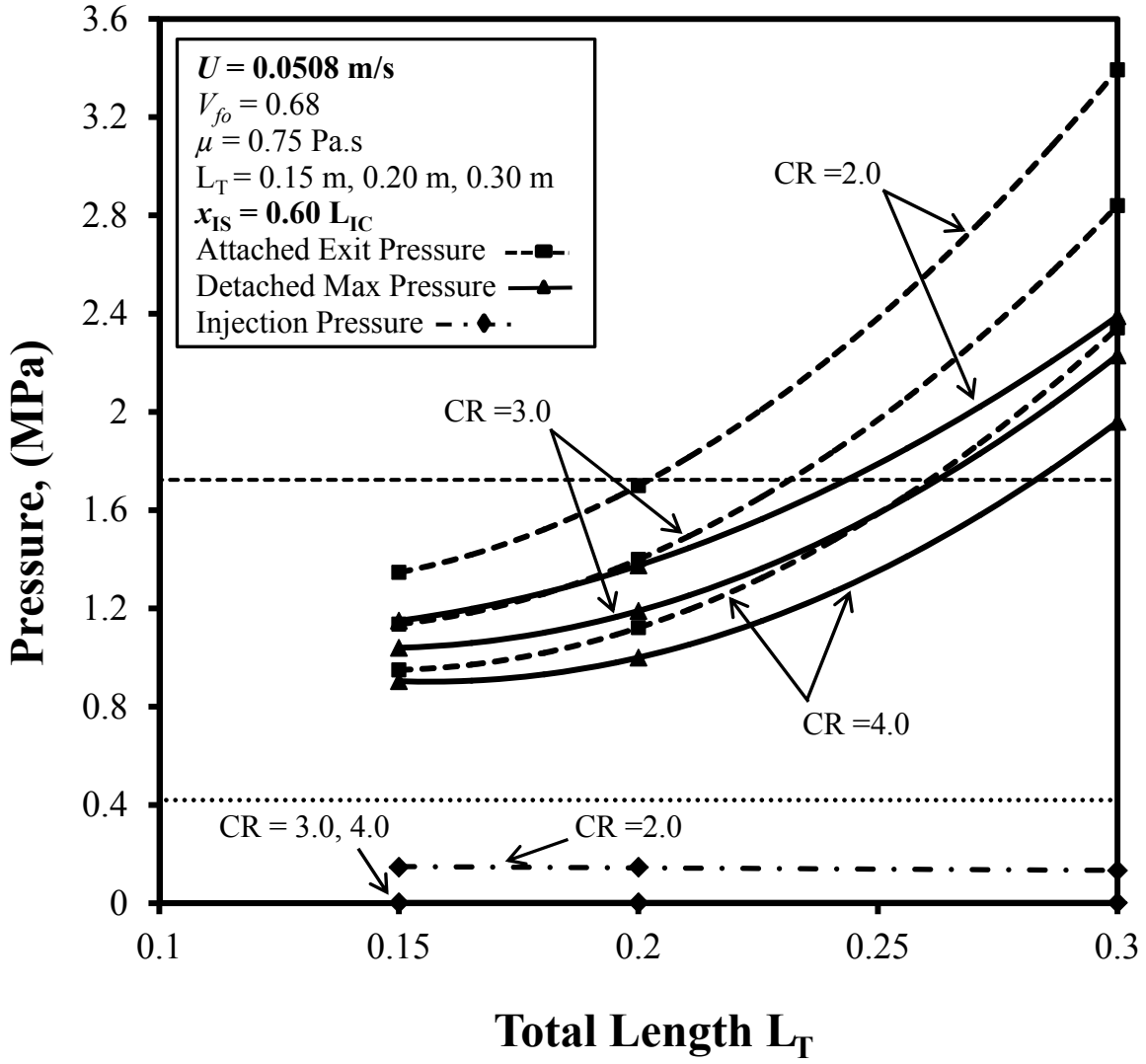

Figure 4-9. Maximum Wall Pressure (——) for Detached Injection Chamber and Exit Wall (Maximum) Pressure (– – –) for Attached Injection Chamber vs. Chamber Length for Various CR, (H_D = 0.0635 m, W_D = 0.00318 m); Minimum Injection Pressure (— · —) to Achieve Complete Wet Out.

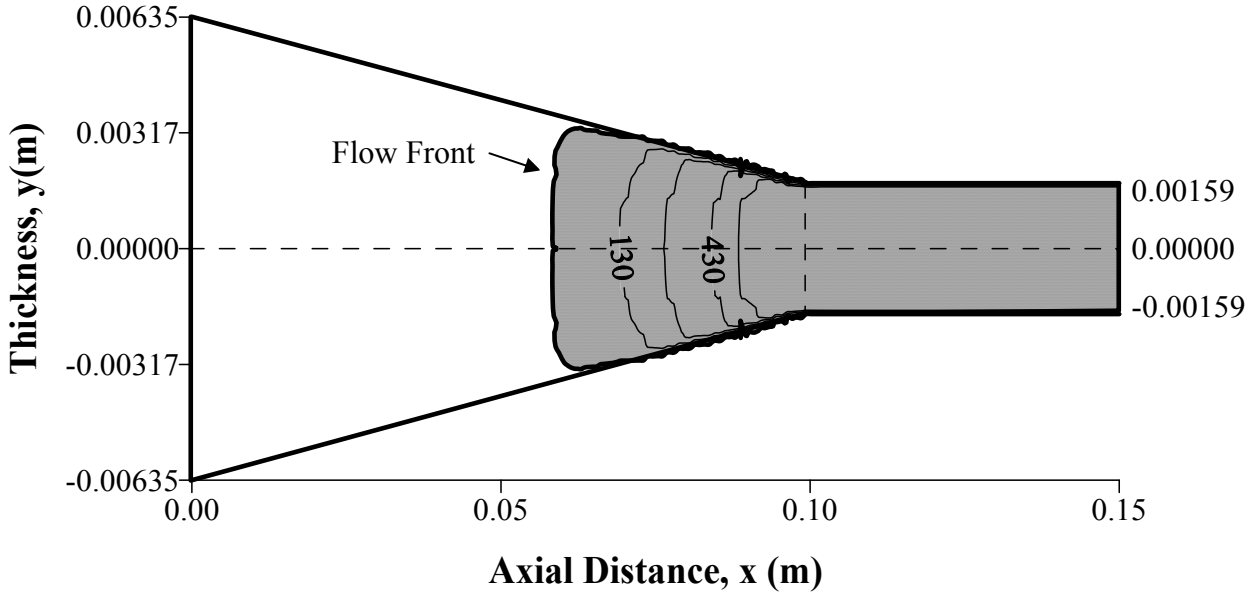

a. Attached Die Configuration

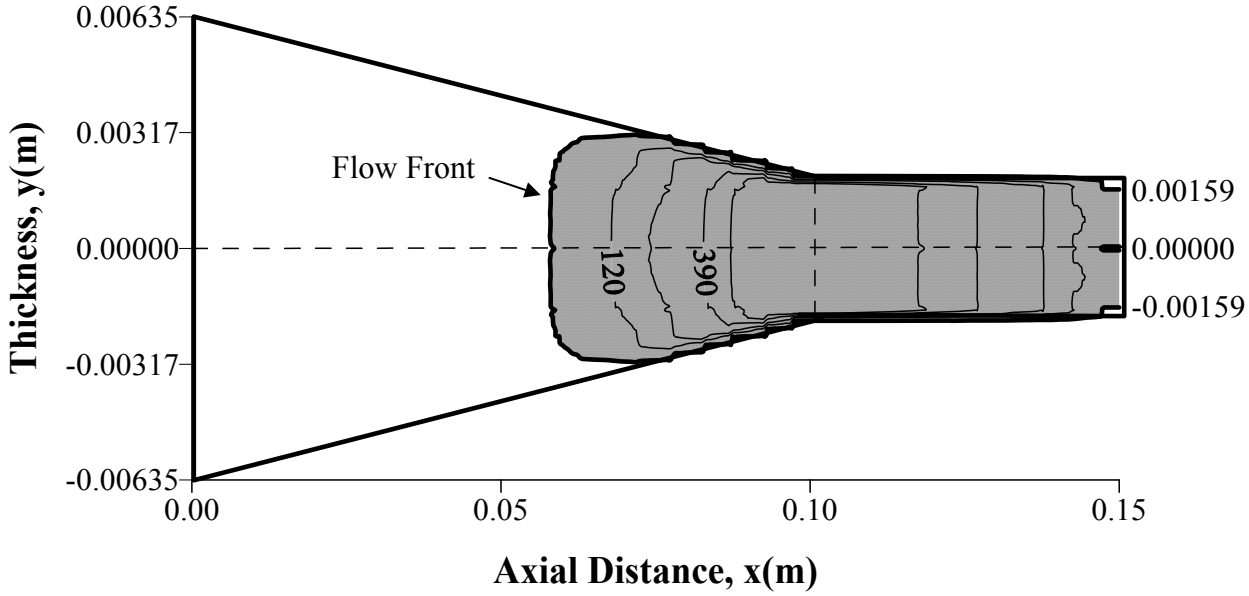

b. Detached Die Configuration

Figure 4-10. Flow Front Profile and Gauge Isopressure (KPa) Contours for Case C3, Table 4-3 with U = 0.0508 m/s for Polyster Resin/Glass Roving, L_T = 0.15 m, CR = 4.0, V_{fo} = 0.68 and μ = 0.75, x_{IS} = 0.60 L_{IC}. (Not to Scale)

configuration can be compared in these two figures. The chamber pressure values are always lower in the detached die configuration system compared to the attached die configuration as can be seen in Fig. 4-10. In the detached die configuration, the isopressure contours can be seen in Region II of the injection chamber due to the decreasing chamber pressure in the Region II and these pressure contours correspond to the same pressure contours as depicted in the Region I of the injection chamber. The plots in the Fig. 4-10 are made out of scale to make it more viewable to the readers.

Figures 4-11, 4-12 and 4-13 depict the chamber wall pressure profile along the interior length of the injection chamber of 0.15 m but for CR values of 2.0, 3.0, and 4.0 respectively. It can be seen that for the CR value of 2.0 (Fig. 4-11), the chamber wall pressure rises to the injection port pressure, decreases slightly after the injection port and then increases to reach the maximum value. But for the higher CR values of 3.0 (Fig. 4-12) and 4.0 (Fig. 4-13), the injection pressure is 0.002 MPa, thus the chamber pressure appears to start near 0 MPa even though it is actually 0.002 MPa, then increases to reach a maximum value. These figures show the chamber wall pressure profile progression inside the injection chamber for both the attached and detached configurations and thus these figures illustrate the difference in the pressure profile development for these two (attached versus detached) configurations. The behavior for $L_T = 0.20$ m (Figs. 4-14, 4-15, 4-16) and 0.30 m (Figs. 4-17, 4-18, 4-19) is very similar to that described above for $L_T = 0.15$ m. Figures 4-13, 4-14 and 4-15 show similar pressure profiles but for an injection chamber length of 0.20 m, and likewise Figs. 4-17, 4-18 and 4-19 depict the pressure profiles for an injection chamber length of 0.30 m.

Figures 4-20, 4-21, and 4-22 demonstrate the pressure profiles in the detached configuration for all the chamber lengths considered for pull speeds of 0.0203 m/s, 0.0254 m/s,

and 0.0508 m/s respectively. These figures illustrate the broad spectrum of pressure profiles for the detached configuration for different CR values depicting how the pressure increases and then decreases back to the atmospheric pressure at the injection chamber exit. For lower pull speed, it is easier to control the process and achieve complete wet out and the corresponding maximum chamber pressure is also low. Among these figures, for the pull speed of 0.0203 m/s, the chamber length of 0.15 m and CR value of 4.0 has the lowest maximum chamber wall pressures. From Fig. 4-22 (Case C3 of Table 4-3), for the pull speed of 0.0508 m/s, the lowest acceptable maximum chamber pressure is 0.904 MPa for chamber length of 0.15 m and CR value of 4.0. Thus, when higher pull speed is desired (0.0508 m/s in this work), a short chamber length of 0.15 m and high CR value of 4.0 is required to have an acceptable pultrusion manufacturing solution which satisfies the pressure constraints on both injection pressures and maximum interior injection chamber pressure. Lower maximum chamber pressures are obtained using the detached configuration; hence, as a result the detached configuration is a better choice for pultrusion manufacturing than the attached configuration.

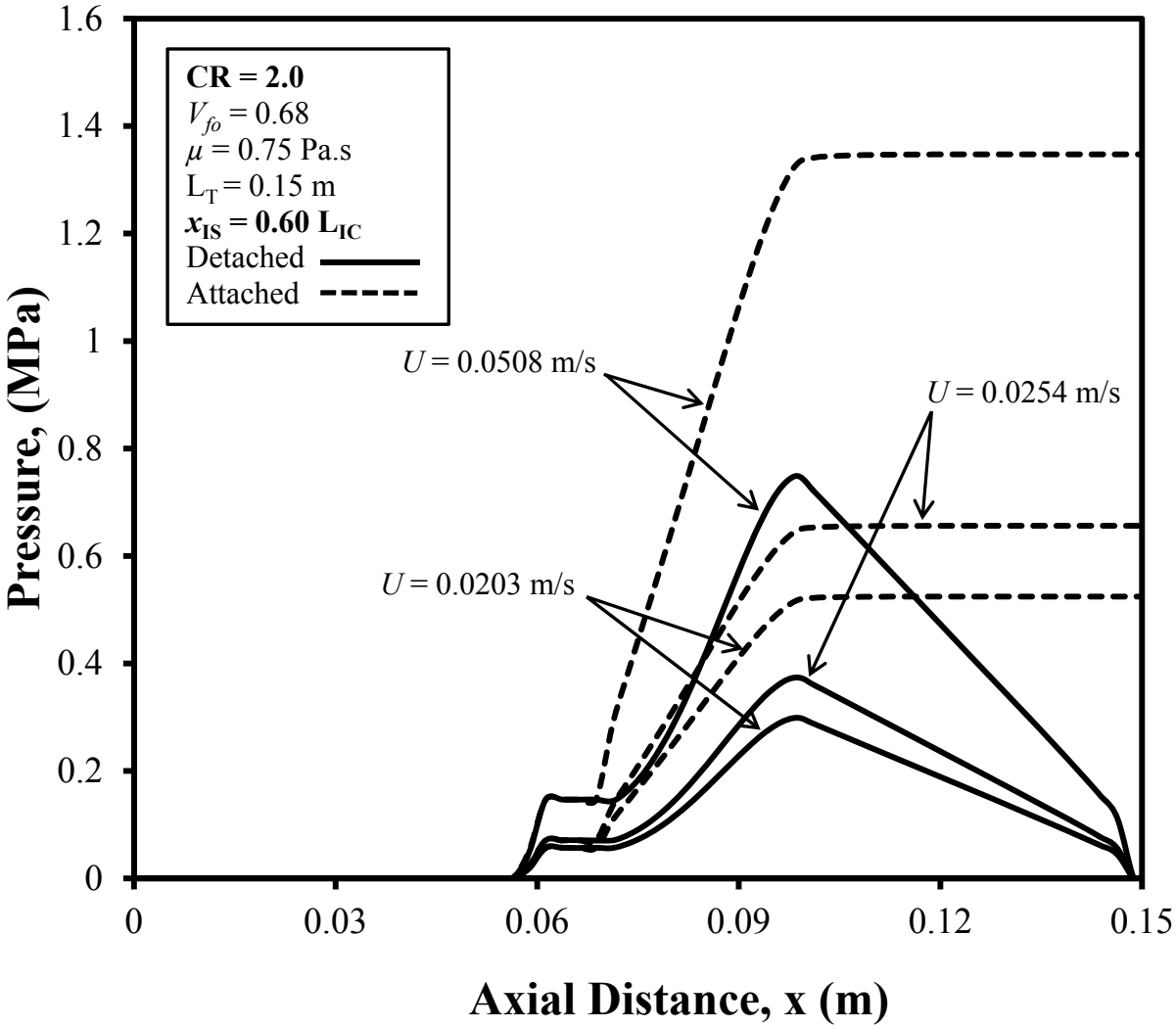

Figure 4-11. Chamber Wall Axial Pressure Profiles for Detached Injection Chamber and Attached Injection Chamber for Chamber Length of 0.15 m for CR = 2.0, (H_D = 0.0635 m, W_D = 0.00318 m).

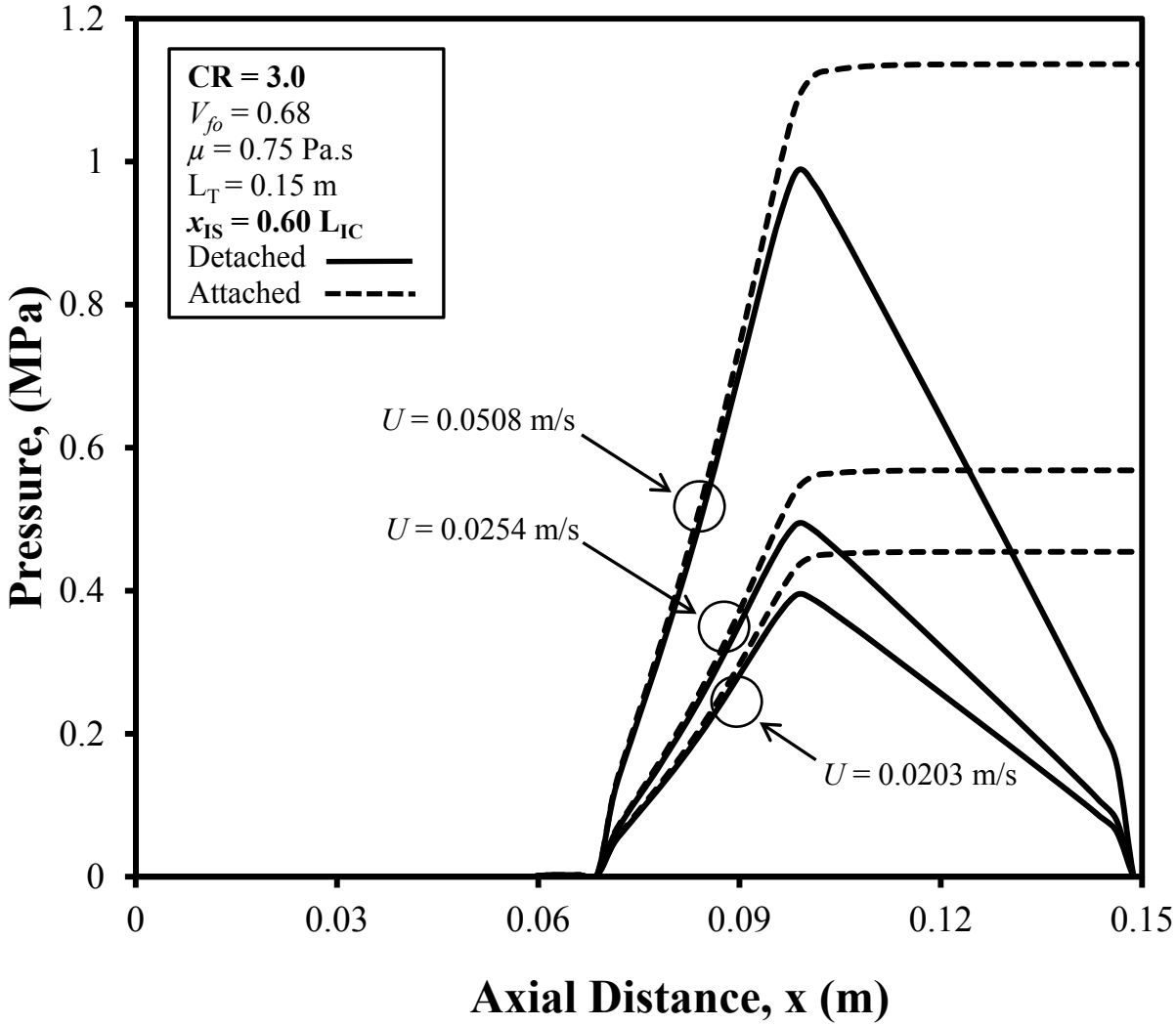

Figure 4-12. Chamber Wall Axial Pressure Profiles for Detached Injection Chamber and Attached Injection Chamber for Chamber Length of 0.15 m for CR = 3.0, (H_D = 0.0635 m, W_D = 0.00318 m).

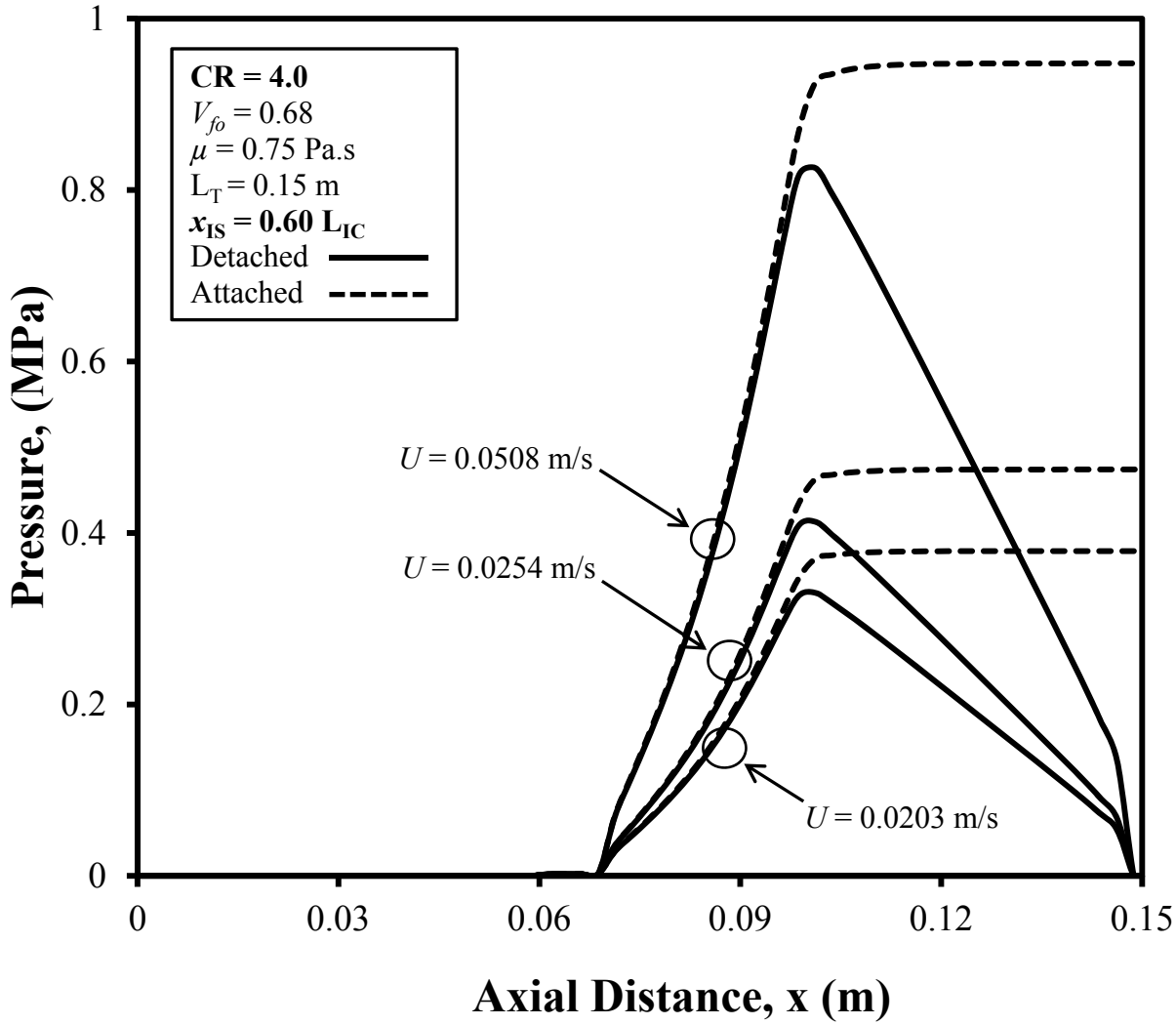

Figure 4-13. Chamber Wall Axial Pressure Profiles for Detached Injection Chamber and Attached Injection Chamber for Chamber Length of 0.15 m for CR = 4.0, (H_D = 0.0635 m, W_D = 0.00318 m).

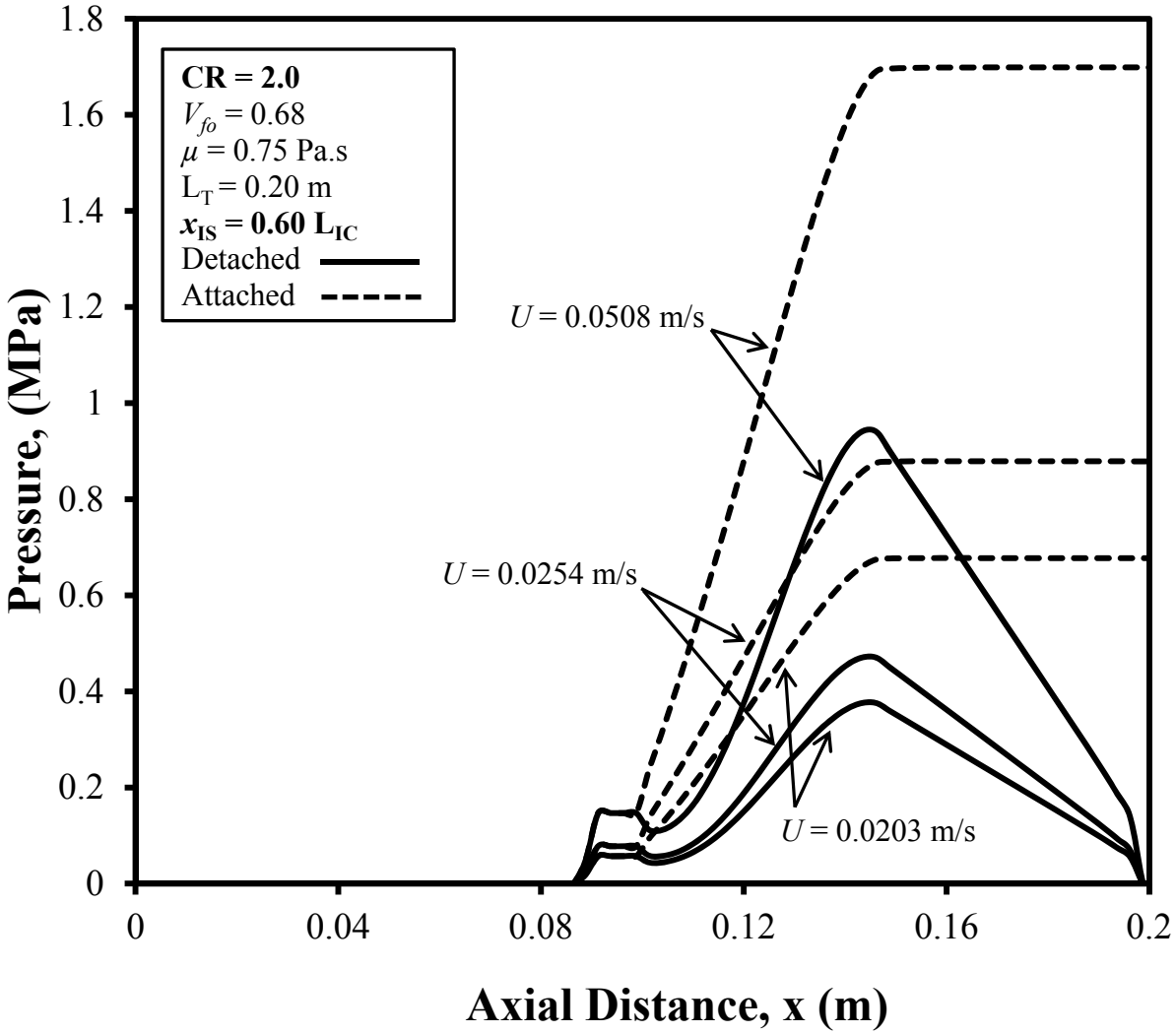

Figure 4-14. Chamber Wall Axial Pressure Profiles for Detached Injection Chamber and Attached Injection Chamber for Chamber Length of 0.20 m for CR = 2.0, (H_D = 0.0635 m, W_D = 0.00318 m).

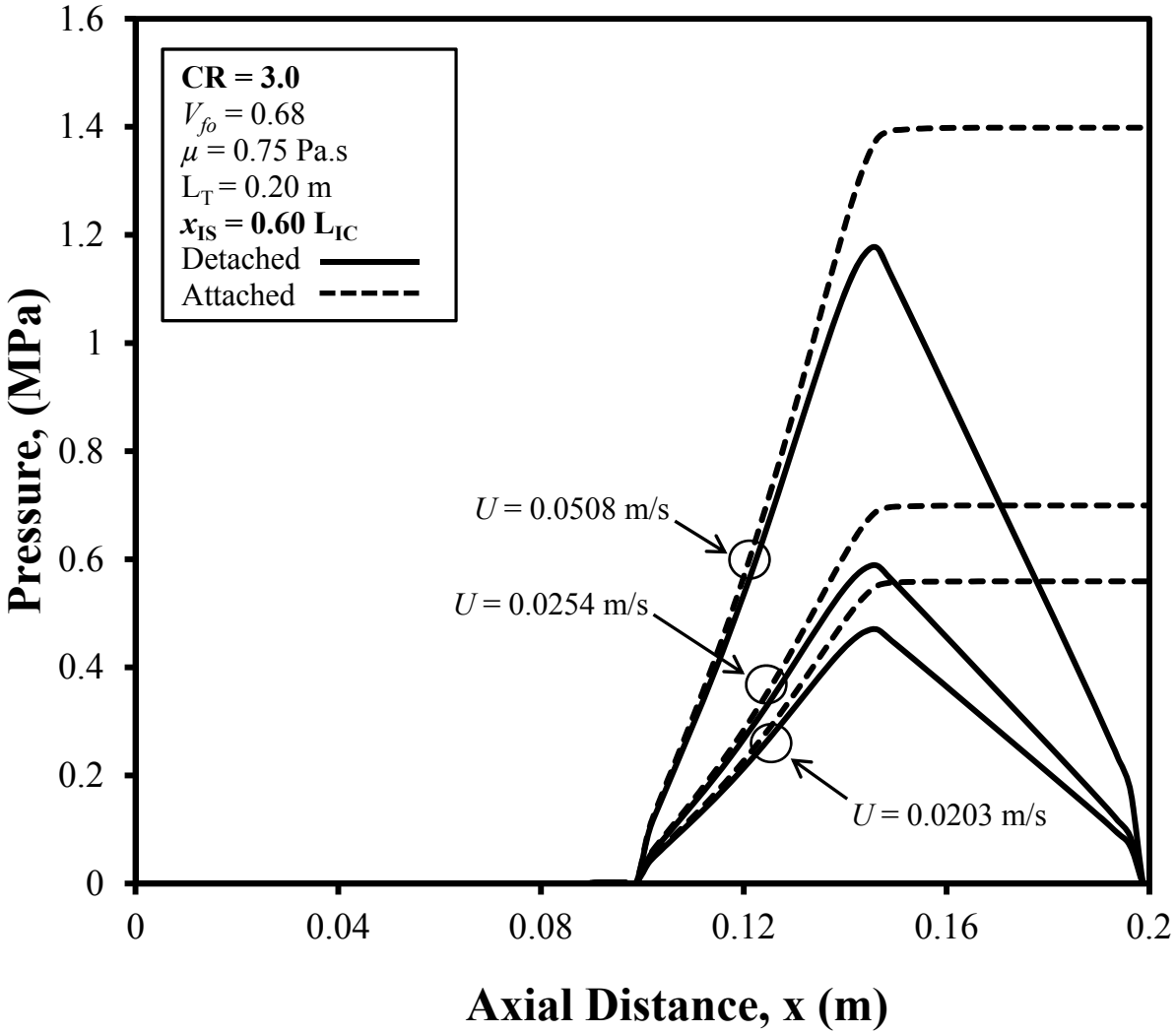

Figure 4-15. Chamber Wall Axial Pressure Profiles for Detached Injection Chamber and Attached Injection Chamber for Chamber Length of 0.20 m for CR = 3.0, (H_D = 0.0635 m, W_D = 0.00318 m).

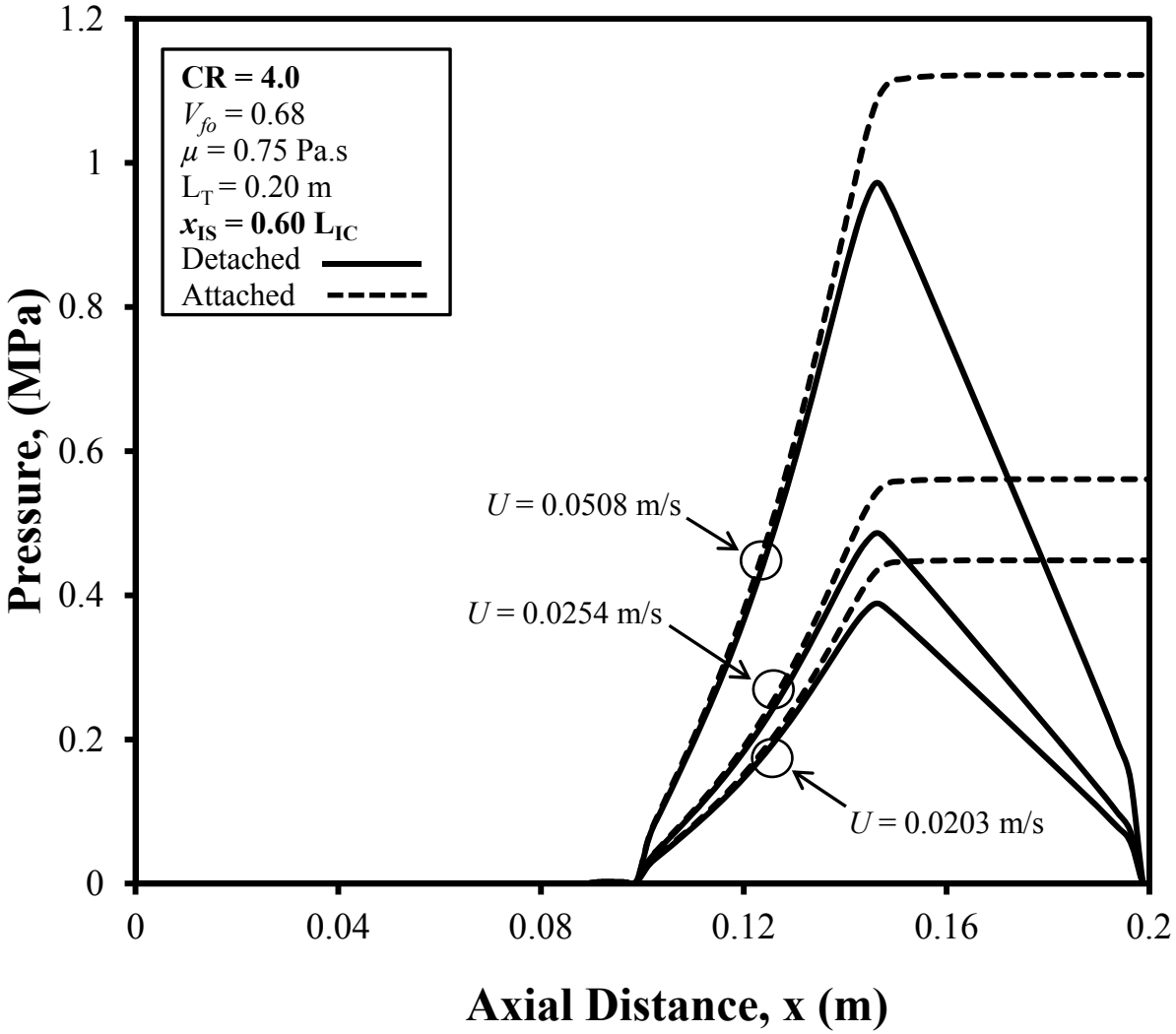

Figure 4-16. Chamber Wall Axial Pressure Profiles for Detached Injection Chamber and Attached Injection Chamber for Chamber Length of 0.20 m for CR = 4.0, (H_D = 0.0635 m, W_D = 0.00318 m).

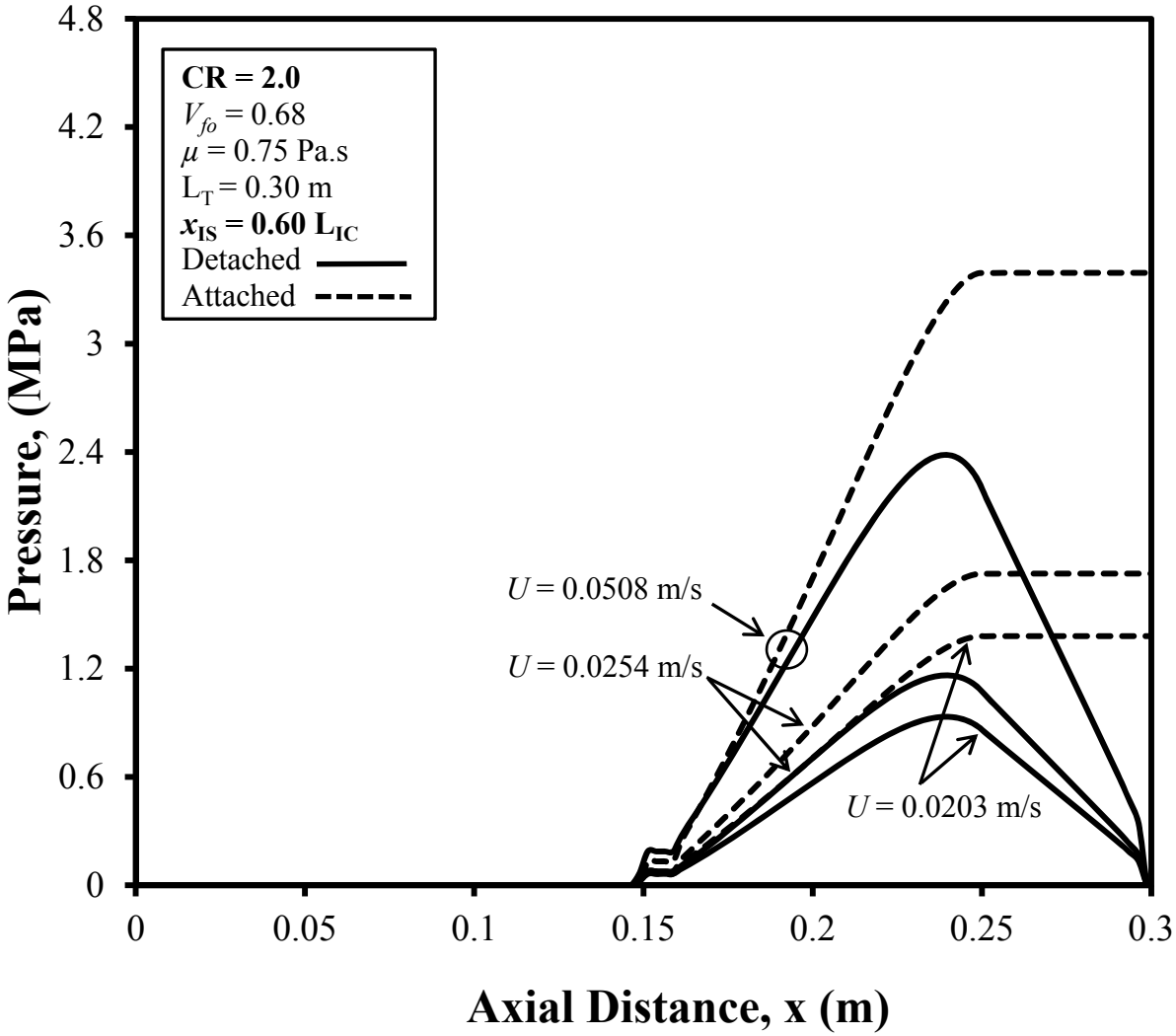

Figure 4-17. Chamber Wall Axial Pressure Profiles for Detached Injection Chamber and Attached Injection Chamber for Chamber Length of 0.30 m for CR = 2.0, (H_D = 0.0635 m, W_D = 0.00318 m).

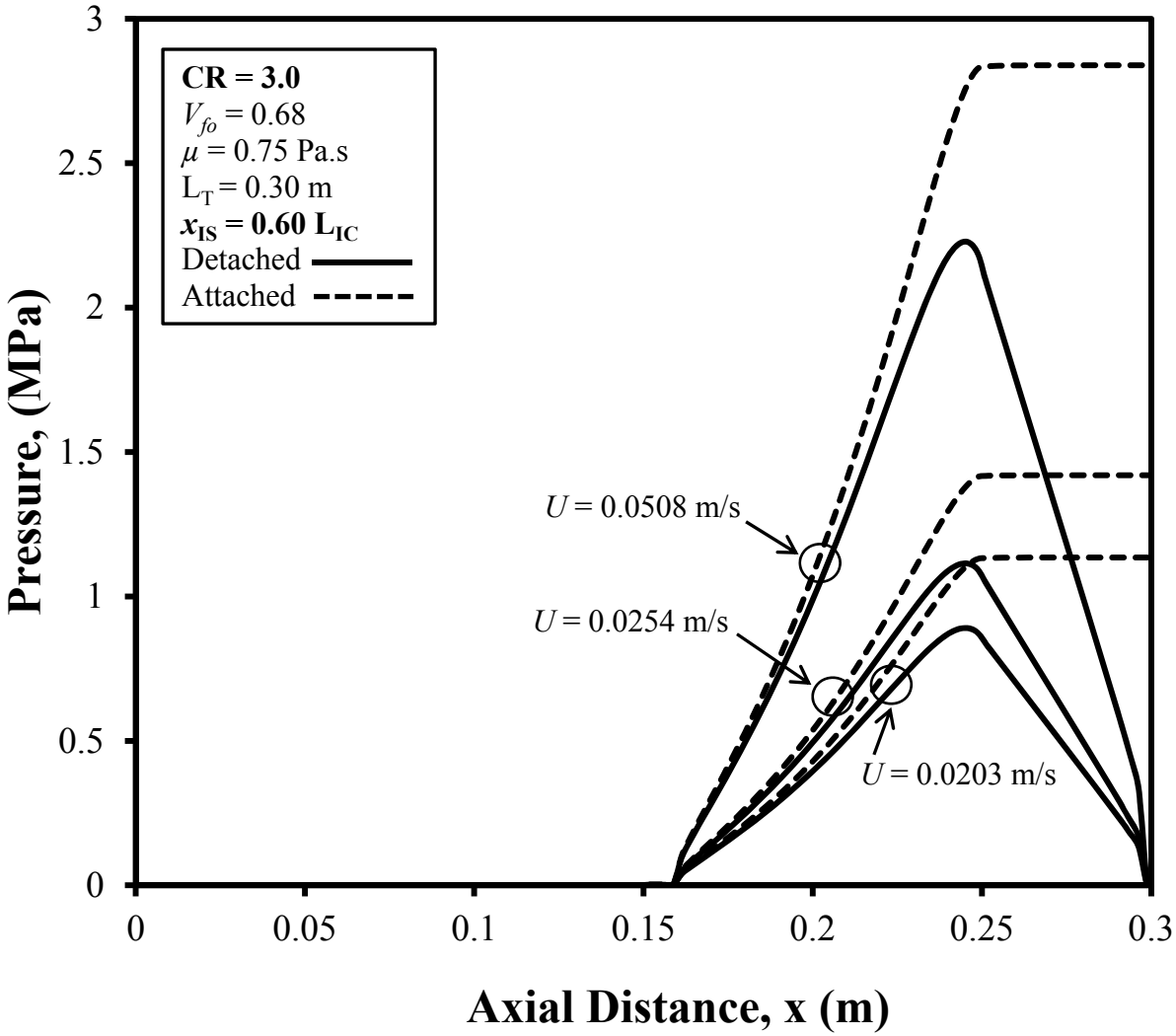

Figure 4-18. Chamber Wall Axial Pressure Profiles for Detached Injection Chamber and Attached Injection Chamber for Chamber Length of 0.30 m for CR = 3.0, (H_D = 0.0635 m, W_D = 0.00318 m).

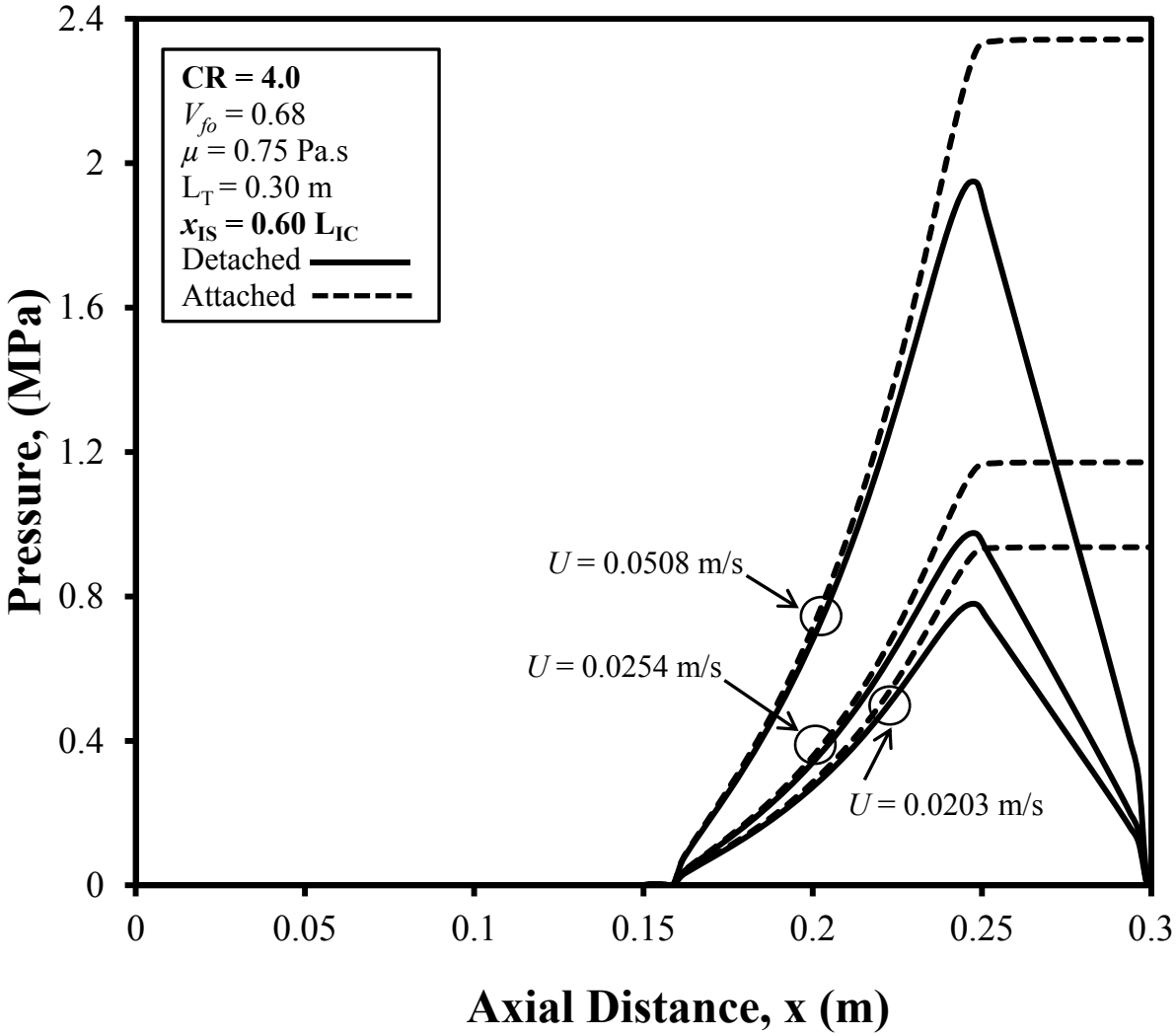

Figure 4-19. Chamber Wall Axial Pressure Profiles for Detached Injection Chamber and Attached Injection Chamber for Chamber Length of 0.30 m for CR = 4.0, (H_D = 0.0635 m, W_D = 0.00318 m).

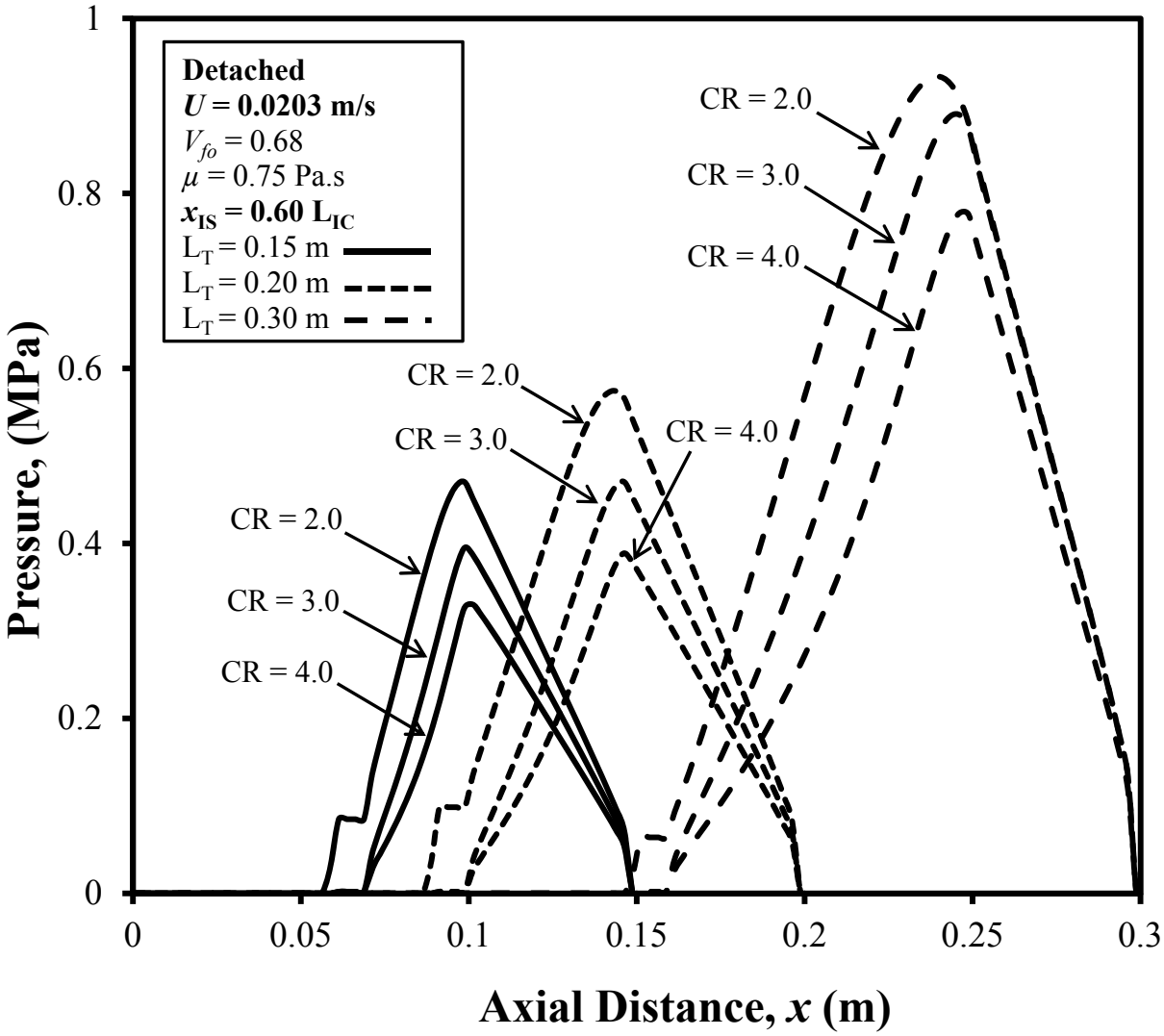

Figure 4-20. Chamber Wall Axial Pressure Profiles of Detached Injection Chamber for different Chamber Lengths of 0.15 m, 0.20 m and 0.30 m for U = 0.0203 m/s, (H_D = 0.0635 m, W_D = 0.00318 m).

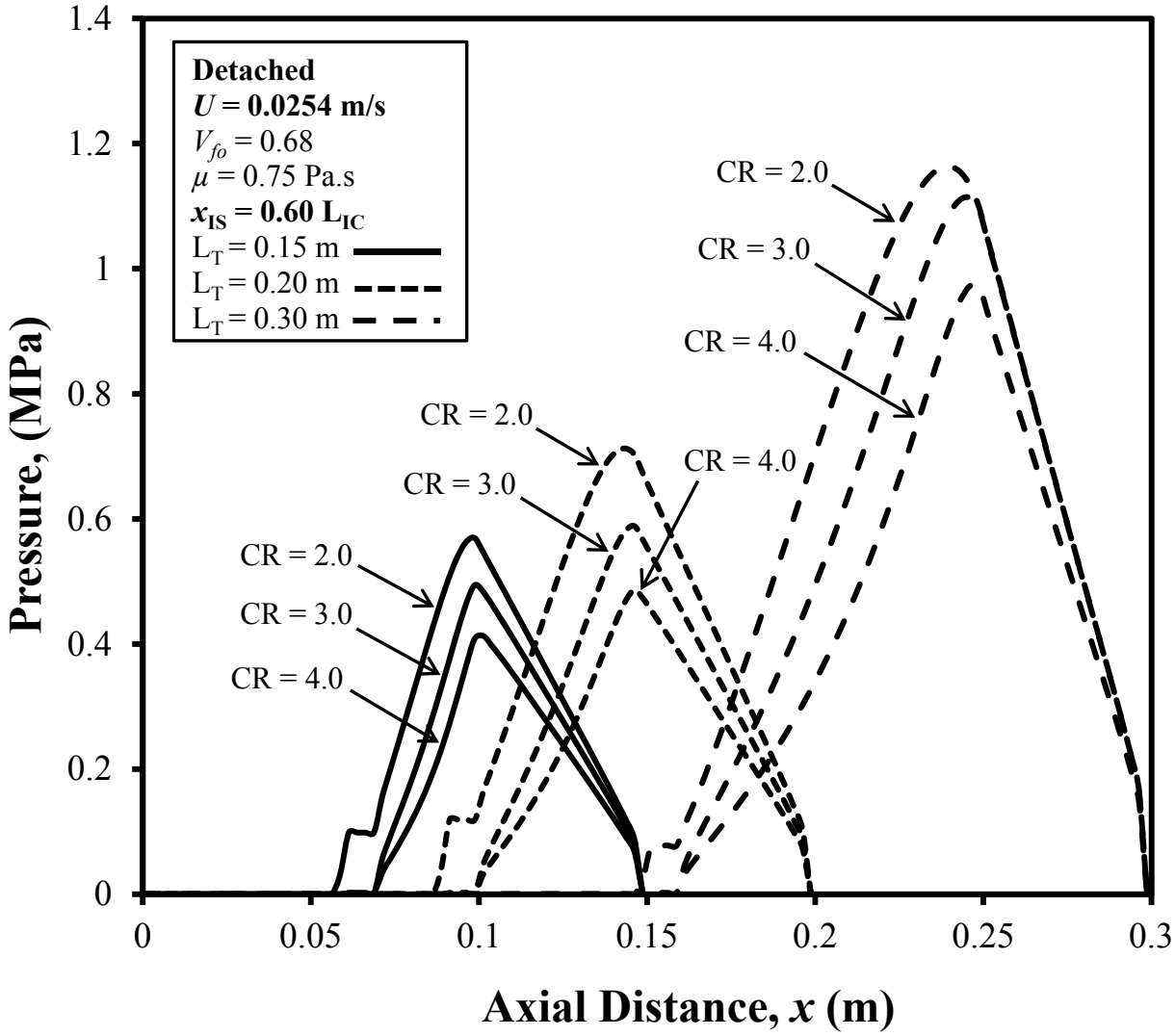

Figure 4-21. Chamber Wall Axial Pressure Profiles of Detached Injection Chamber for different Chamber Lengths of 0.15 m, 0.20 m and 0.30 m for U = 0.0254 m/s, (H_D = 0.0635 m, W_D = 0.00318 m).

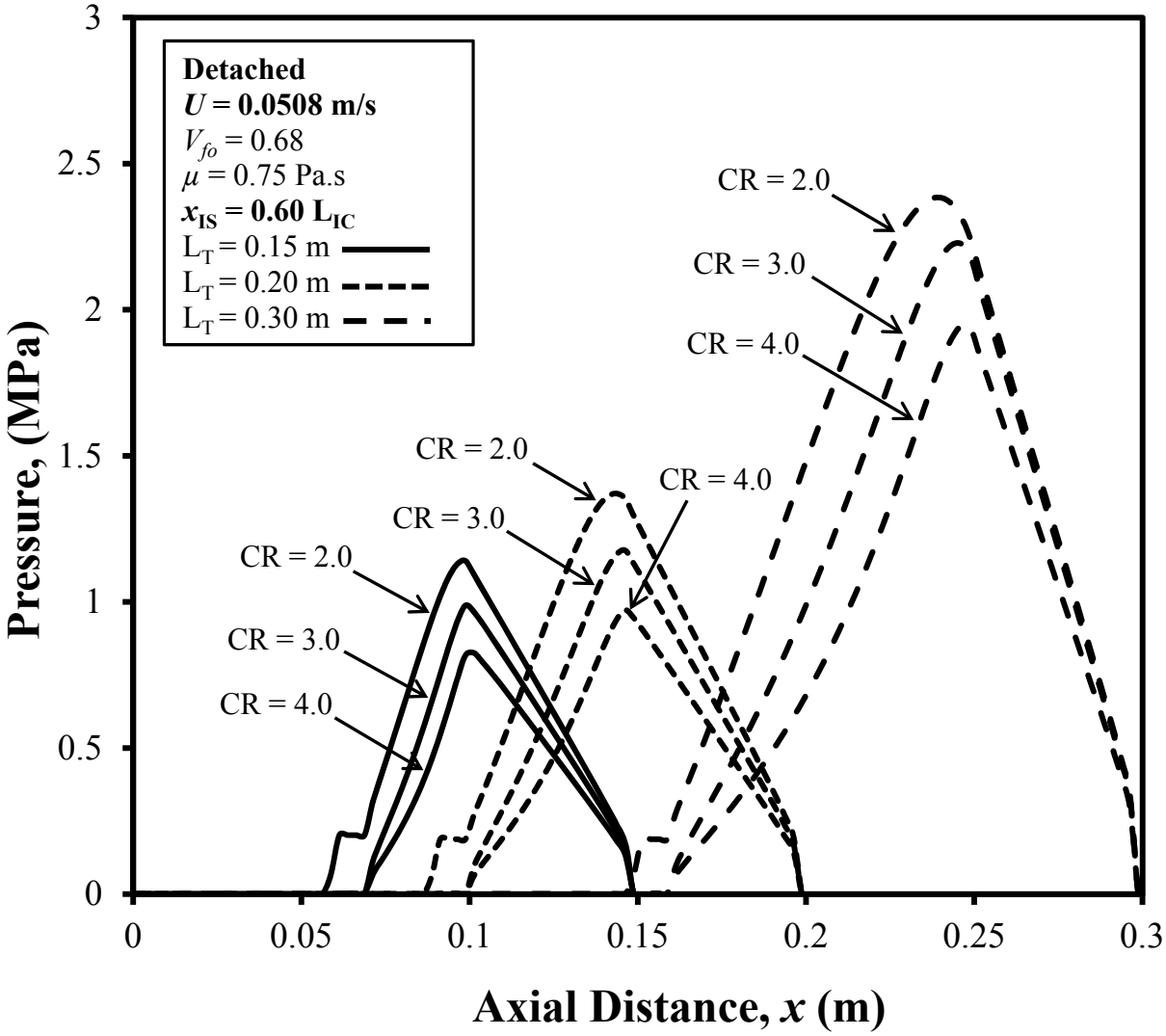

Figure 4-22. Chamber Wall Axial Pressure Profiles of Detached Injection Chamber for different Chamber Lengths of 0.15 m, 0.20 m and 0.30 m for U = 0.0508 m/s, (H_D = 0.0635 m, W_D = 0.00318 m).

4.2. Effect of Fiber Volume Fraction, V_{fo}

Fiber volume fraction is another important processing parameter. Its impact on the strength of the final composite is important since higher fiber volume fraction composites generally yield higher strength. Manufacturing composites with higher fiber volume fraction are more difficult because higher fiber volume fractions require higher injection pressures to achieve complete wet out and thus yield higher maximum interior chamber wall pressures. The investigation of the effect of the fiber volume fraction, for suitable composite strength, on the minimum injection pressure to achieve complete wet out and the associated maximum chamber resin pressure is important. The simulation cases for the effect of fiber volume fraction on the minimum injection pressure to achieve complete wet out and maximum interior chamber pressure are presented in Table 4-4. From Table 4-4, it can be seen that three cases for the attached die configuration and only one case for detached die configuration have non-feasible solutions for the parameters investigated. Table 4-4 also shows that the maximum chamber pressure for the detached die configuration is always less than the exit (maximum) pressure for the attached die configuration. This will be clearly illustrated in the upcoming figures in this section. The resistance to the flow of resin through the fiber bed increases as the fiber volume fraction increases due to the increased amount of fiber blockage. Thus the higher fiber volume fraction (V_{fo}) increases the injection pressure required for the complete wet out and hence yields a higher corresponding maximum chamber pressure. After complete wet out, which is where the flow front reaching the centerline, the resin pressure rises rapidly as the resin is compressed due to the tapering of the injection chamber walls.

For the CR value of 2.0, as the fiber volume fraction increases, the injection pressure

Table 4-4. Effect of Fiber Volume Fraction, V_{fo}, on Minimum Injection Pressure Necessary to Achieve Complete Wet out for Different Processing Parameters for Slot Width = 0.01 m, Part Width = 0.0635 m, Part Thickness = 0.00318 m at a Proportional Slot Location x_{IS} = 0.60 L_{IC}.

Case	CR	U (m/s)	V_{fo}	μ Pa·s	Injection Pressure (Gauge) (MPa)	Total Length L_T (m)	Location of x_{IS} (m)	Exit Pressure (Gauge) (MPa) (Attached)	Maximum Chamber Pressure (Gauge) (MPa) (Detached)
A4	2	0.0254	0.64	0.75	0.064	0.15	0.06	0.487	0.388
A2	2	0.0254	0.68	0.75	0.071	0.15	0.06	0.656	0.570
A5	2	0.0254	0.72	0.75	0.092	0.15	0.06	0.968	0.827
B4	3	0.0254	0.64	0.75	0.002	0.15	0.06	0.417	0.367
B2	3	0.0254	0.68	0.75	0.002	0.15	0.06	0.570	0.520
B5	3	0.0254	0.72	0.75	0.002	0.15	0.06	0.784	0.728
C4	4	0.0254	0.64	0.75	0.002	0.15	0.06	0.355	0.334
C2	4	0.0254	0.68	0.75	0.002	0.15	0.06	0.474	0.452
C5	4	0.0254	0.72	0.75	0.002	0.15	0.06	0.639	0.620
D4	2	0.0254	0.64	0.75	0.078	0.20	0.09	0.631	0.522
D2	2	0.0254	0.68	0.75	0.078	0.20	0.09	0.880	0.715
D5	2	0.0254	0.72	0.75	0.133	0.20	0.09	1.273	1.030
E4	3	0.0254	0.64	0.75	0.002	0.20	0.09	0.518	0.434
E2	3	0.0254	0.68	0.75	0.002	0.20	0.09	0.700	0.590
E5	3	0.0254	0.72	0.75	0.002	0.20	0.09	0.953	0.827
F4	4	0.0254	0.64	0.75	0.002	0.20	0.09	0.426	0.375
F2	4	0.0254	0.68	0.75	0.002	0.20	0.09	0.561	0.501
F5	4	0.0254	0.72	0.75	0.002	0.20	0.09	0.743	0.675
G4	2	0.0254	0.64	0.75	0.064	0.30	0.15	1.210	0.801
G2*	2	0.0254	0.68	0.75	0.078	0.30	0.15	**1.727**	1.198
G5*	2	0.0254	0.72	0.75	0.147	0.30	0.15	**2.440**	**1.747**
H4	3	0.0254	0.64	0.75	0.002	0.30	0.15	1.040	0.801
H2	3	0.0254	0.68	0.75	0.002	0.30	0.15	1.420	1.120
H5*	3	0.0254	0.72	0.75	0.002	0.30	0.15	**1.960**	1.581
I4	4	0.0254	0.64	0.75	0.002	0.30	0.15	0.876	0.721
I2	4	0.0254	0.68	0.75	0.002	0.30	0.15	1.171	0.984
I5	4	0.0254	0.72	0.75	0.002	0.30	0.15	1.583	1.356

***** Bold font indicates non-acceptable manufacturing solutions, not satisfying the following criteria: injection pressure ≤ 0.42 MPa (60 psi) and corresponding exit pressure (attached configuration) or maximum wall pressure (detached configuration) ≤ 1.72 MPa (250 psi).

necessary for the complete wet out increases due to the higher blockage resistance to the flow of resin through the fiber system. But for CR values of 3.0 and 4.0, the injection gauge pressure necessary for complete wet out has a constant (low) value of about 0.002 MPa (15 psi absolute), and thus the minimum injection pressure to achieve complete wet out is essentially no longer a function of the fiber volume fraction. For CR = 3.0 and 4.0, the local fiber volume fraction at the injection port location is so low that only a very low injection pressure is needed to achieve complete wet out.

Figures 4-23, 4-24, and 4-25 show the impact of fiber volume fraction on the minimum injection pressure to achieve wet out and the maximum chamber wall pressure for the detached die configuration and attached die configuration for CR values of 2.0, 3.0 and 4.0 respectively for chamber lengths (L_T) of 0.15 m, 0.2 m, and 0.3 m. In these figures, the lower horizontal dotted line (0.42 MPa) and the upper horizontal dashed line (1.72 MPa) represent the limits for the acceptable manufacturing solutions for the resin injection pressure and the maximum chamber wall pressure respectively. To be an acceptable pultrusion manufacturing solution, both the maximum chamber pressure must be below the 1.72 MPa horizontal dashed line and the minimum injection pressure to achieve complete wet out must be below the 0.42 MPa horizontal dotted line simultaneously. Since the resin is more compressed as the fiber volume fraction increases, the maximum chamber wall pressure increases with an increase in the fiber volume fraction. The injection pressure lines for the CR value of 2.0 can be seen in the Fig. 4-23; but for the CR values of 3.0 and 4.0 (Figs. 4-24 and 4-25) the injection pressure values are essentially 0.002 MPa (near zero) and thus cannot be seen distinctly. Hence for a CR value of 3.0 or greater

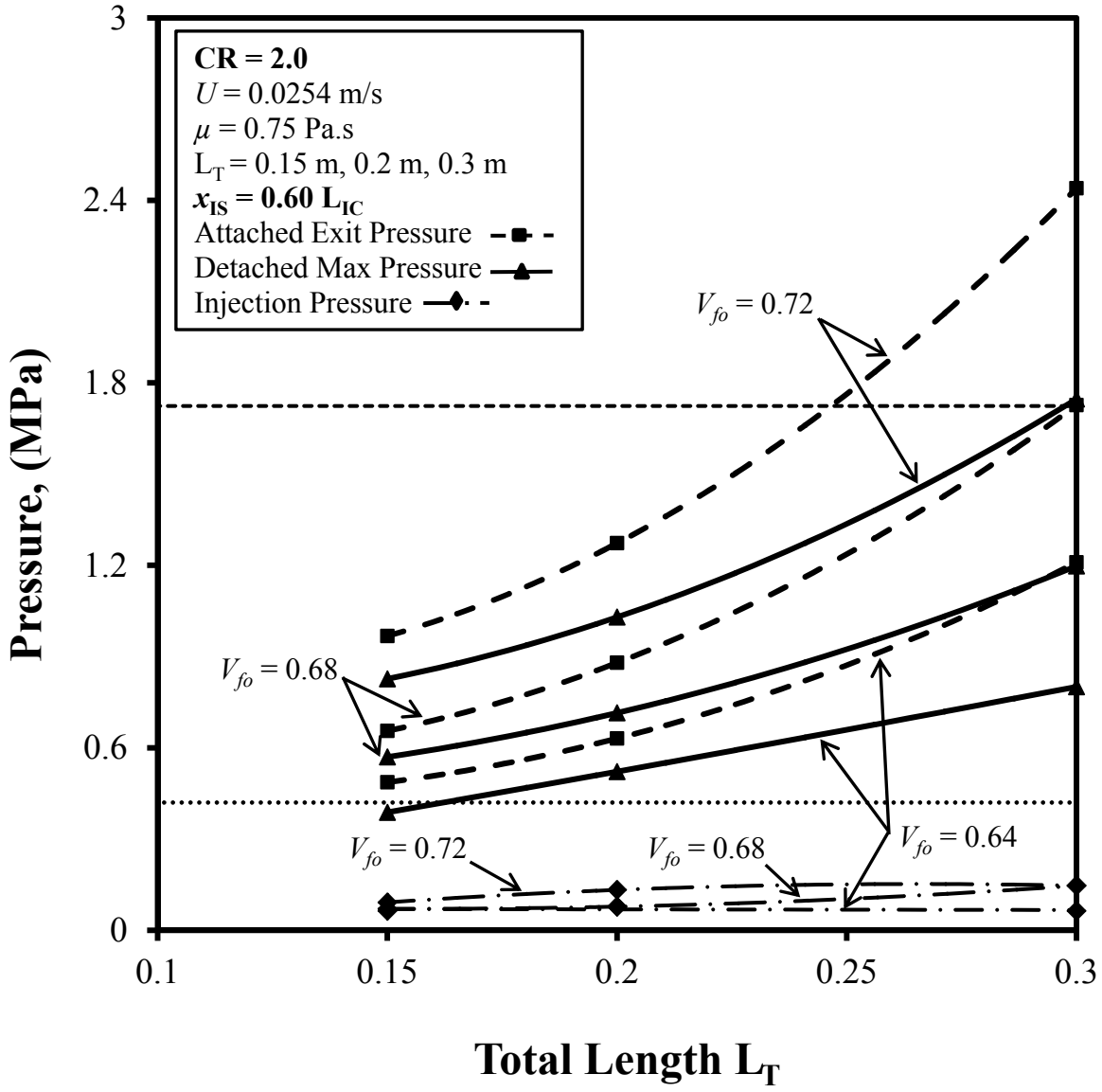

Figure 4-23. Maximum Wall Pressure (——) for Detached Injection Chamber and Exit Wall (Maximum) Pressure (– – –) for Attached Injection Chamber vs. Chamber Length for CR = 2.0 (H_D = 0.0635 m, W_D = 0.00318 m); Minimum Injection Pressure (— · —) to Achieve Complete Wet Out.

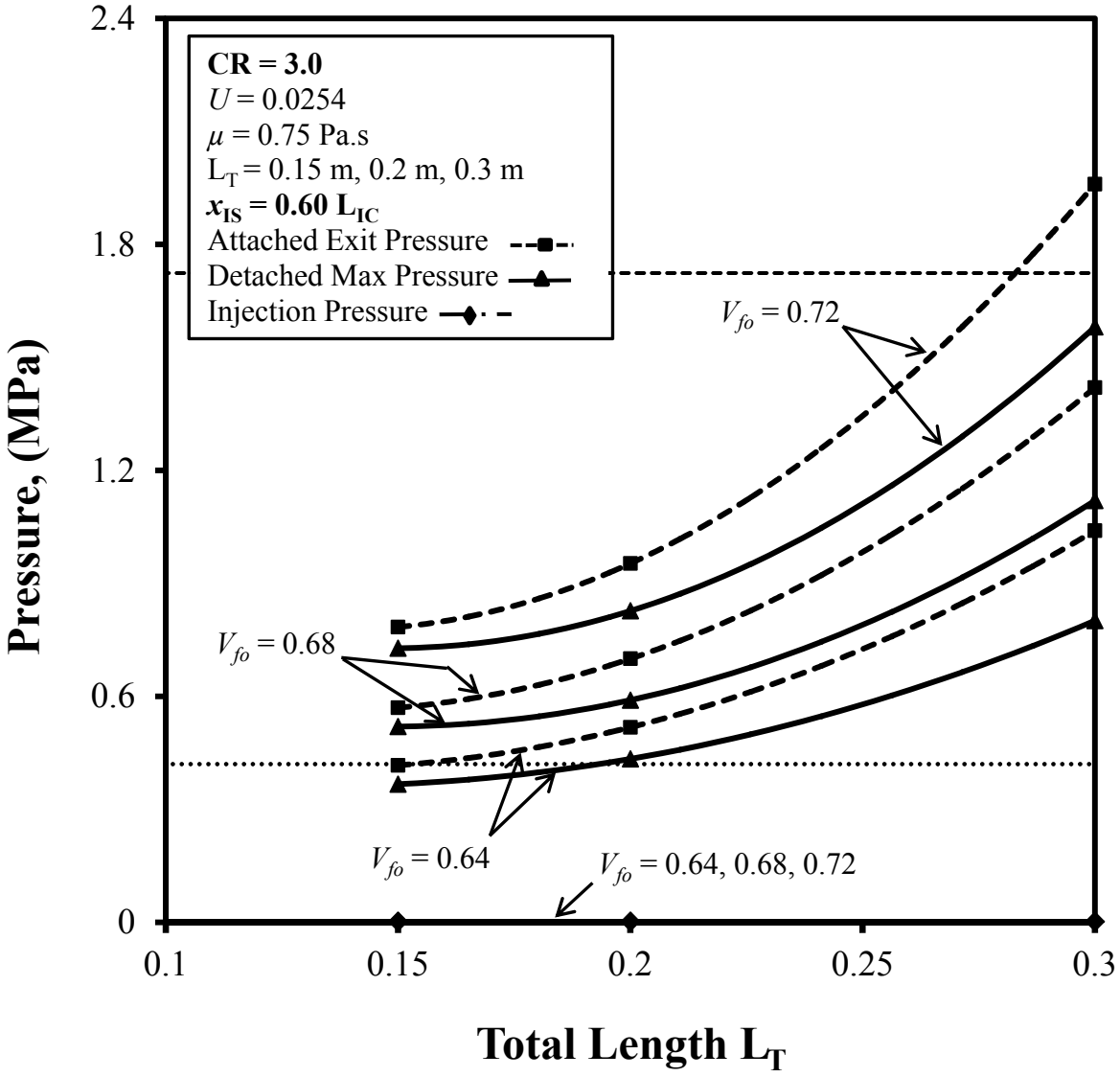

Figure 4-24. Maximum Wall Pressure (——) for Detached Injection Chamber and Exit Wall (Maximum) Pressure (– – –) for Attached Injection Chamber vs. Chamber Length for CR = 3.0, (H_D = 0.0635 m, W_D = 0.00318 m); Minimum Injection Pressure (— · —) to Achieve Complete Wet Out.

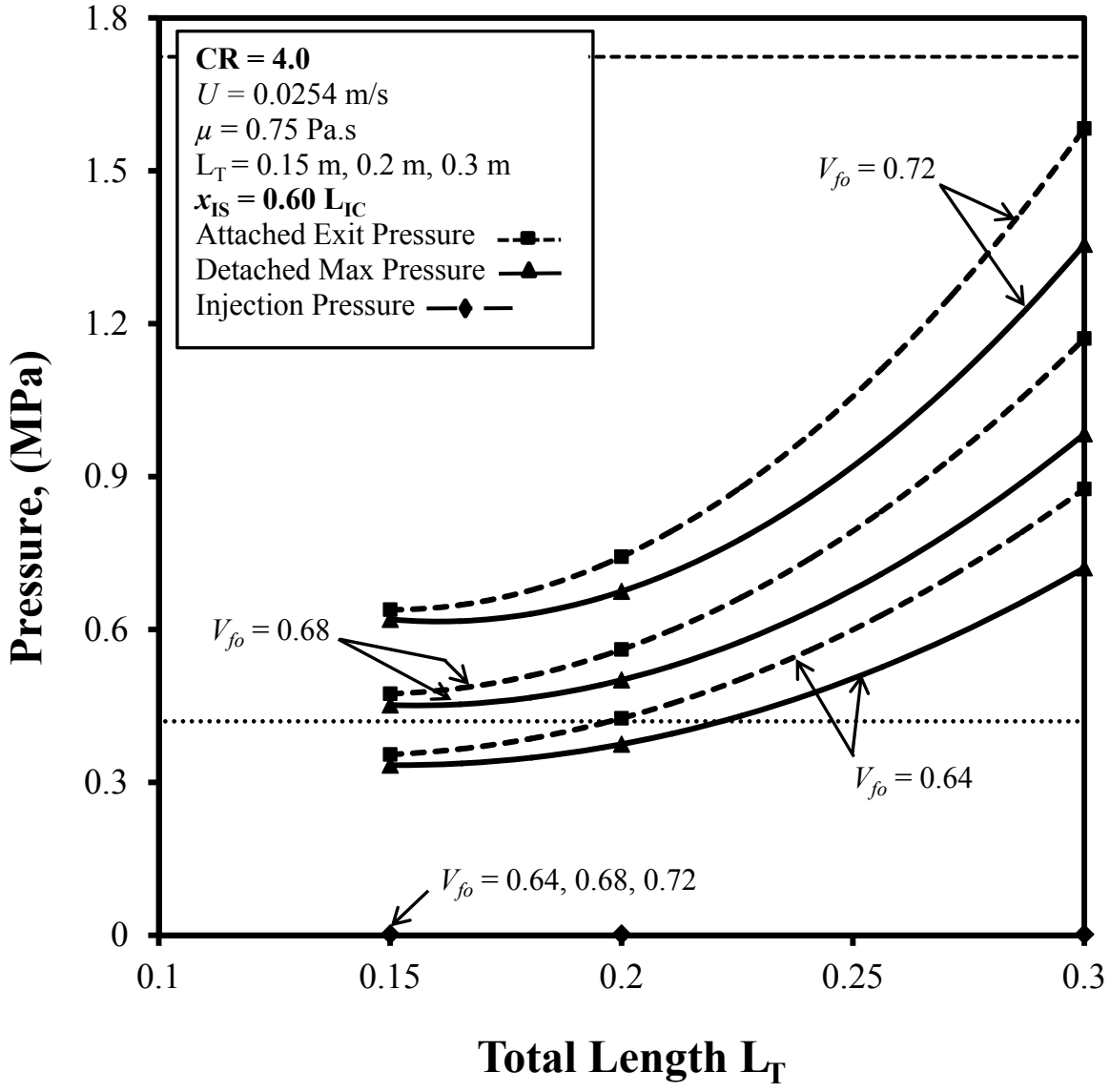

Figure 4-25. Maximum Wall Pressure (——) for Detached Injection Chamber and Exit Wall (Maximum) Pressure (– – –) for Attached Injection Chamber vs. Chamber Length for CR = 4.0, (H_D = 0.0635 m, W_D = 0.00318 m); Minimum Injection Pressure (— · —) to Achieve Complete Wet Out.

(Figs. 4-24 and 4-25), the injection pressure to achieve complete wet out is essentially no longer a function of fiber volume fraction. In Fig. 4-23, for CR value of 2.0, different injection pressure lines can be seen as a weak function of injection chamber length for different fiber volume fractions; for L_T = 0.15 m, 0.2 m, and 0.3 m, for V_{fo} = 0.64, the injection pressure increases slightly; for V_{fo} = 0.68, it increases and remains constant; for V_{fo} = 0.72, it remains essentially constant. But for the CR value of 2.0 (Fig. 4-23) for a specific injection chamber length, the resin injection pressure for complete wet out is always anticipated to increase as the fiber volume fraction increases due to the higher resistance for resin to penetrate through the fiber for higher fiber volume fraction. In Figs. 4-23, 4-24 and 4-25, it can be seen that as the length of the injection chamber increases, the corresponding maximum interior chamber wall pressure sharply increases. This pressure rise is due to the source term in Eq. (3-24h) which occurs as the result of tapering the injection chamber walls in Region I; the maximum pressure increases as the tapered length (L_{IC}) increases due to the longer distance over which the resin is compressed. The increase in maximum chamber wall pressure for longer injection chamber lengths is also due to the increased volume of resin in the longer injection chambers. For CR values of 3.0 and 4.0 (Figs. 4-24 and 4-25), the behavior of the curves looks similar for the attached and detached die configurations for all the values of fiber volume fraction; this indicates that for these specific conditions, the maximum chamber wall pressure is a continuous increasing function of injection chamber length and fiber volume fraction.

Figures 4-26, 4-27, and 4-28 show the minimum injection pressure to achieve complete wet out and the corresponding maximum chamber pressure trends for different CR values for the fiber volume fraction of V_{fo} = 0.64, 0.68, and 0.72 respectively. These figures demonstrate the pressure behavior for different fiber volume fractions and thus illustrate the difference in the

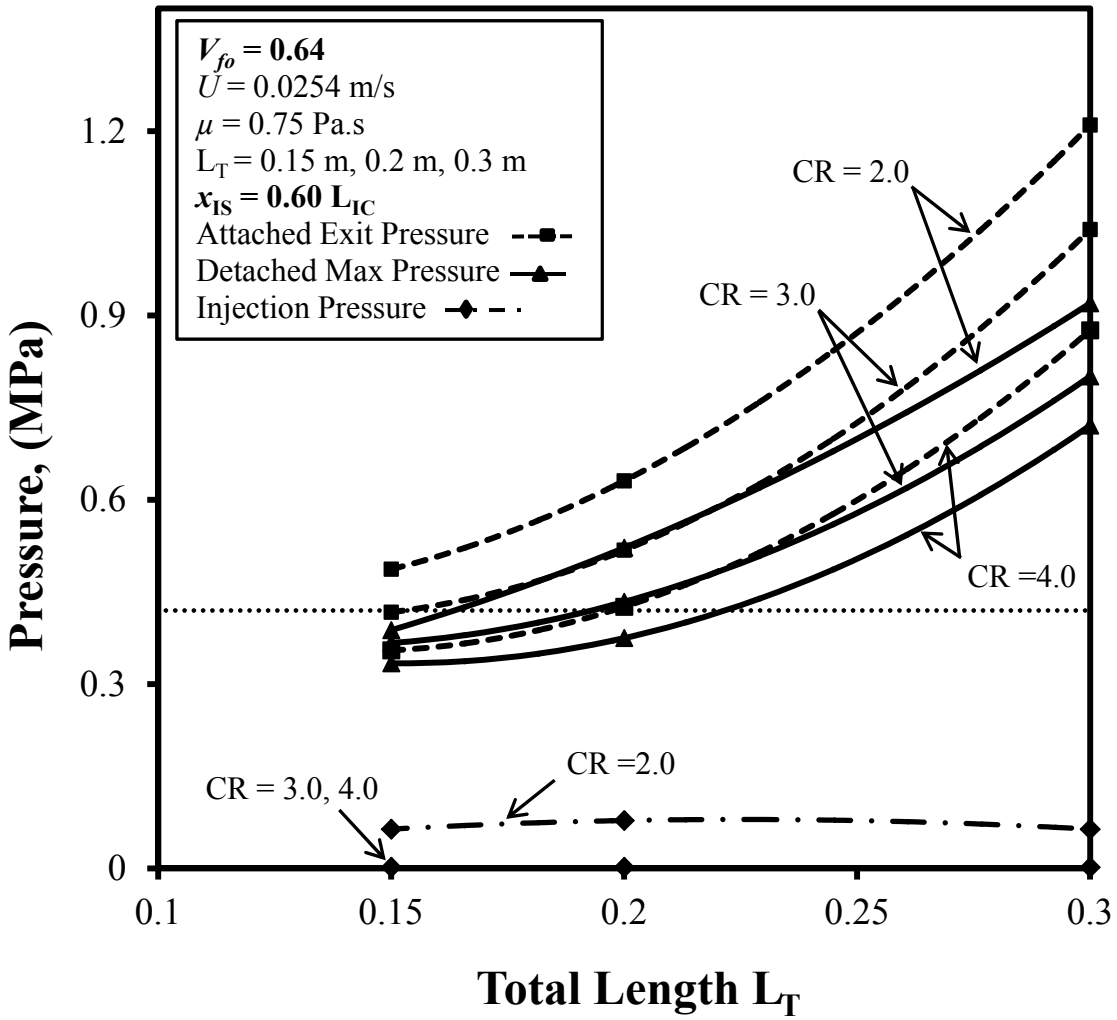

Figure 4-26. Maximum Wall Pressure (———) for Detached Injection Chamber and Exit Wall (Maximum) Pressure (– – –) for Attached Injection Chamber vs. Chamber Length for Various CR, (H_D = 0.0635 m, W_D = 0.00318 m); Minimum Injection Pressure(— · —) to Achieve Complete Wet Out.

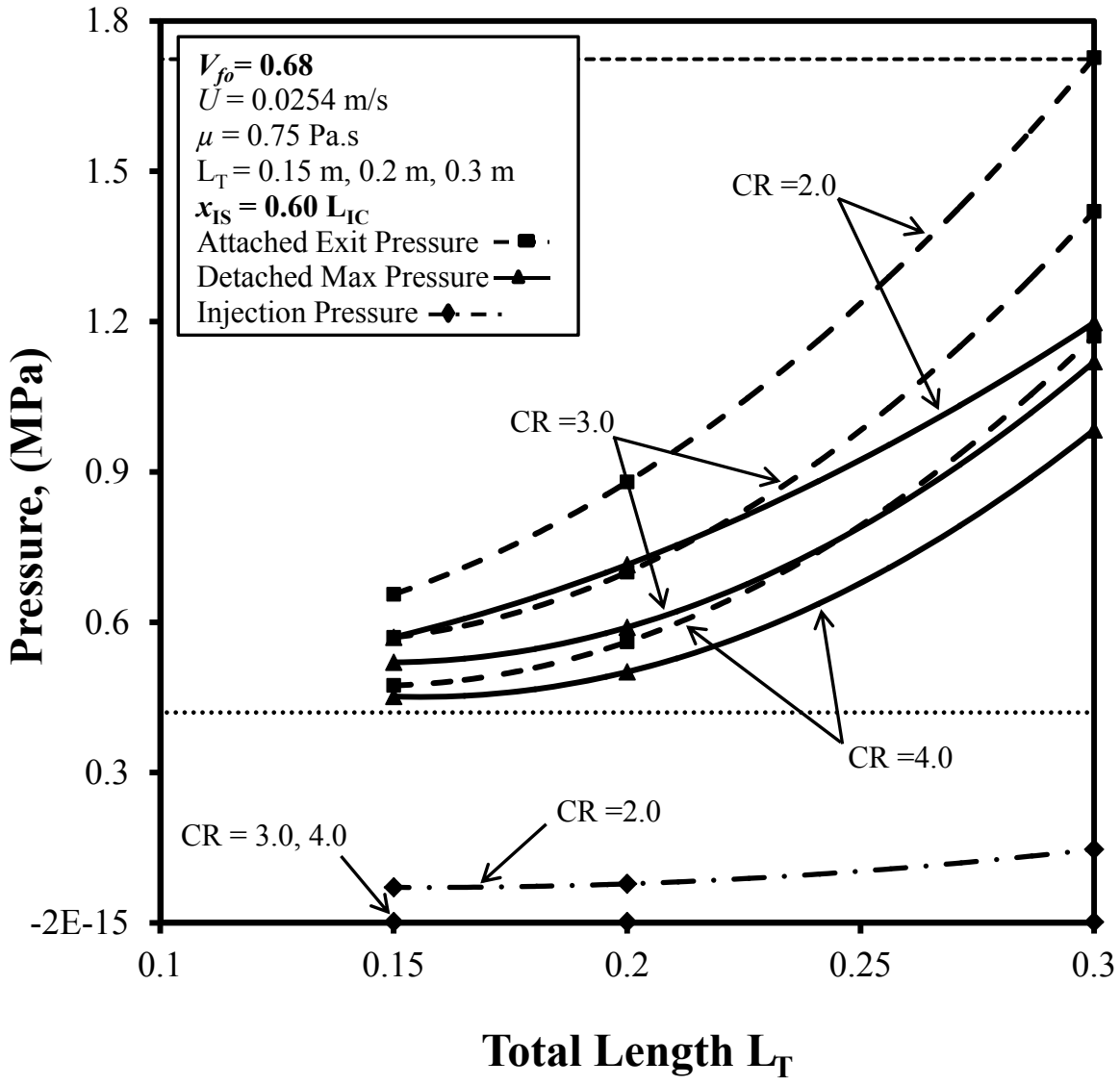

Figure 4-27. Maximum Pressure (——) for Detached Injection Chamber and Exit (Maximum) Pressure (– – –) for Attached Injection Chamber vs. Chamber Length for Various CR, (H_D = 0.0635 m, W_D = 0.00318 m). Minimum Injection Pressure (— · —) to Achieve Complete Wet Out.

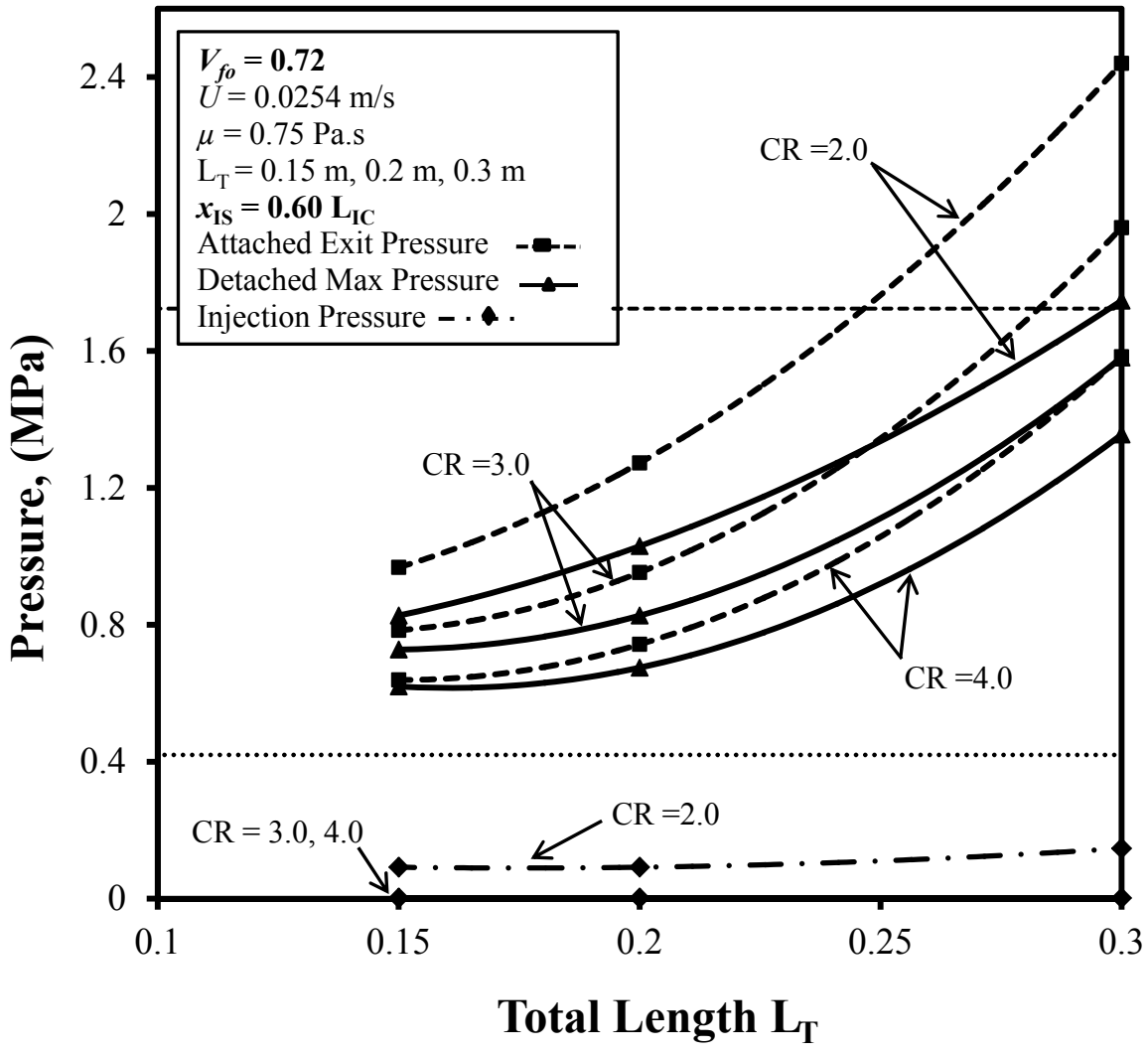

Figure 4-28. Maximum Pressure (——) for Detached Injection Chamber and Exit (Maximum) Pressure (– – –) for Attached Injection Chamber vs. Chamber Length for Various CR, (H_D = 0.0635 m, W_D = 0.00318 m). Minimum Injection Pressure (— · —) to Achieve Complete Wet Out.

maximum chamber wall pressure between the attached die configuration and detached die for injection chamber lengths (L_T = 0.15 m, 0.2 m, and 0.3 m) and CR value of 2.0, 3.0, and 4.0. The pressure difference (ΔP) between the maximum chamber wall pressure for the attached die configuration and detached die configuration decreases as the CR value increases.

The maximum chamber wall pressure increases with an increase in fiber volume fraction (V_{fo}) and the injection chamber length (L_T) for all CR values. In Fig. 4-28, for the highest fiber volume fraction considered, V_{fo} = 0.72, the non-feasible manufacturing solutions due to the excessive maximum chamber wall pressure can be seen for the attached die configuration for CR values of 2.0 and 3.0 and for the detached die configuration for the CR value of 2.0 for the injection chamber length of L_T = 0.3 m. It is clear from Fig. 4-28, that longer injection chamber lengths (L_T) can generate unacceptable maximum chamber wall pressures. Thus the longer chamber lengths and the lower CR values yield unfavorable conditions for pultrusion manufacturing of composites with high fiber volume fractions. From Fig. 4-28, it can be seen that for the highest fiber volume fraction considered, V_{fo} = 0.72, the most favorable combination for an acceptable chamber wall pressure is the detached die configuration with CR value of 4.0 and an injection chamber length of L_T = 0.15m.

Figure 4-29 shows the resin flow front profile through the fiber reinforcement for the most favorable case with an injection chamber length of 0.15 m and CR = 4 for the highest pull speed of 0.0508 m/s considered and other nominal processing parameters (V_{fo} = 0.68 and μ = 0.75 Pa·s). The white portion inside the injection chamber is dry fiber and the shaded region is the resin and fiber mixture. The thick dark line corresponds to the flow front of the resin/fiber system and the thin lines show the isopressure contours labeled with pressure values in KPa. The resin flow front and the pressure values for the attached die configuration and the detached die

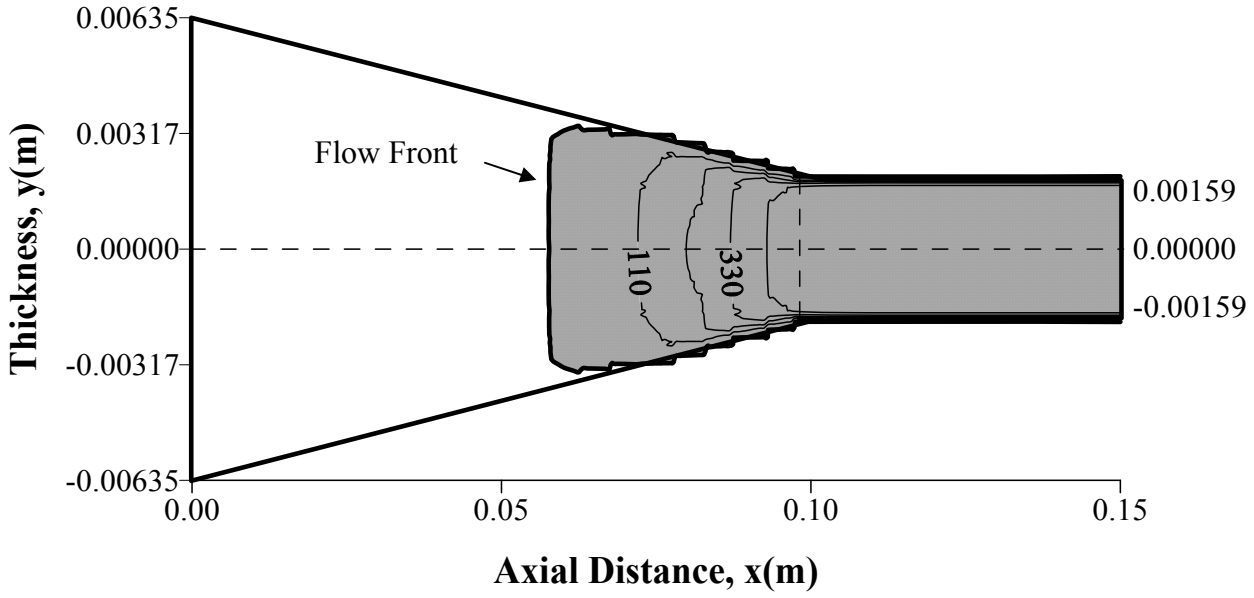

a. Attached Die Configuration

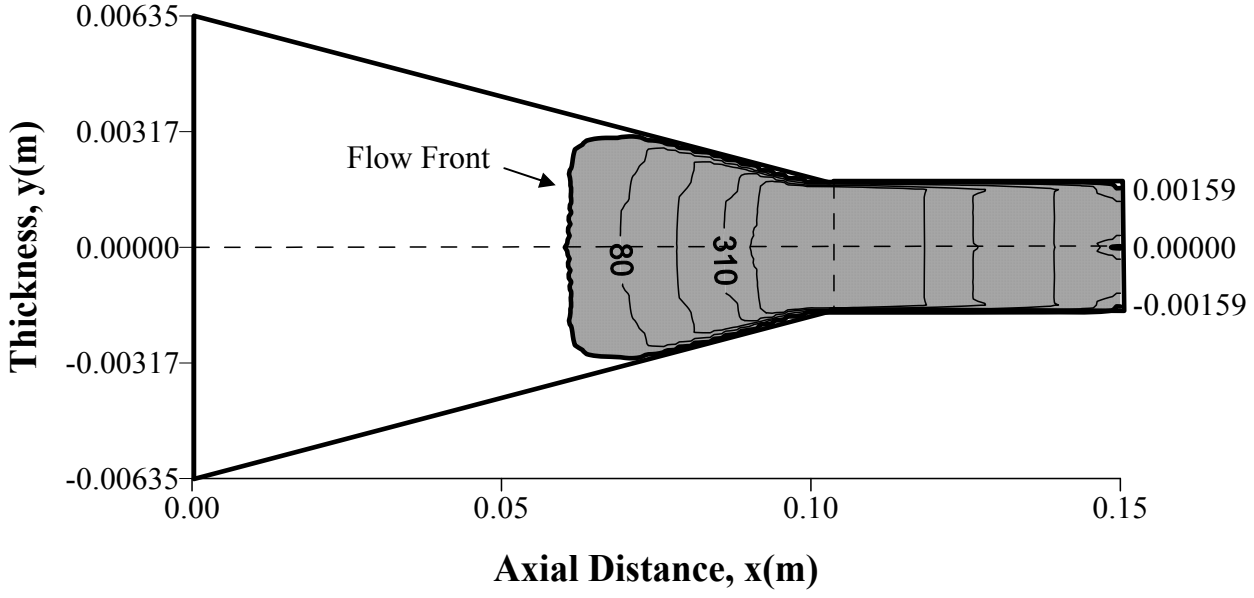

b. Detached Die Configuration

Figure 4-29. Flow Front Profile and Gauge Isopressure (KPa) contours for Case C5, Table 4-4 with V_{fo} = 0.72, L_T = 0.15 m, CR = 4.0, U = 0.0254 m/s for Polyster Resin/Glass Roving and μ = 0.75, x_{IS} = 0.60 L_{IC}. (Not to Scale)

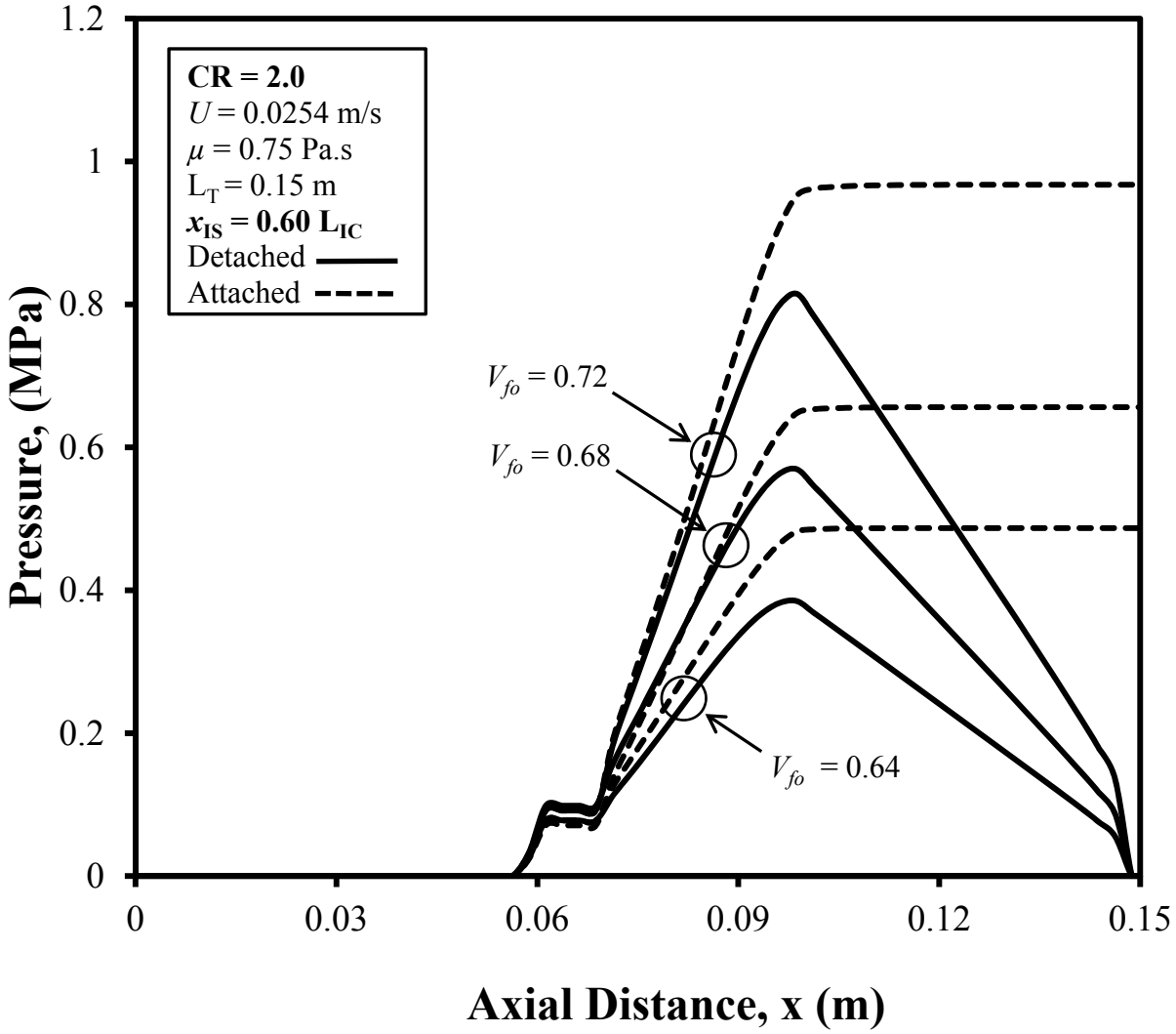

Figure 4-30. Chamber Wall Axial Pressure Profiles for Detached Injection Chamber and Attached Injection Chamber for Chamber Length of 0.15 m for CR = 2.0, (H_D = 0.0635 m, W_D = 0.00318 m).

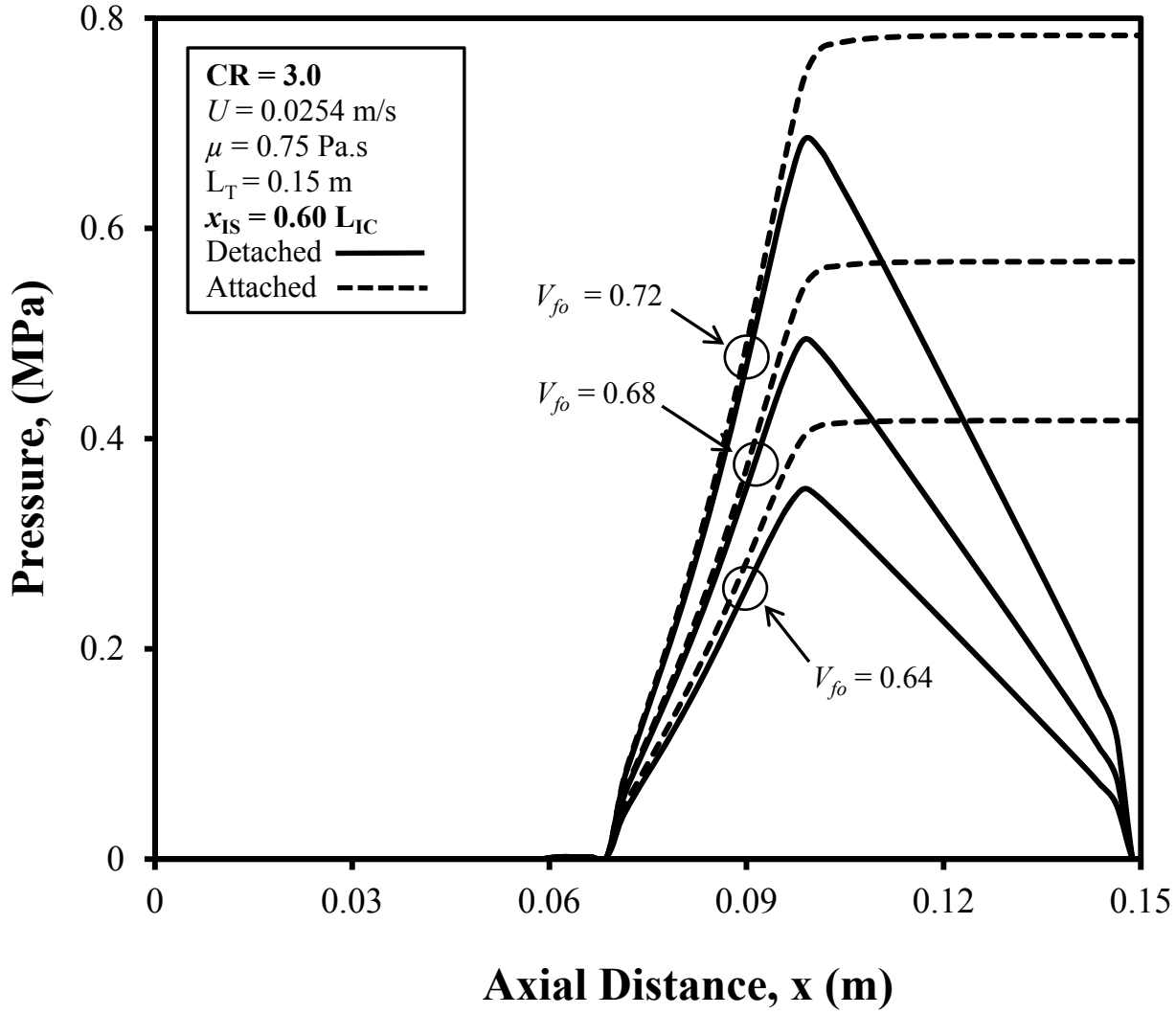

Figure 4-31. Chamber Wall Axial Pressure Profiles for Detached Injection Chamber and Attached Injection Chamber for Chamber Length of 0.15 m for CR = 3.0, (H_D = 0.0635 m, W_D = 0.00318 m).

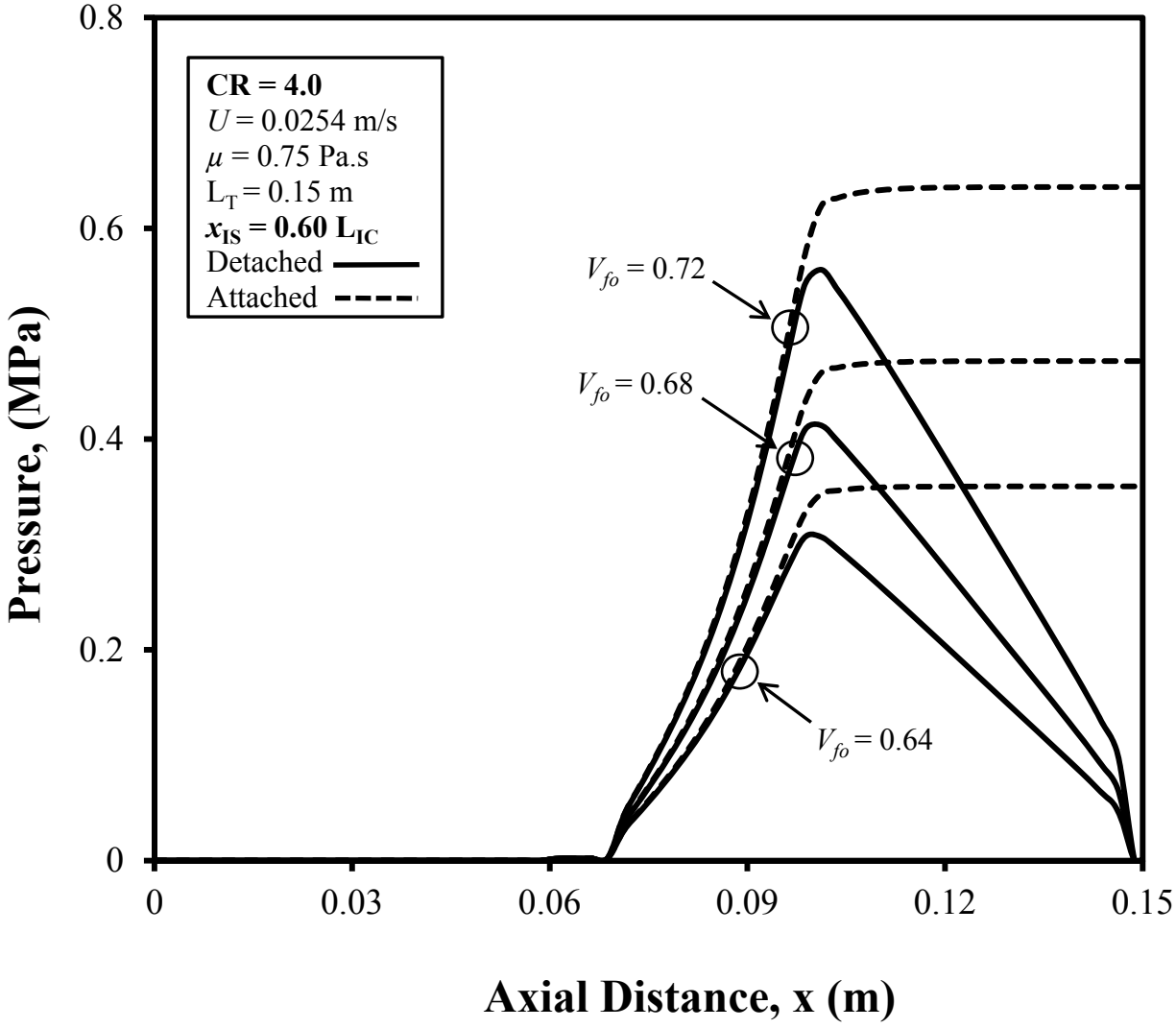

Figure 4-32. Chamber Wall Axial Pressure Profiles for Detached Injection Chamber and Attached Injection Chamber for Chamber Length of 0.15 m for CR = 4.0, (H_D = 0.0635 m, W_D = 0.00318 m).

configuration can be compared in these two figures. The chamber pressure values are always lower in the detached die configuration system compared to the attached die configuration as can be seen in Fig. 4-29. In the detached die configuration, the isopressure contours can be seen in Region II of the injection chamber due to the decreasing chamber pressure in the Region II and these pressure contours correspond to the same pressure contours as depicted in the Region I of the injection chamber. The plots in the Fig. 4-29 are made out of scale to make it more viewable to the readers.

Figures 4-30, 4-31, and 4-32 depict the chamber wall pressure profile within the injection chamber for different fiber volume fractions, V_{fo}, of 0.64, 0.68 and 0.72 along the interior length of the injection chamber for L_T = 0.15 m and for the CR values of 2.0, 3.0 and 4.0 respectively. These pressure profiles show how the internal chamber wall pressures change along the injection chamber length for these different fiber volume fractions. In Fig. 4-30 (CR = 2.0), it can be seen that the chamber wall gauge pressure starts at zero and then rises to the injection port pressure, decreases slightly and then increases to reach its maximum value; whereas, for the CR values of 3.0 and 4.0 (Figs. 4-31 and 4-32), the chamber wall pressure follows the same trend but it starts at a very low injection pressure of 0.002 MPa for these cases. These figures show the differences in the pressure profile development for attached and detached die configurations for various fiber volume fractions. The pressure profiles behavior for L_T = 0.20 m (Figs. 4-33, 4-34, 4-35) and 0.30 m (Figs. 4-36, 4-37, 4-38) are very similar to that described above for L_T = 0.15 m (Figs. 4-30, 4-31, 4-32). Figures 4-33, 4-34 and 4-35 show similar pressure profiles but for an injection chamber length of L_T = 0.20 m, and likewise Figs. 4-36, 4-37 and 4-38 depict the pressure profiles for an injection chamber length of L_T = 0.30 m.

Fig. 4-32 provides the useful design information for an injection chamber with the maximum fiber volume fraction (V_{fo} = 0.72) considered. The most favorable combination for the minimum chamber wall pressure is the obtained with CR value of 4.0 and an injection chamber length of 0.15m (Fig. 4-32); thus this condition (Fig. 4-32) is of primary significance. In Fig. 4-32, the maximum chamber wall pressure for the attached die configuration and detached die configuration occur at around an injection chamber *x*-location length of about 0.10 m, i.e. near the end of the Region I (tapered region). For the attached die configuration the maximum chamber wall pressure occurs a little beyond the injection chamber location of x = 0.10 m and slightly into Region II, and then remains constant throughout Region II. For the detached die configuration, the maximum chamber wall pressure occurs almost at the end of Region I, and then it decreases and finally reaches atmospheric pressure at the end of Region II (injection chamber exit). But for all other cases (Figs. 4-30, 4-31, 4-33, 4-34, 4-35, 4-36, 4-37, 4-38), for the attached die configuration, the maximum chamber wall pressure occurs near the end of Region I, and for the detached die configuration, the maximum chamber wall pressure occur just before the end of Region I. As the CR value increases for each injection chamber length, the peak of the chamber wall pressure for the detached die configuration moves closer to the end of the Region I.

The detached die configuration always performed the best and thus the preferred choice for the pultrusion manufacturing process as compared to the attached die configuration, since it provides lower maximum chamber wall pressure due to the pressure release at the injection chamber exit. Figures 4-39, 4-40, and 4-41 demonstrate the pressure profiles in the detached die configuration for all the chamber lengths considered for fiber volume fractions, V_{fo}, of 0.64, 0.68, and 0.72 respectively. These figures illustrate how the chamber wall pressure increases, reaches

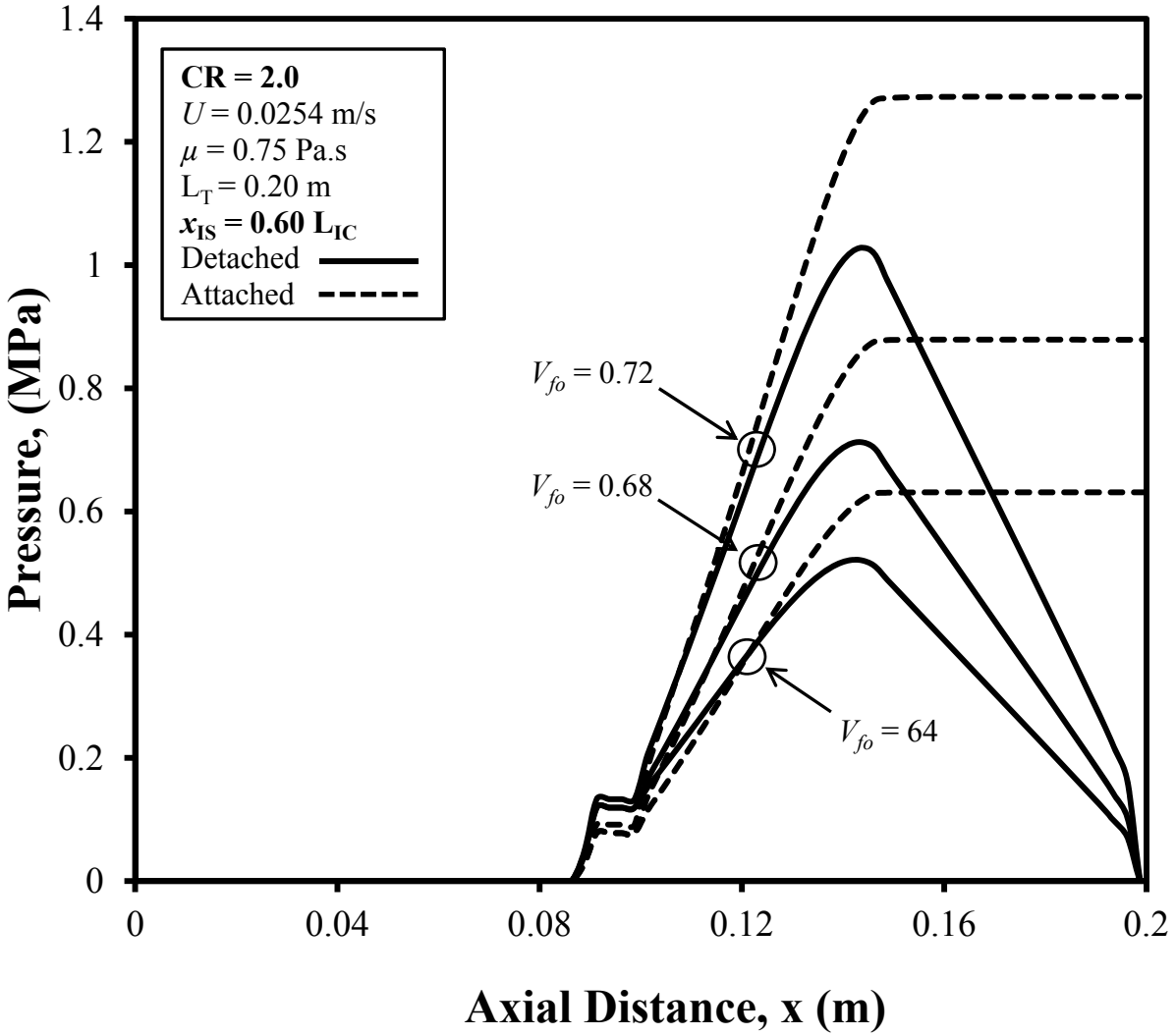

Figure 4-33. Chamber Wall Axial Pressure Profiles for Detached Injection Chamber and Attached Injection Chamber for Chamber Length of 0.20 m for CR = 2.0, (H_D = 0.0635 m, W_D = 0.00318 m).

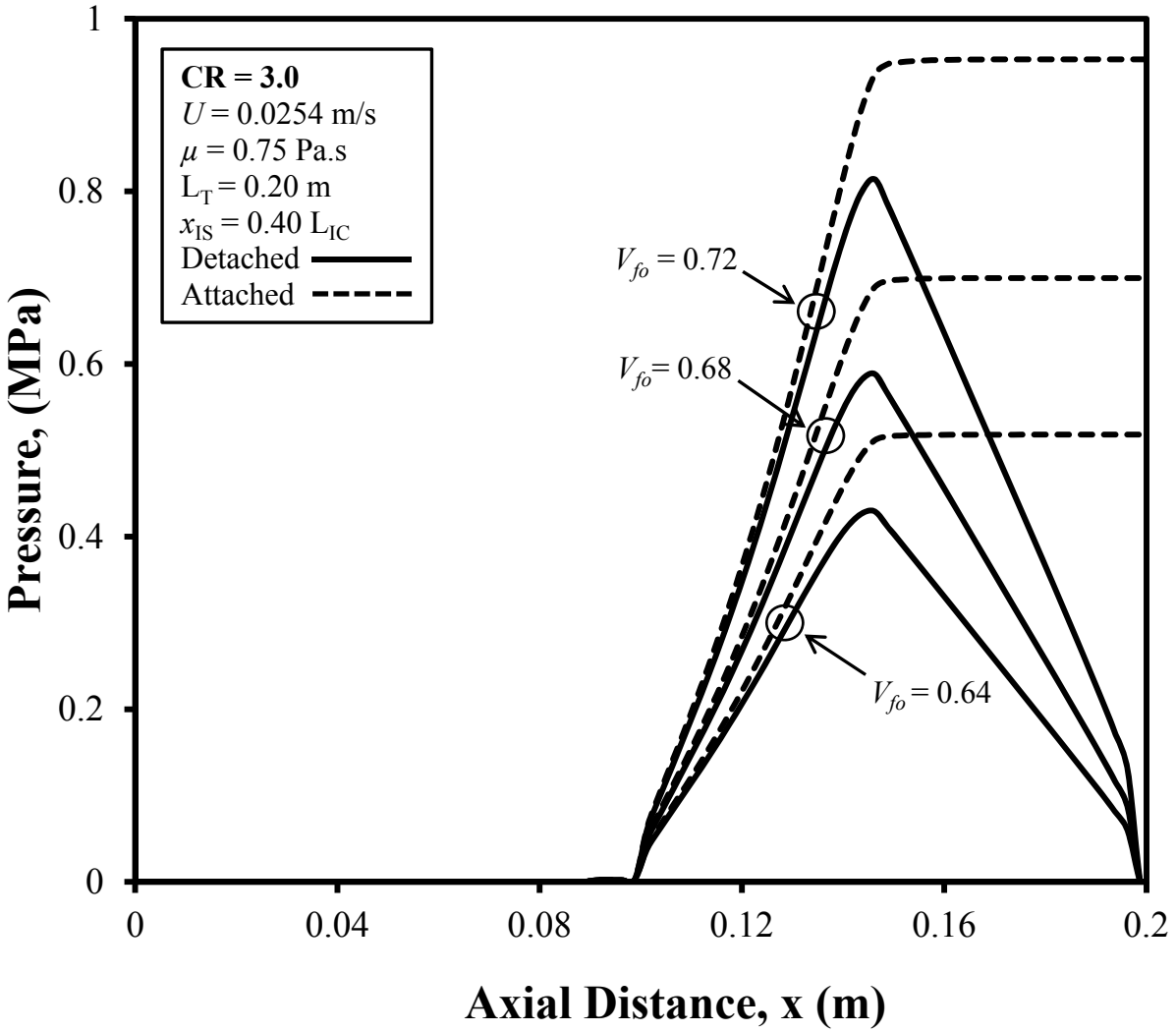

Figure 4-34. Chamber Wall Axial Pressure Profiles for Detached Injection Chamber and Attached Injection Chamber for Chamber Length of 0.20 m for CR = 3.0, (H_D = 0.0635 m, W_D = 0.00318 m).

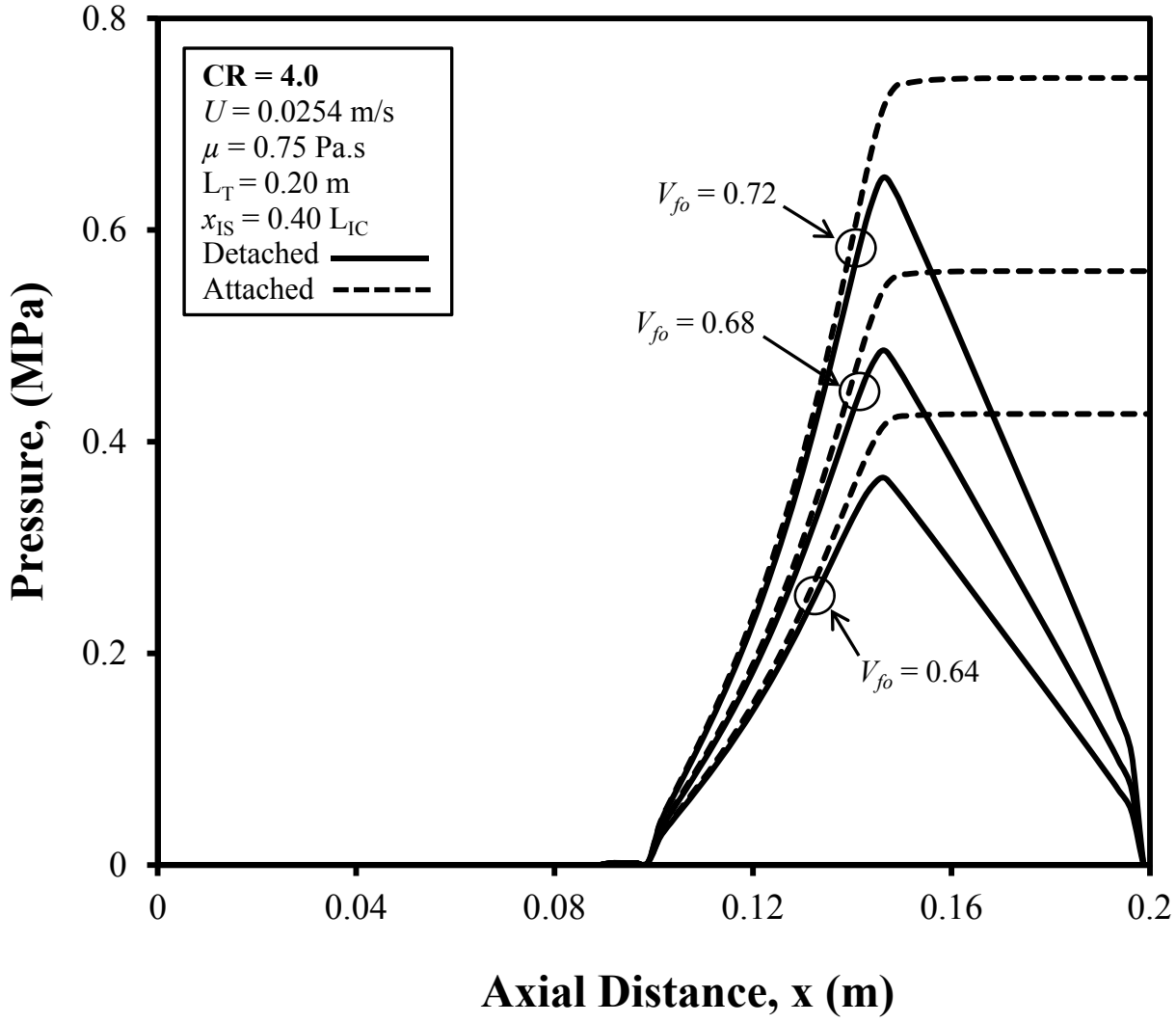

Figure 4-35. Chamber Wall Axial Pressure Profiles for Detached Injection Chamber and Attached Injection Chamber for Chamber Length of 0.20 m for CR = 4.0, (H_D = 0.0635 m, W_D = 0.00318 m).

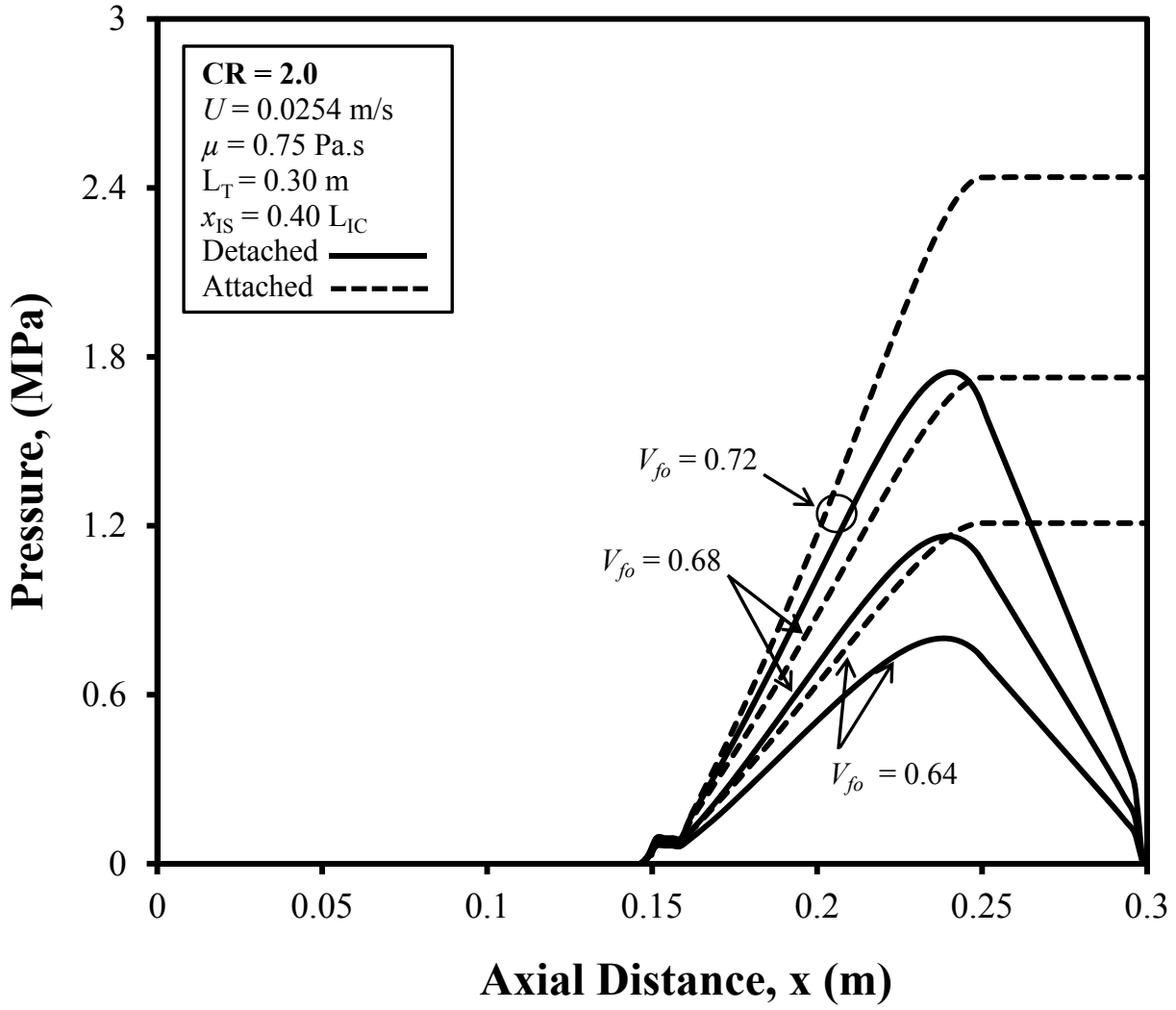

Figure 4-36. Chamber Wall Axial Pressure Profiles for Detached Injection Chamber and Attached Injection Chamber for Chamber Length of 0.30 m for CR = 2.0, (H_D = 0.0635 m, W_D = 0.00318 m).

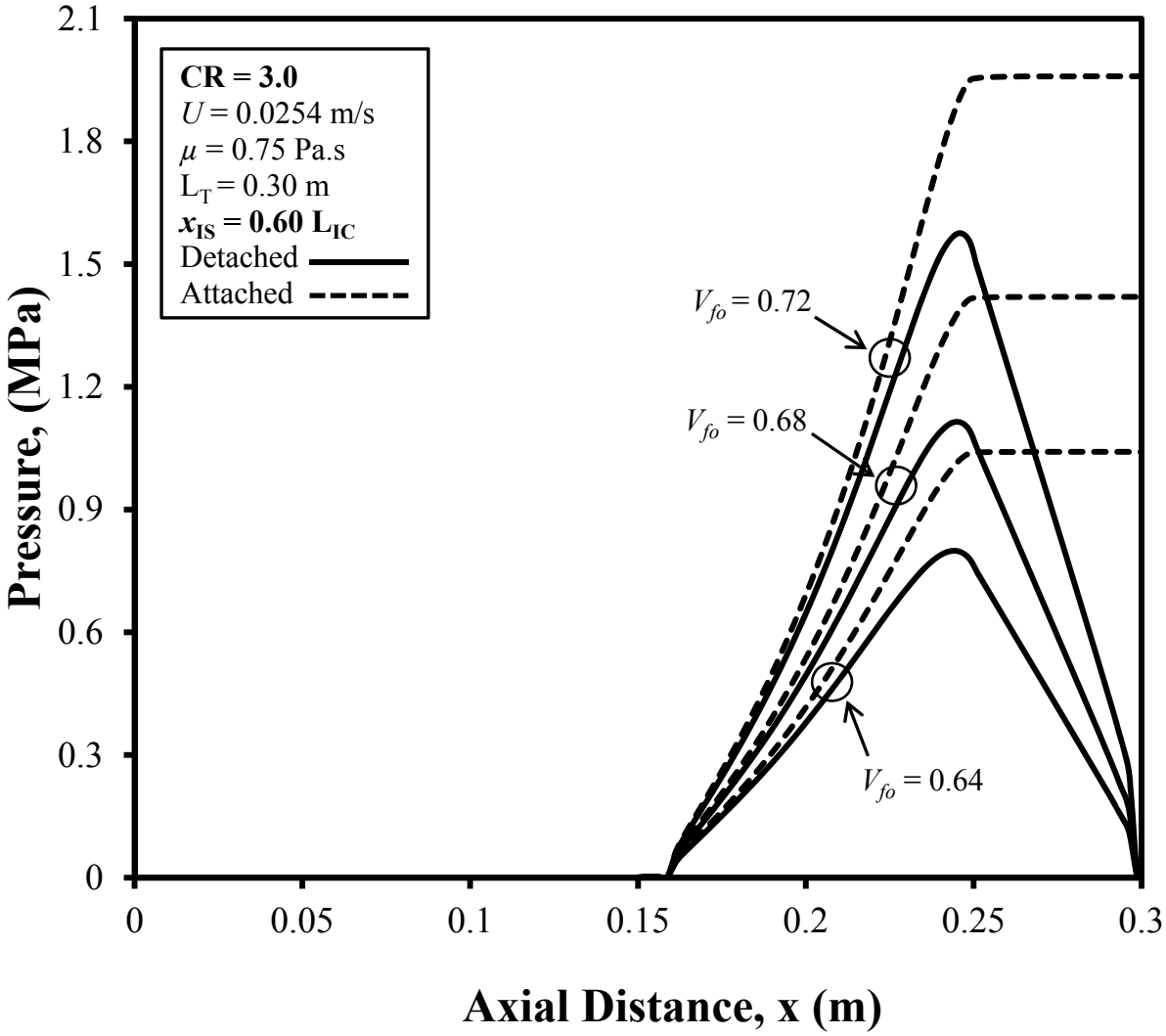

Figure 4-37. Chamber Wall Axial Pressure Profiles for Detached Injection Chamber and Attached Injection Chamber for Chamber Length of 0.30 m for CR = 3.0, (H_D = 0.0635 m, W_D = 0.00318 m).

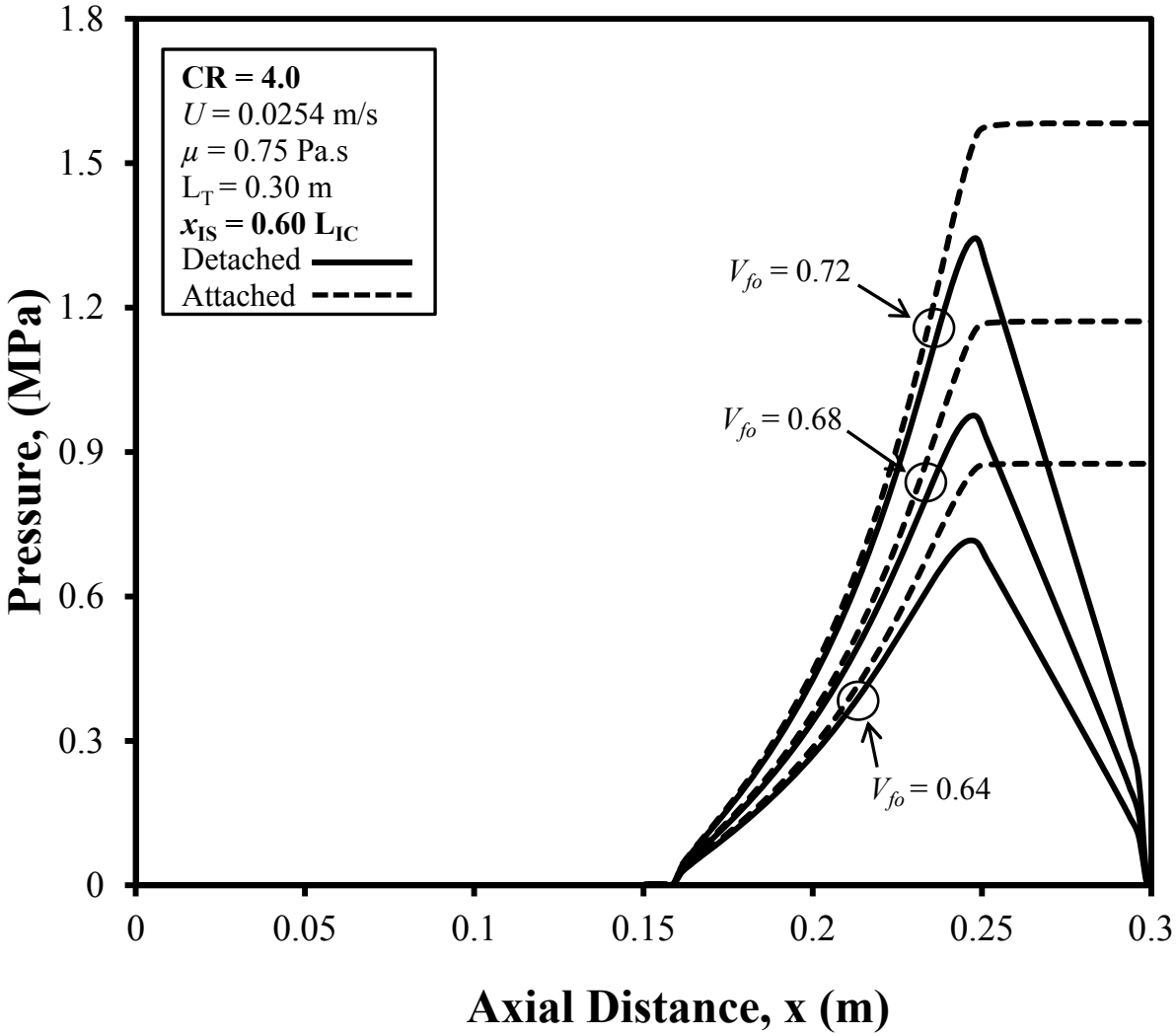

Figure 4-38. Chamber Wall Axial Pressure Profiles for Detached Injection Chamber and Attached Injection Chamber for Chamber Length of 0.30 m for CR = 4.0, (H_D = 0.0635 m, W_D = 0.00318 m).

a peak value and then decreases back to atmospheric pressure for all the different injection chamber lengths and different CR values considered. Figure 4-41 shows the pressure profile and the maximum chamber wall pressure for the maximum value of fiber volume fraction considered, V_{fo} = 0.72, for various injection chamber lengths and CR values. Figure 4-41 gives the general spectrum of the maximum chamber wall pressure at different injection chamber lengths. As the CR value increases, the maximum chamber wall pressure decreases, and as the injection chamber length increases the maximum chamber wall pressure increases. From Fig. 4-41, it is clear that composite pultrusion manufacturing at higher fiber volume fractions is achievable with higher CR values and with lower injection chamber lengths. In this work, for the highest fiber volume fraction of 0.72 considered, the most favorable condition for the lowest acceptable maximum chamber wall pressure of 0.620 MPa (Case C5 of Table 4-4) is the one having CR value of 4.0 with injection chamber length of 0.15 m.

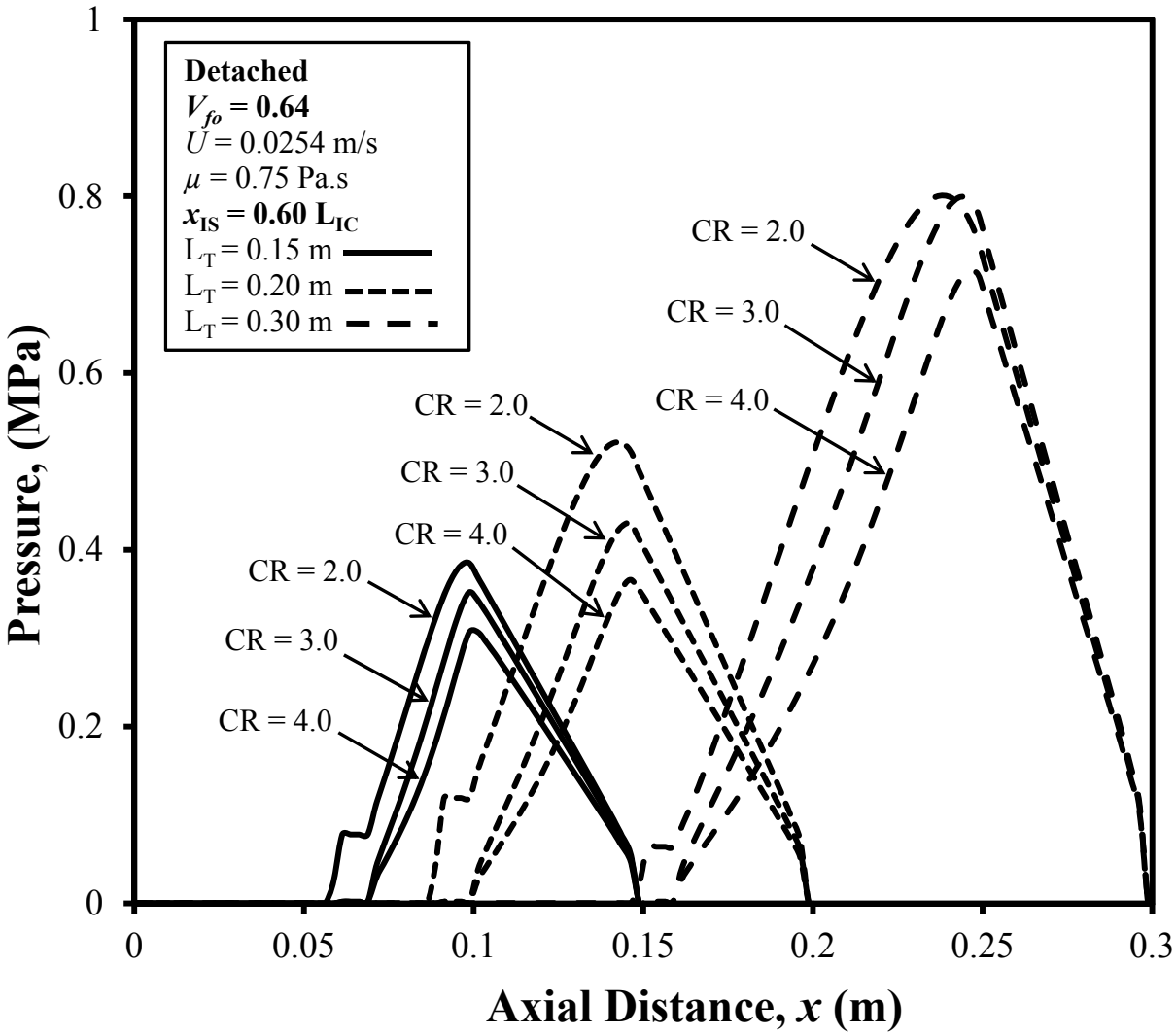

Figure 4-39. Chamber Wall Axial Pressure Profiles of Detached Injection Chamber for different Chamber Lengths of 0.15 m, 0.20 m and 0.30 m for V_{fo} = 0.64, (H_D = 0.0635 m, W_D = 0.00318 m).

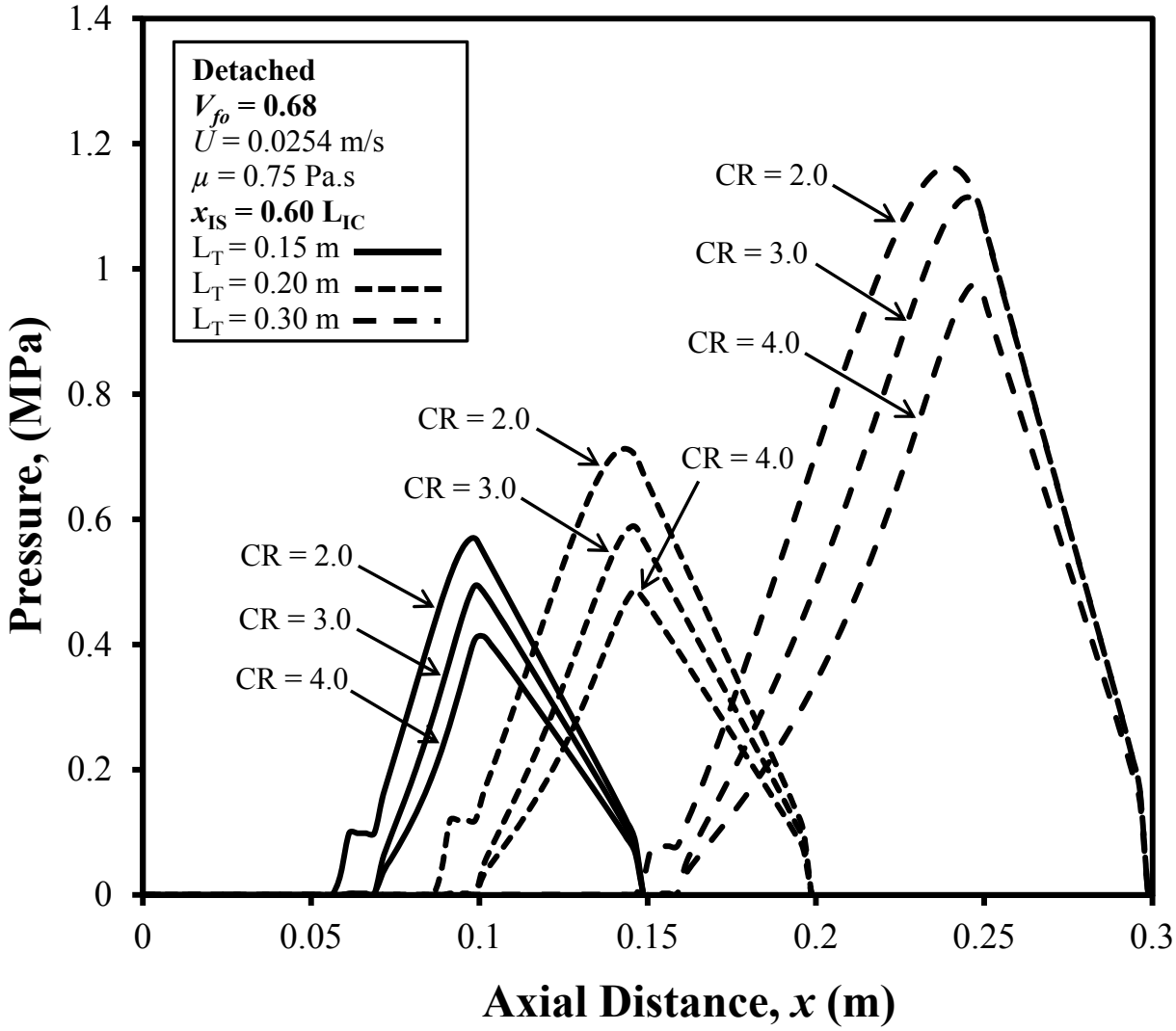

Figure 4-40. Chamber Wall Axial Pressure Profiles of Detached Injection Chamber for different Chamber Lengths of 0.15 m, 0.20 m and 0.30 m for V_{fo} = 0.68, (H_D = 0.0635 m, W_D = 0.00318 m).

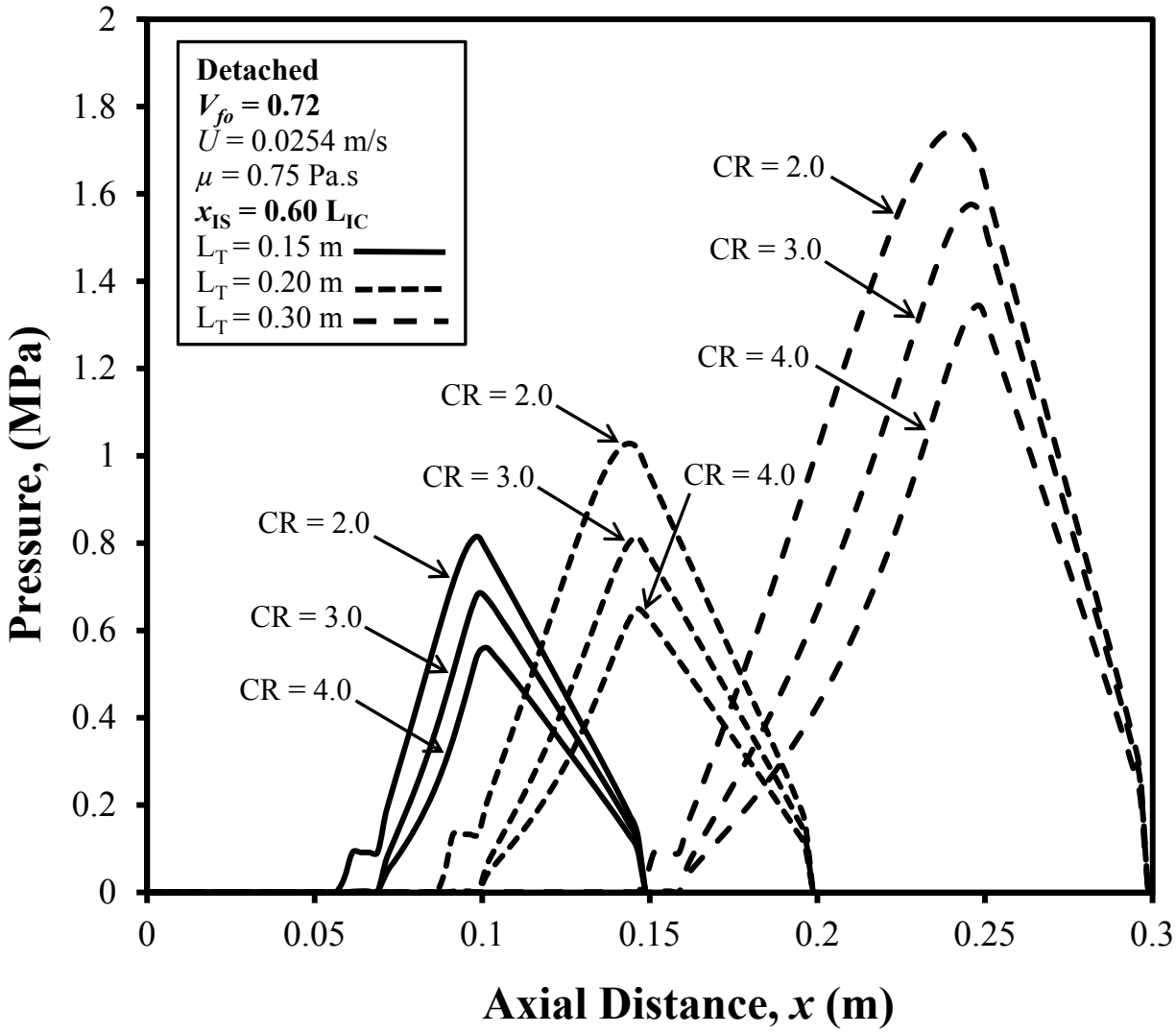

Figure 4-41. Chamber Wall Axial Pressure Profiles of Detached Injection Chamber for different Chamber Lengths of 0.15 m, 0.20 m and 0.30 m for V_{fo} = 0.72, (H_D = 0.0635 m, W_D = 0.00318 m).

4.3 Effect of Viscosity, μ

The selection of a resin for a composite manufacturing involves several factors. Viscosity is one of the main fluid characteristics which is needed to be considered in order to determine the operating and processing conditions for a specific resin. Resin viscosity offers resistance to the flow of resin through the fiber bed. Thus a lower resin viscosity should yield a lower minimum injection pressure for achieving complete wet out; whereas a higher resin viscosity should increase the minimum injection pressure accordingly. The resin viscosity is an important processing parameter to be considered for the pultrusion manufacturing of composites. The injection pressures required for complete wet out and the associated interior maximum chamber wall pressure were determined from simulation cases for the different viscosities values of 0.50 Pa·s, 0.75 Pa·s and 1.00 Pa·s in this work which are appropriate for phenolic resin systems. The other processing parameters (pull speed and fiber volume fraction) are kept constant at their nominal values of U = 0.0254 m/s and V_{fo} = 0.68 respectively for investigating the effect of resin viscosity on the minimum injection pressure required for the complete wet out of the fiber bed, and the corresponding maximum chamber wall pressure. For all the results presented in this section the injection slot is located at a proportional slot location of x_{IS} = 0.60 L_{IC}. The resin viscosity simulation cases are presented in Table 4-5; this table shows that there were three non-feasible manufacturing (bolded cases) solutions for the "attached" die configuration; whereas all the cases are feasible manufacturing solutions for the "detached" die configuration.

From Table 4-5 it can be seen that for the CR value of 2.0 as the resin viscosity increases, the minimum injection pressure required for complete wet out also increases. This is due to the

Table 4-5. Effect of Resin Viscosity, μ, on Minimum Injection Pressure Necessary to Achieve Complete Wetout for Different Processing Parameters for Slot Width = 0.01 m, Part Width = 0.0635 m, Part Thickness = 0.00318 m at a Proportional Slot Location (x_{IS}) of x_{IS} = 0.60 L_{IC}.

Case	CR	U (m/s)	V_{fo}	μ Pa·s	Injection Pressure (Gauge) (MPa)	Total Length L_T (m)	Location of x_{IS} (m)	Exit Pressure (Gauge) (MPa) (Attached)	Maximum Chamber Pressure (Gauge) (MPa) (Detached)
A6	2	0.0254	0.68	0.50	0.064	0.15	0.06	0.471	0.383
A2	2	0.0254	0.68	0.75	0.071	0.15	0.06	0.656	0.570
A7	2	0.0254	0.68	1.00	0.100	0.15	0.06	0.900	0.743
B6	3	0.0254	0.68	0.50	0.002	0.15	0.06	0.379	0.346
B2	3	0.0254	0.68	0.75	0.002	0.15	0.06	0.570	0.520
B7	3	0.0254	0.68	1.00	0.002	0.15	0.06	0.758	0.691
C6	4	0.0254	0.68	0.50	0.002	0.15	0.06	0.316	0.302
C2	4	0.0254	0.68	0.75	0.002	0.15	0.06	0.474	0.452
C7	4	0.0254	0.68	1.00	0.002	0.15	0.06	0.632	0.603
D6	2	0.0254	0.68	0.50	0.050	0.20	0.09	0.583	0.491
D2	2	0.0254	0.68	0.75	0.078	0.20	0.09	0.880	0.715
D7	2	0.0254	0.68	1.00	0.105	0.20	0.09	1.174	0.926
E6	3	0.0254	0.68	0.50	0.002	0.20	0.09	0.470	0.397
E2	3	0.0254	0.68	0.75	0.002	0.20	0.09	0.700	0.590
E7	3	0.0254	0.68	1.00	0.002	0.20	0.09	0.933	0.793
F6	4	0.0254	0.68	0.50	0.002	0.20	0.09	0.374	0.330
F2	4	0.0254	0.68	0.75	0.002	0.20	0.09	0.561	0.501
F7	4	0.0254	0.68	1.00	0.002	0.20	0.09	0.748	0.670
G6	2	0.0254	0.68	0.50	0.050	0.30	0.15	1.150	0.853
G2*	2	0.0254	0.68	0.75	0.078	0.30	0.15	**1.727**	1.198
G7*	2	0.0254	0.68	1.00	0.092	0.30	0.15	***2.263**	1.584
H6	3	0.0254	0.68	0.50	0.002	0.30	0.15	0.947	0.745
H2	3	0.0254	0.68	0.75	0.002	0.30	0.15	1.420	1.120
H7*	3	0.0254	0.68	1.00	0.002	0.30	0.15	***1.900**	1.490
I6	4	0.0254	0.68	0.50	0.002	0.30	0.15	0.781	0.656
I2	4	0.0254	0.68	0.75	0.002	0.30	0.15	1.171	0.984
I7	4	0.0254	0.68	1.00	0.002	0.30	0.15	1.562	1.310

***** Bold font indicates non-acceptable manufacturing solutions, not satisfying the following criteria: injection pressure ≤ 0.42 MPa (60 psi) and corresponding exit pressure (attached configuration) or maximum wall pressure (detached configuration) ≤ 1.72 MPa (250 psi).

essentially constant (low) value of about 0.002 MPa. For CR ≥ 3.0, the wall taper angles at the injection slot location are higher which result in a lower local fiber volume fraction at the injection slot location. This lower local fiber volume fraction $V_f(x)$ yields less resistance to the resin flow; the resistance due to the resin viscosity is dominated by the reduction in flow resistance offered by the lower local fiber volume fraction. Thus the minimum injection pressure required for complete wet out is slightly above atmospheric pressure (0.002 MPa gauge or 15 psi absolute) and the minimum injection pressure to achieve complete wet out is essentially no longer a function of resin viscosity.

Figures 4-42, 4-43 and 4-44 illustrate the trends of the minimum injection pressure required to achieve compete wet out and the maximum chamber wall pressure inside the injection chamber for different resin viscosities for the attached die configuration and the detached die configuration at CR values of 2.0, 3.0 and 4.0, respectively, and for total injection chamber lengths (L_T) of 0.15 m, 0.20 m and 0.30 m. These figures show the impact of the resin viscosity on the minimum injection pressure required for complete wet out and the corresponding maximum chamber wall pressure. To be an acceptable manufacturing solution, both the maximum chamber pressure must be below the 1.72 MPa horizontal dashed line and the minimum injection pressure to achieve complete wet out must be below the 0.42 MPa horizontal dotted line simultaneously. For the CR values of 2.0 and 3.0 shown in Figs. 4-42 and 4-43 there are two non-acceptable manufacturing solution cases and one non-acceptable case respectively for the attached die configuration. For the CR value of 4.0 (Fig. 4-44) all the simulation cases yield acceptable manufacturing solutions; this shows that as the CR value increases the corresponding maximum chamber wall pressure decreases resulting in more acceptable manufacturing solutions. Higher resistance offered by the resin itself to the flow of resin into the

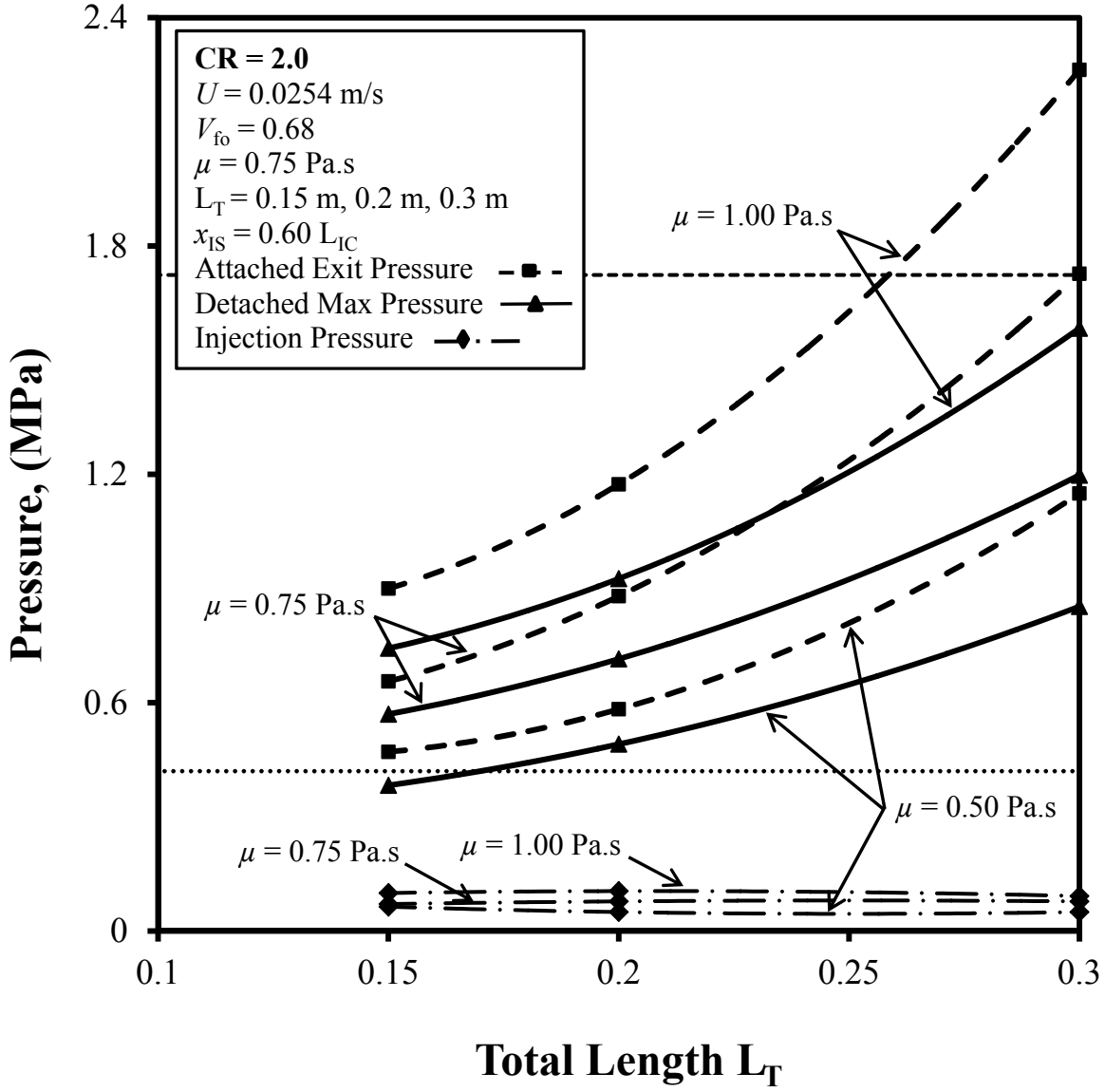

Figure 4-42. Maximum Wall Pressure (——) for Detached Injection Chamber and Exit Wall (Maximum) Pressure (– – –) for Attached Injection Chamber vs. Chamber Length for CR = 2.0 (H_D = 0.0635 m, W_D = 0.00318 m); Minimum Injection Pressure (— · —) to Achieve Complete Wet Out.

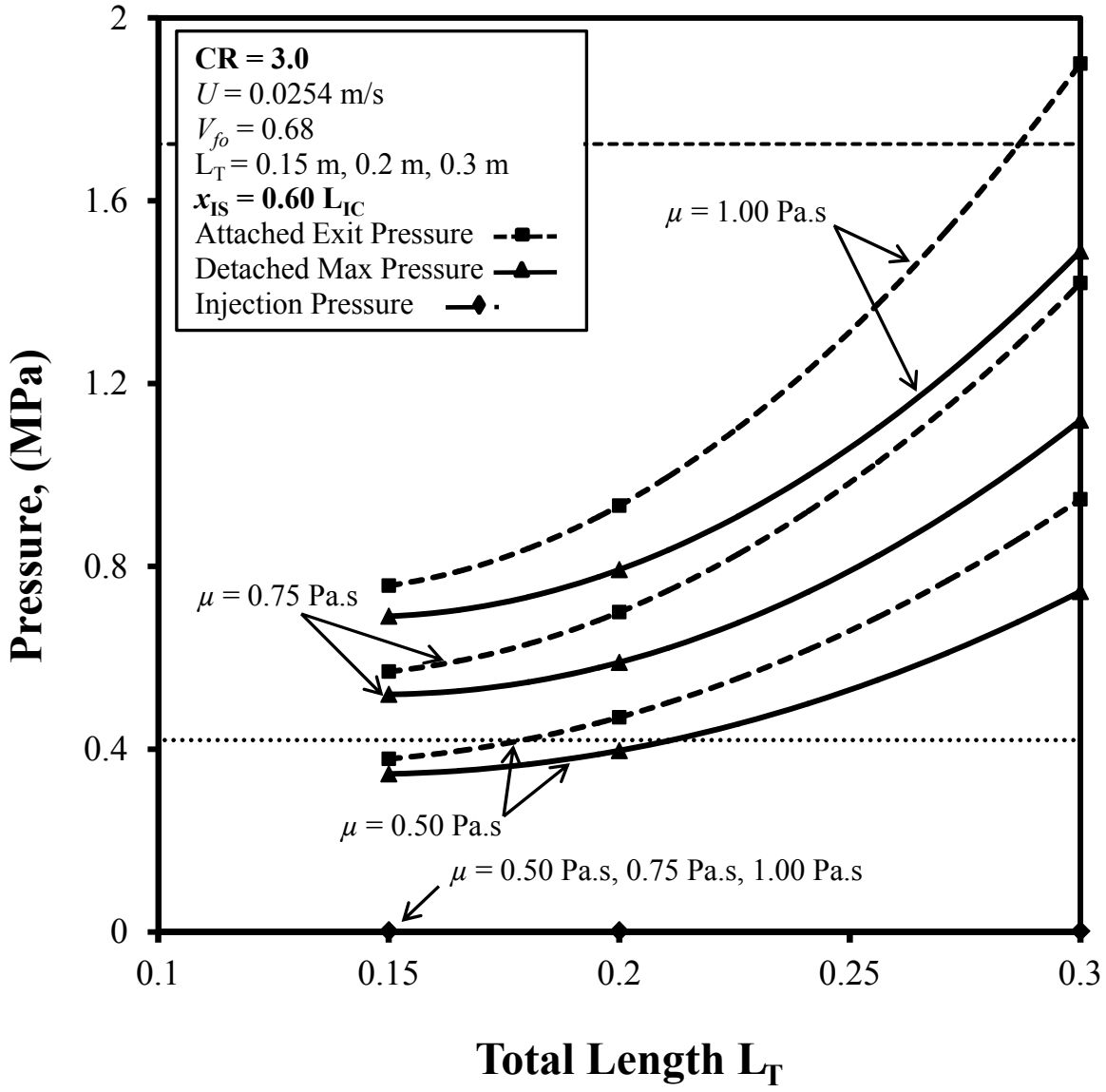

Figure 4-43. Maximum Wall Pressure (——) for Detached Injection Chamber and Exit Wall (Maximum) Pressure (– – –) for Attached Injection Chamber vs. Chamber Length for CR = 3.0, (H_D = 0.0635 m, W_D = 0.00318 m); Minimum Injection Pressure (— · —) to Achieve Complete Wet Out.

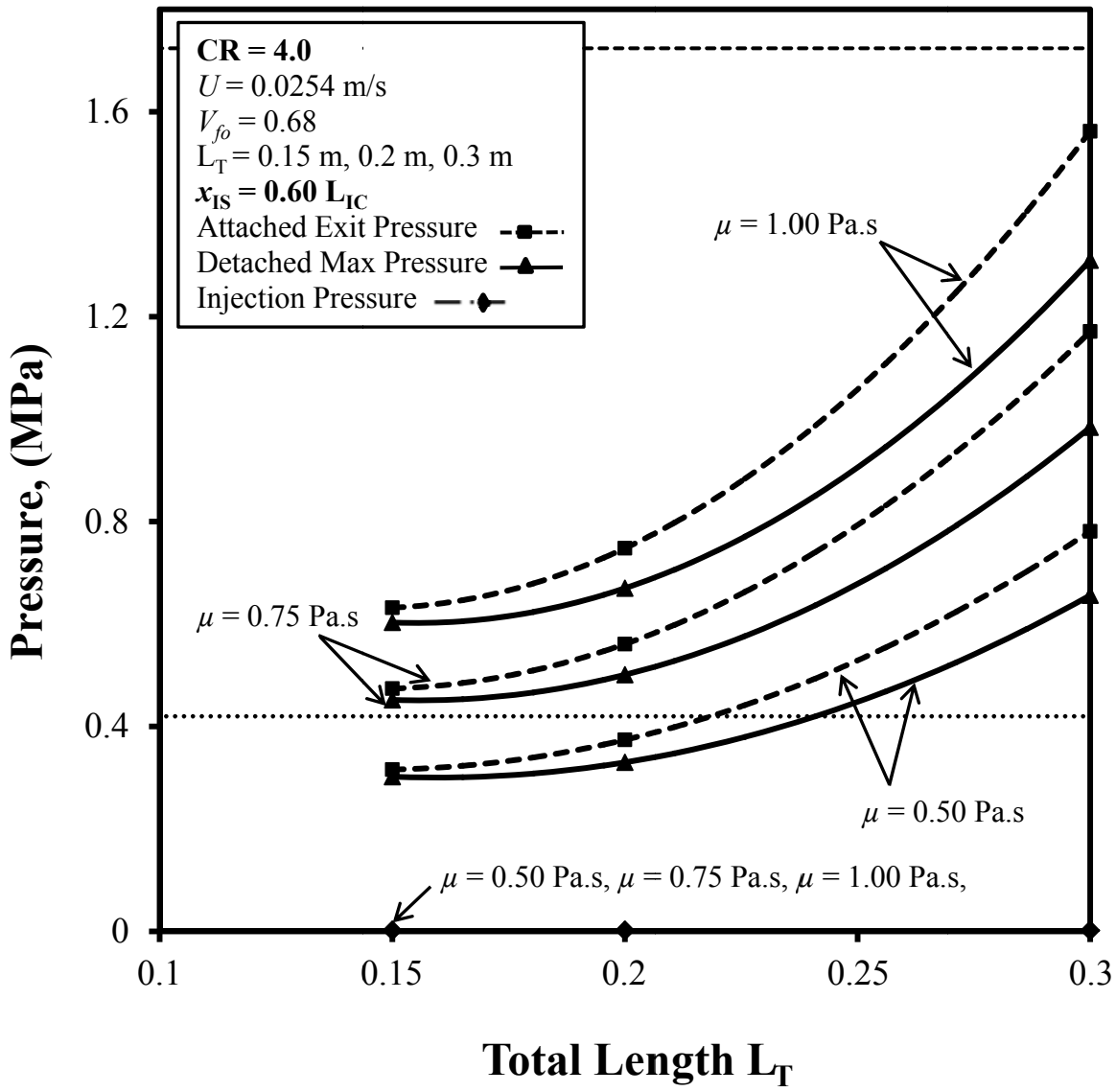

Figure 4-44. Maximum Wall Pressure (——) for Detached Injection Chamber and Exit Wall (Maximum) Pressure (– – –) for Attached Injection Chamber vs. Chamber Length for CR = 4.0, (H_D = 0.0635 m, W_D = 0.00318 m); Minimum Injection Pressure (—·—) to Achieve Complete Wet Out.

fiber bed.

It can be seen in the Fig. 4-42 that as the resin viscosity increases the minimum injection pressure required for complete wet out also increases for each of the specific chamber lengths (0.15 m, 0.20 m, and 0.30 m) due to the increase in the resistance offered by the higher resin viscosity. For the CR values of 3.0 and 4.0 (Figs. 4-43 and 4-44) the injection pressure values are essentially 0.002 MPa (slightly above zero) and thus cannot be seen distinctly. This indicates that for the CR values 3.0 or 4.0, the injection pressure is essentially no longer function of resin viscosity or total chamber length (L_T).

Figures 4-42, 4-43 and 4-44 show the comparison of maximum chamber wall pressure for the attached die configuration and detached die configuration for different resin viscosity values; the maximum chamber wall pressure for the attached die configuration is always higher than that for the detached die configuration. For the CR values of 3.0 and 4.0 (Figs. 4-43 and 4-44), the maximum chamber wall pressure lines for attached and detached have similar patterns for each viscosity value. This indicates that for these specific conditions, the maximum chamber wall pressure is a monotonically increasing function of injection chamber length and resin viscosity.

Figures 4-45, 4-46 and 4-47 depict the minimum injection pressure to achieve complete wet out and the corresponding maximum chamber pressure trends for different CR values for the specific resin viscosity values of 0.50 Pa·s, 0.75 Pa·s and 1.00 Pa·s respectively. In these figures, it can be seen that as the injection chamber length (L_T) increases, the maximum chamber wall pressure also increases accordingly. Figures 4-45, 4-46 and 4-47 show that as the length of the injection chamber increases, the corresponding maximum interior chamber wall pressure also increases. This pressure rise is due to the tapering of the injection chamber walls in Region I; the maximum pressure increases as the tapered length (L_{IC}) increases due to the longer distance over

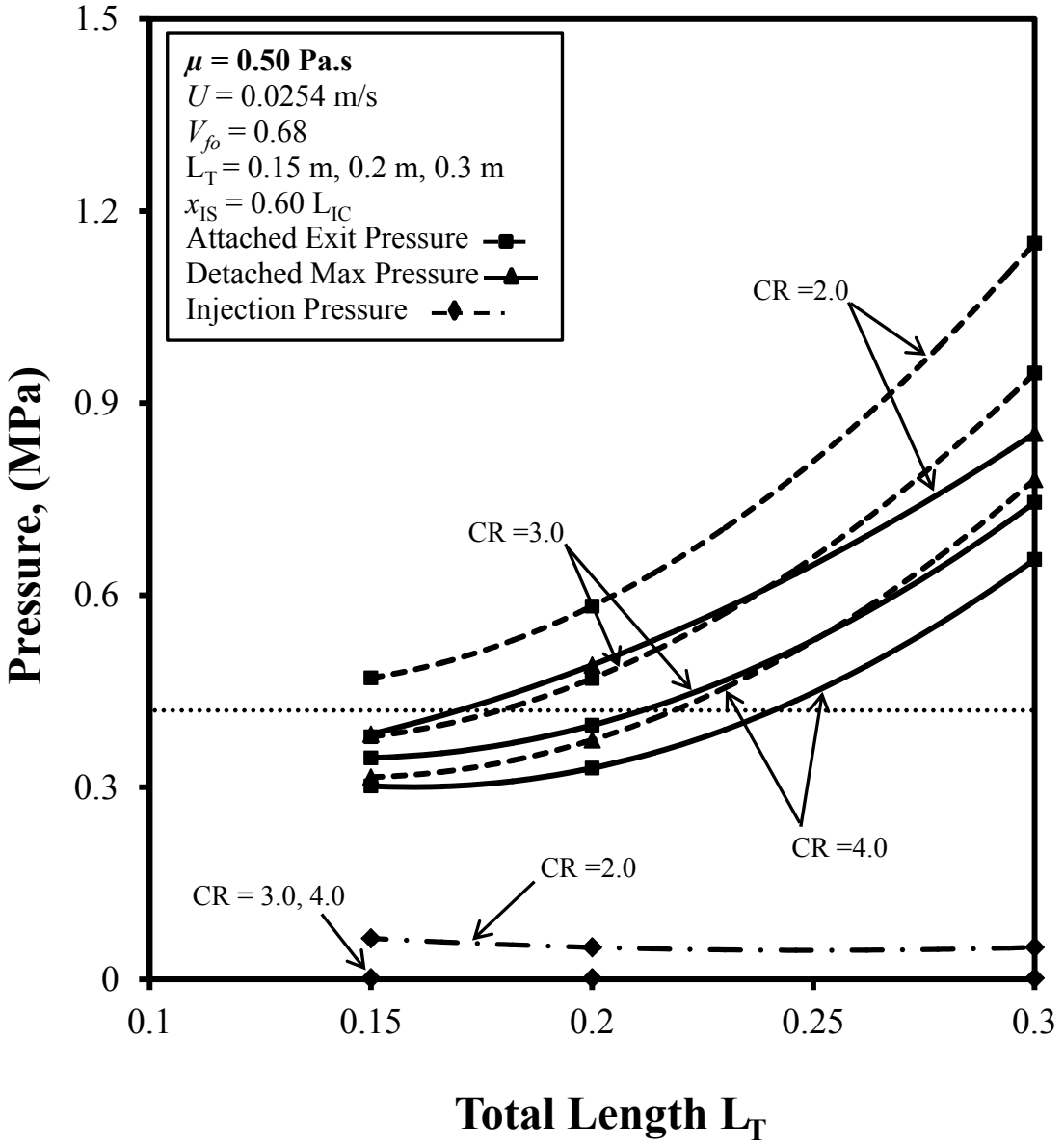

Figure 4-45. Maximum Wall Pressure (– – –) for Detached Injection Chamber and Exit Wall (Maximum) Pressure (——) for Attached Injection Chamber vs. Chamber Length for Various CR, (H_D = 0.0635 m, W_D = 0.00318 m); Minimum Injection Pressure(— · —) to Achieve Complete Wet Out.

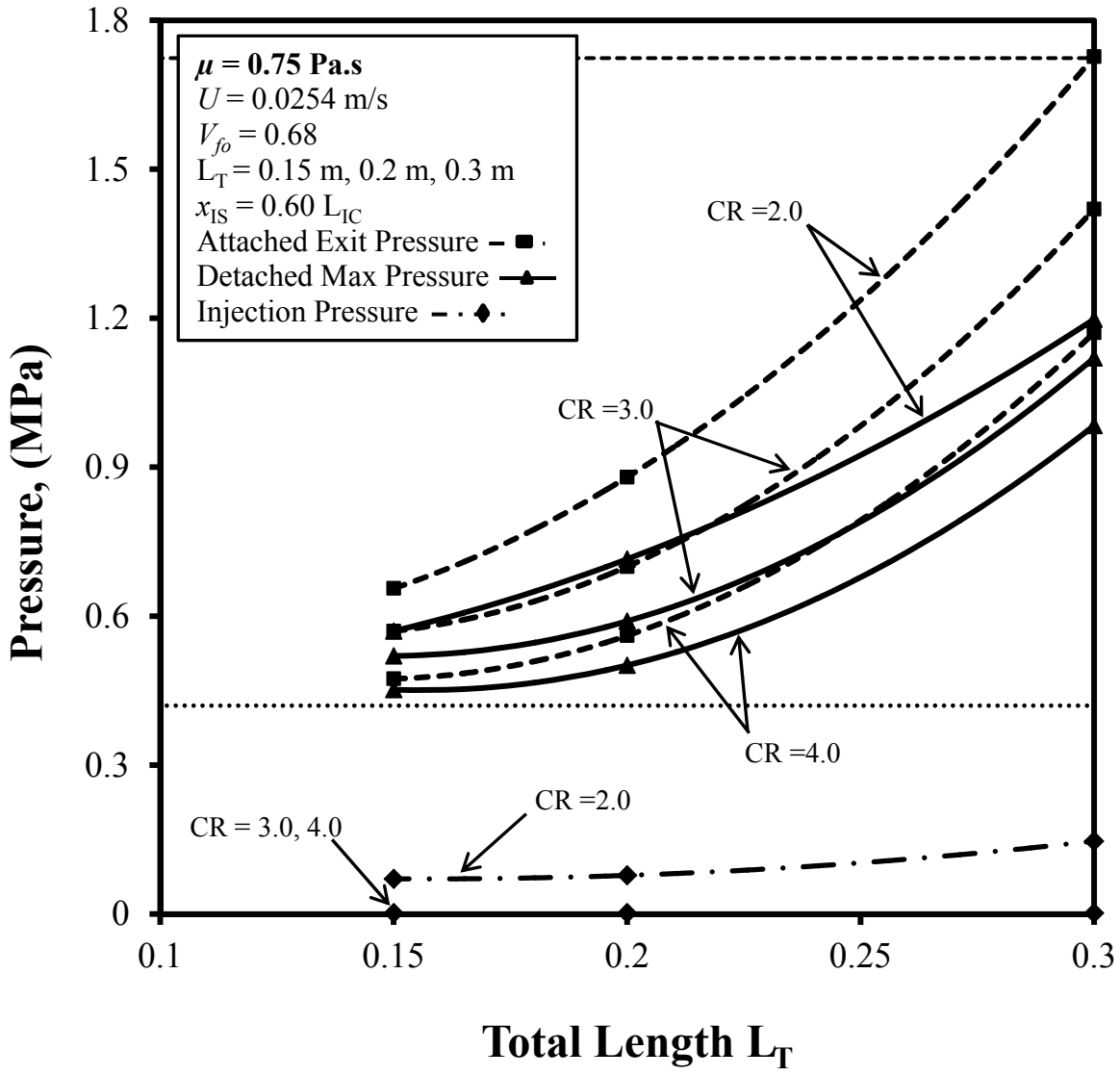

Figure 4-46. Maximum Pressure (——) for Detached Injection Chamber and Exit (Maximum) Pressure (– – –) for Attached Injection Chamber vs. Chamber Length for Various CR, (H_D = 0.0635 m, W_D = 0.00318 m). Minimum Injection Pressure (— · —) to Achieve Complete Wet Out.

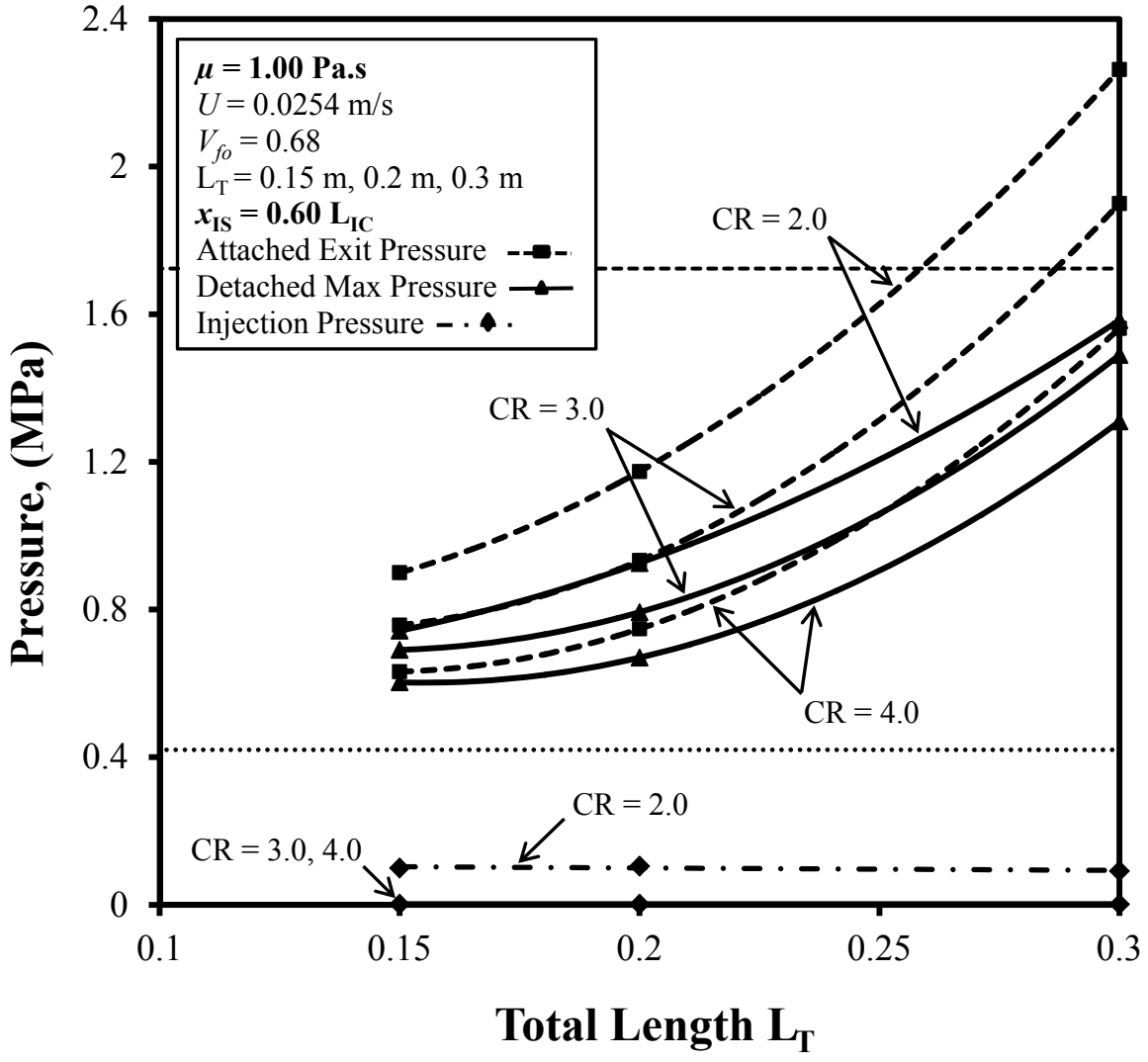

Figure 4-47. Maximum Pressure (——) for Detached Injection Chamber and Exit (Maximum) Pressure (– – –) for Attached Injection Chamber vs. Chamber Length for Various CR, (H_D = 0.0635 m, W_D = 0.00318 m). Minimum Injection Pressure (— · —) to Achieve Complete Wet Out.

which the resin is compressed. Figures 4-45, 4-46 and 4-47 demonstrate the pressure behavior for the resin viscosity values of 0.50 Pa·s, 0.75 Pa·s and 1.00 Pa·s, respectively, and thus illustrate the difference in the maximum chamber wall pressure between the attached die configuration and detached die configuration for the injection chamber lengths (L_T = 0.15 m, 0.20 m, and 0.30 m) and CR value of 2.0, 3.0, and 4.0.

Figure 4-48 shows the resin flow front profile through the fiber reinforcement for the most favorable case with an injection chamber length of 0.15 m and CR = 4 for the highest pull speed of 0.0508 m/s considered and other nominal processing parameters (V_{fo} = 0.68 and μ = 0.75 Pa·s). The white portion inside the injection chamber is dry fiber and the shaded region is the resin and fiber mixture. The thick dark line corresponds to the flow front of the resin/fiber system and the thin lines show the isopressure contours labeled with pressure values in KPa. The resin flow front and the pressure values for the attached die configuration and the detached die configuration can be compared in these two figures. The chamber pressure values are always lower in the detached die configuration system compared to the attached die configuration as can be seen in Fig. 4-48. In the detached die configuration, the isopressure contours can be seen in Region II of the injection chamber due to the decreasing chamber pressure in the Region II and these pressure contours correspond to the same pressure contours as depicted in the Region I of the injection chamber. The plots in the Fig. 4-48 are made out of scale to make it more viewable to the readers.

The non-feasible manufacturing solutions due to the excessive maximum chamber wall pressure can be observed for the higher viscosity values of 0.75 Pa·s (Fig. 4-49) and 1.00 Pa·s (Fig. 4-50) for the injection chamber length of 0.30 m with the attached die configuration. Hence, the higher maximum chamber wall pressure is obtained for the higher viscosity (μ)

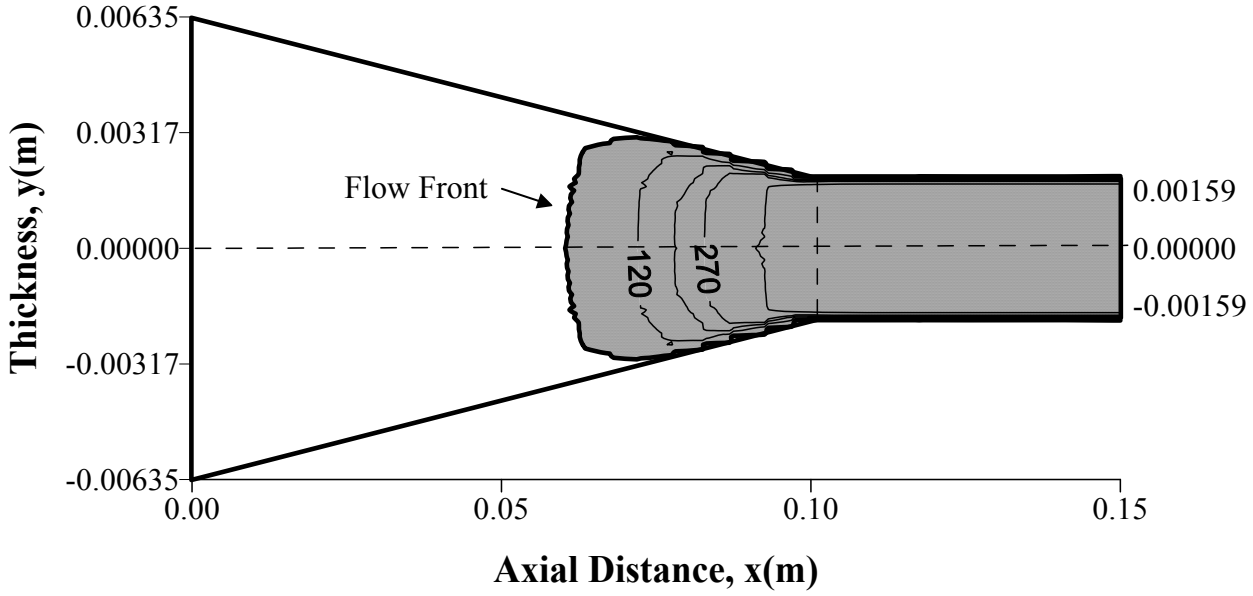

a. Attached Die Configuration

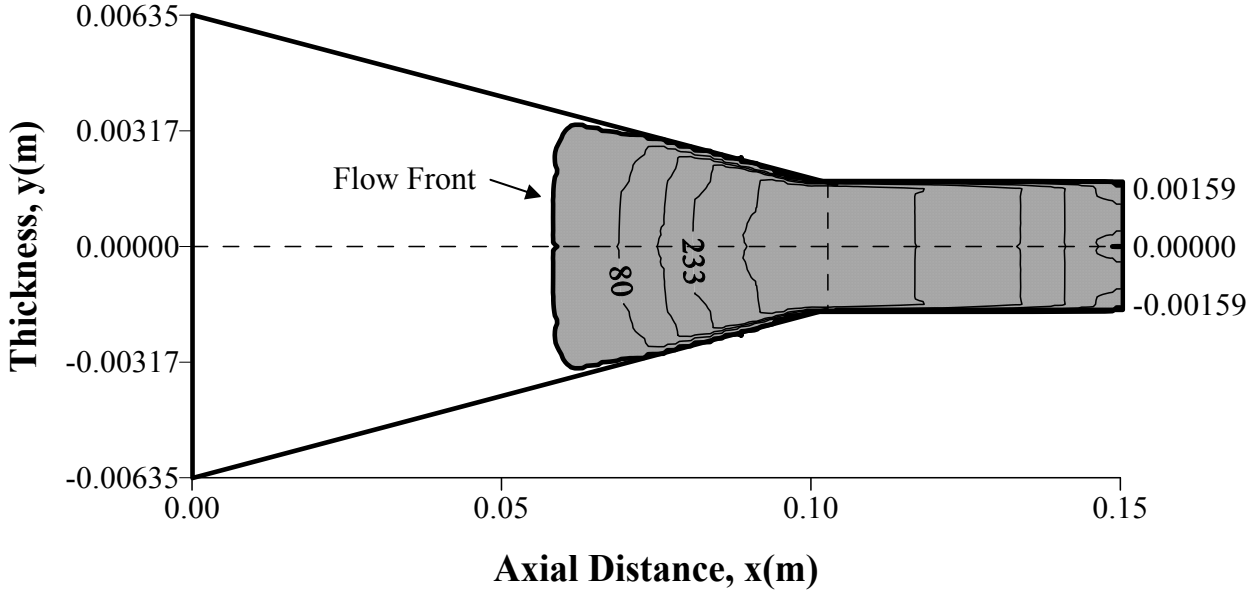

b. Detached Die Configuration

Figure 4-48. Flow Front Profile and Gauge Isopressure (KPa) Contours for Case C7, Table 4-5 with μ = 1.00 for Polyster Resin/Glass Roving, L_T = 0.15 m, CR = 0.60 L_{IC}, U = 0.0254 m/s and V_{fo} = 0.68, x_{IS} = 0.60 L_{IC}. (Not to Scale)

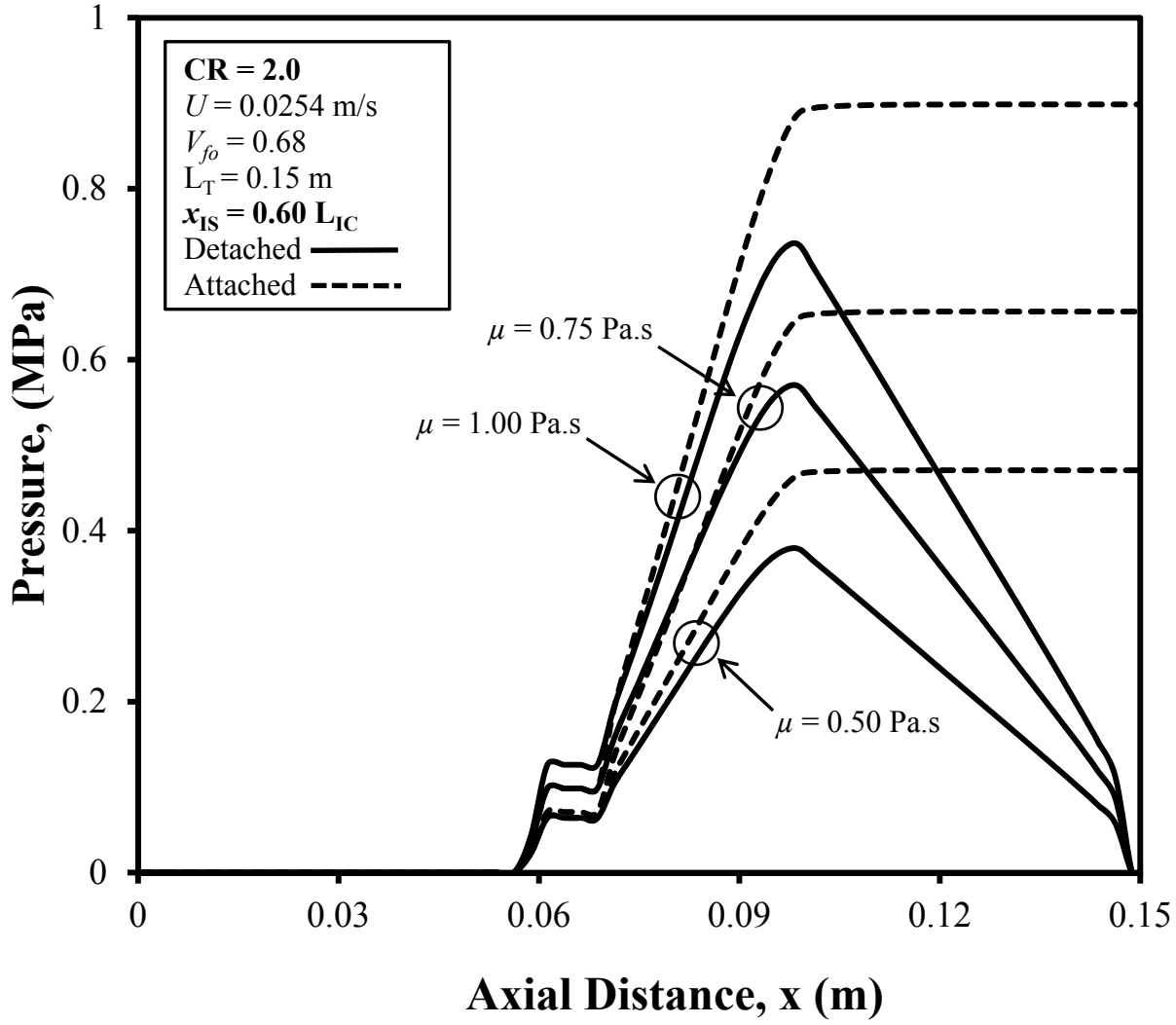

Figure 4-49. Chamber Wall Axial Pressure Profiles for Detached Injection Chamber and Attached Injection Chamber for Chamber Length of 0.15 m for CR = 2.0, (H_D = 0.0635 m, W_D = 0.00318 m).

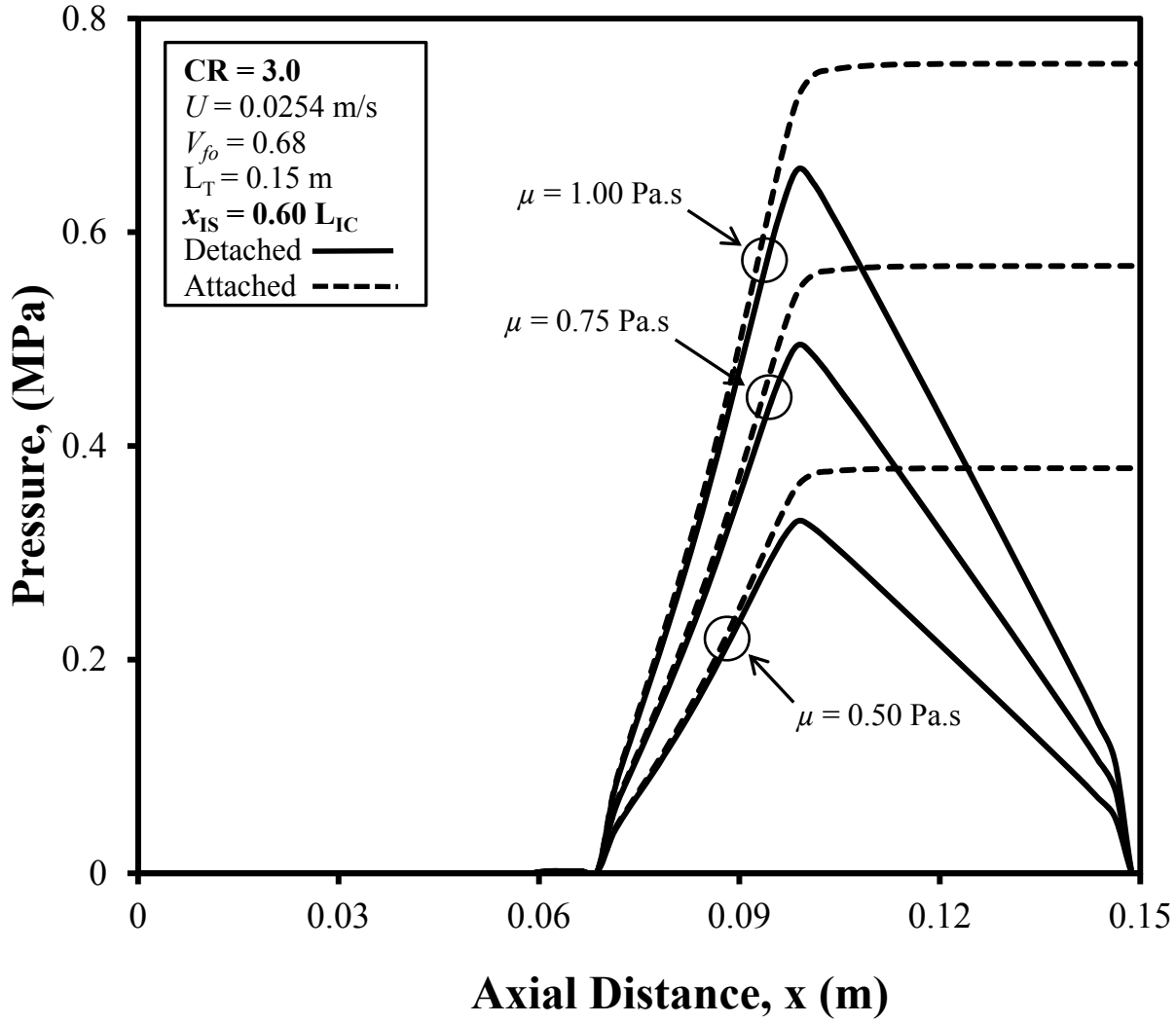

Figure 4-50. Chamber Wall Axial Pressure Profiles for Detached Injection Chamber and Attached Injection Chamber for Chamber Length of 0.15 m for CR = 3.0, (H_D = 0.0635 m, W_D = 0.00318 m).

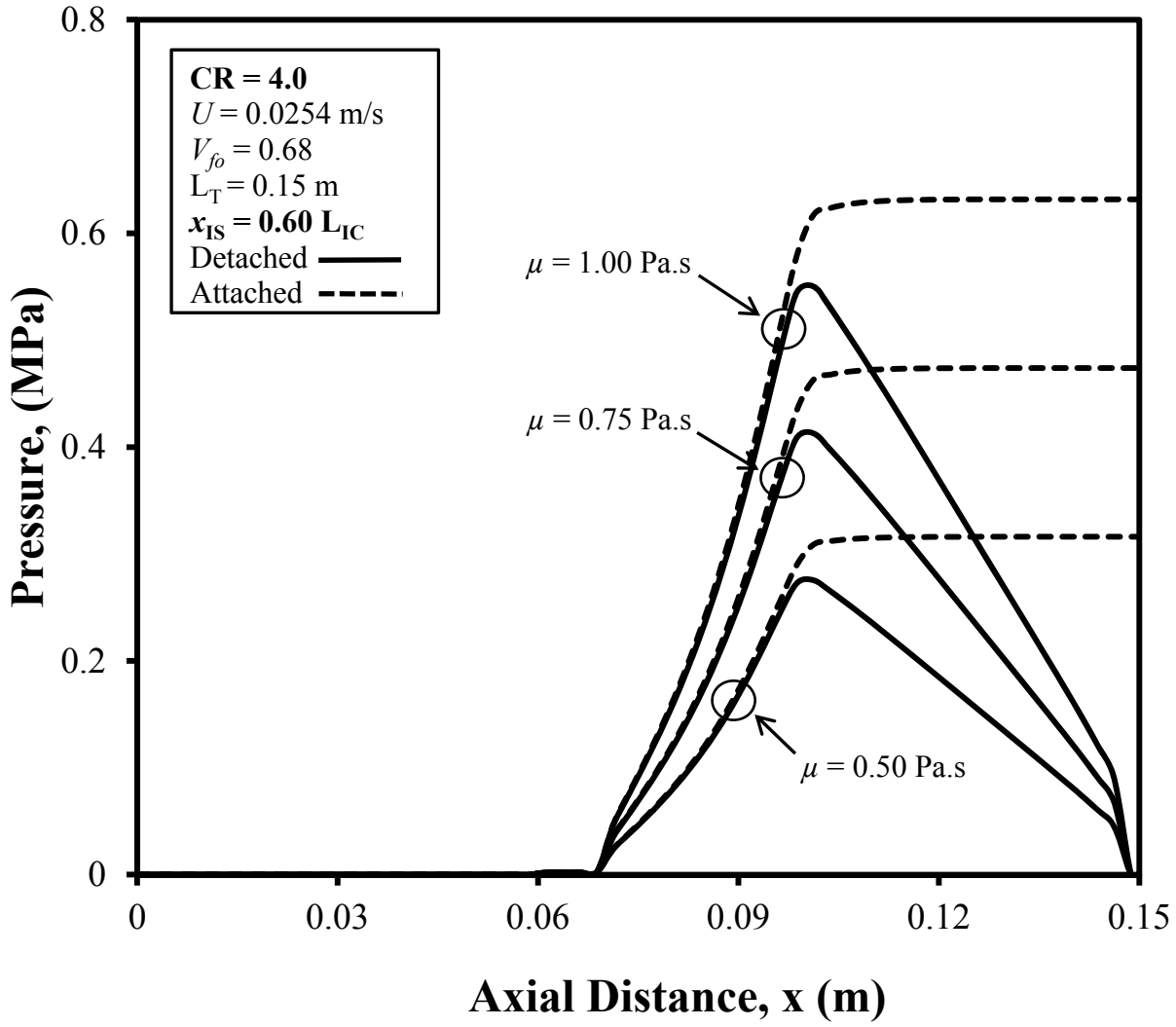

Figure 4-51. Chamber Wall Axial Pressure Profiles for Detached Injection Chamber and Attached Injection Chamber for Chamber Length of 0.15 m for CR = 4.0, (H_D = 0.0635 m, W_D = 0.00318 m).

values, lower CR values and longer injection chamber lengths (L_T). Thus from a design perspective for the pultrusion manufacturing of composites with a higher viscosity, an injection chamber with higher CR values and shorter total length is most favorable. For the highest viscosity, μ = 1.0 considered in this work, the most favorable combination for the acceptable chamber wall pressure can be observed in Fig. 4-50; the detached die configuration with CR value of 4.0 and an injection chamber length of L_T = 0.15 m.

Figures 4-49, 4-50 and 4-51 depict the chamber wall pressure profiles for the attached die configuration and the detached die configuration along the interior length of the injection chamber for L_T = 0.15 m at resin viscosity values of 0.50 Pa·s, 0.75 Pa·s and 1.00 Pa·s for CR values of 2.0, 3.0, and 4.0, respectively. By comparing the pressure profiles for different resin viscosities and different CR values for the attached die configuration and detached die configuration, it is observed that the maximum chamber wall pressures are significantly higher for the attached die configuration as compared to the maximum resin pressure in the detached die configuration. It can be seen that for the CR value of 2.0 (Fig. 4-49), the chamber wall pressure rises to the injection port pressure, decreases slightly after the injection port and then increase to reach the maximum value. But for the higher CR values of 3.0 (Fig. 4-50) and 4.0 (Fig. 4-51), the injection pressure is only 0.002 MPa, thus the chamber pressure appears to start near zero even though it is actually 0.002 MPa, then increases to reach a maximum value. These figures show the chamber wall pressure profile progression inside the injection chamber for both the attached and detached configurations and thus these figures illustrate the difference in the pressure profile development for these two (attached versus detached) configurations. The behavior for L_T = 0.20 m (Figs. 4-52, 4-53, 4-54) and L_T = 0.30 m (Figs. 4-55, 4-56, 4-57) are very similar to that described above for L_T = 0.15 m. Thus, Figs. 4-52, 4-53 and 4-54 show

similar pressure profiles but for an injection chamber length of 0.20 m, and likewise Figs. 4-55, 4-56 and 4-57 depict the pressure profiles for an injection chamber length of 0.30 m. For all the detached pressure profiles the chamber pressure decreases to zero due to the gap at the end of the injection chamber being at a gauge pressure of zero or an absolute pressure of atmospheric pressure.

Figures 4-58, 4-59, and 4-60 demonstrate the pressure profiles in the detached configuration for all the chamber lengths considered for resin viscosity values of 0.50 Pa·s, 0.75 Pa·s and 1.00 Pa·s, respectively. These figures illustrate a broad spectrum of pressure profiles for the detached configuration for different CR values; how the chamber wall pressure increases, reaches a peak value and then decreases back to atmospheric pressure (zero gauge pressure). These figures exhibit the trend, occurrence and change in the maximum chamber wall pressure inside the injection chamber for different chamber lengths, CR values and for the different viscosity values considered. Among these figures, for the highest resin viscosity value of 1.00 Pa·s considered, the chamber length of 0.15 m and CR value of 4.0 has the lowest maximum chamber wall pressure. For manufacturing the composites with higher viscosity value (1.00 Pa·s in this work), the short chamber length of 0.15 m and the high CR value of 4.0 were required to achieve an acceptable pultrusion manufacturing solution which satisfies the pressure constraints on both injection pressure and maximum interior chamber pressure. Thus the detached die configuration with shorter injection chamber length and higher CR value is recommended for the pultrusion manufacturing of composites with higher viscosity values.

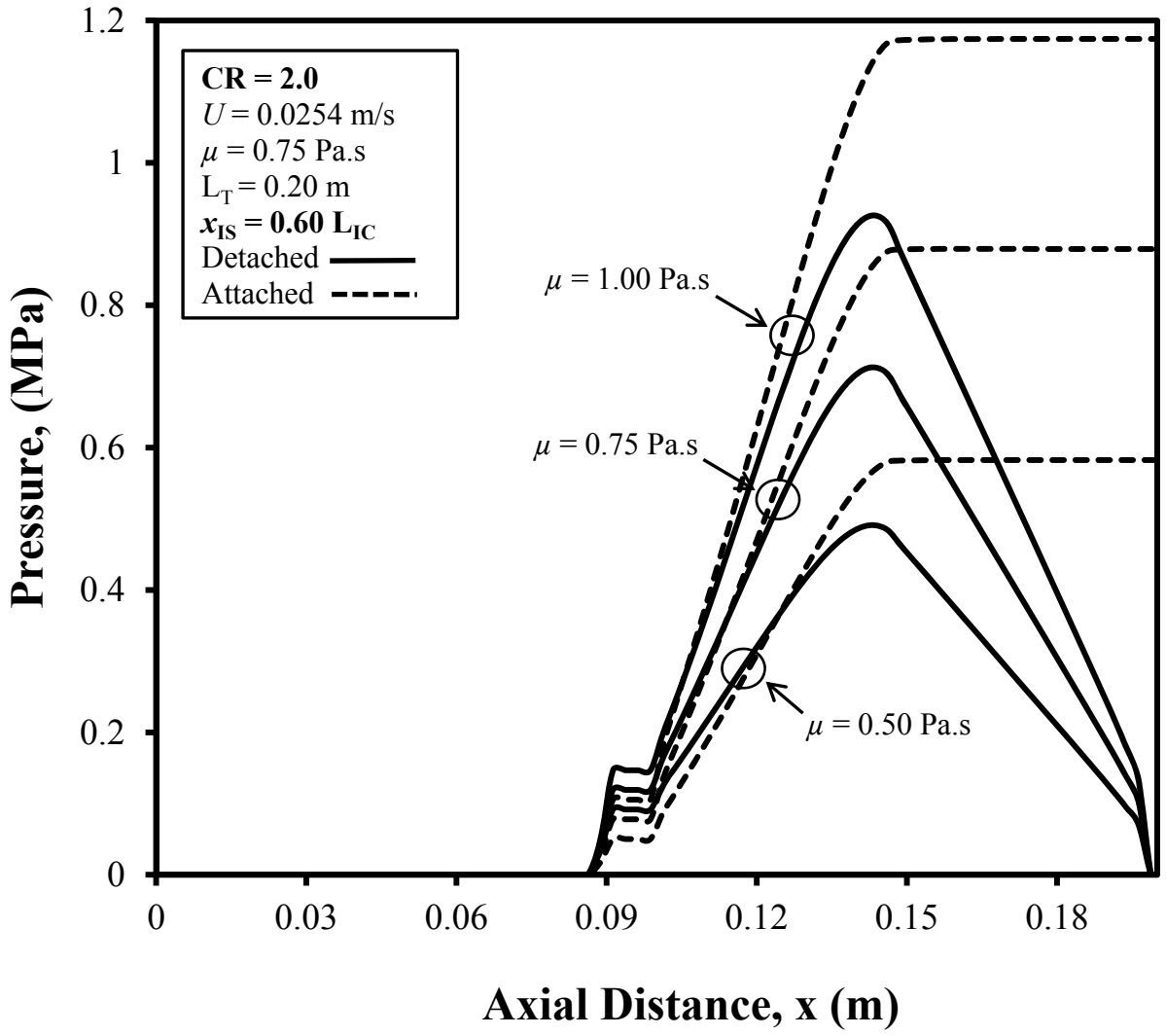

Figure 4-52. Chamber Wall Axial Pressure Profiles for Detached Injection Chamber and Attached Injection Chamber for Chamber Length of 0.20 m for CR = 2.0, (H_D = 0.0635 m, W_D = 0.00318 m).

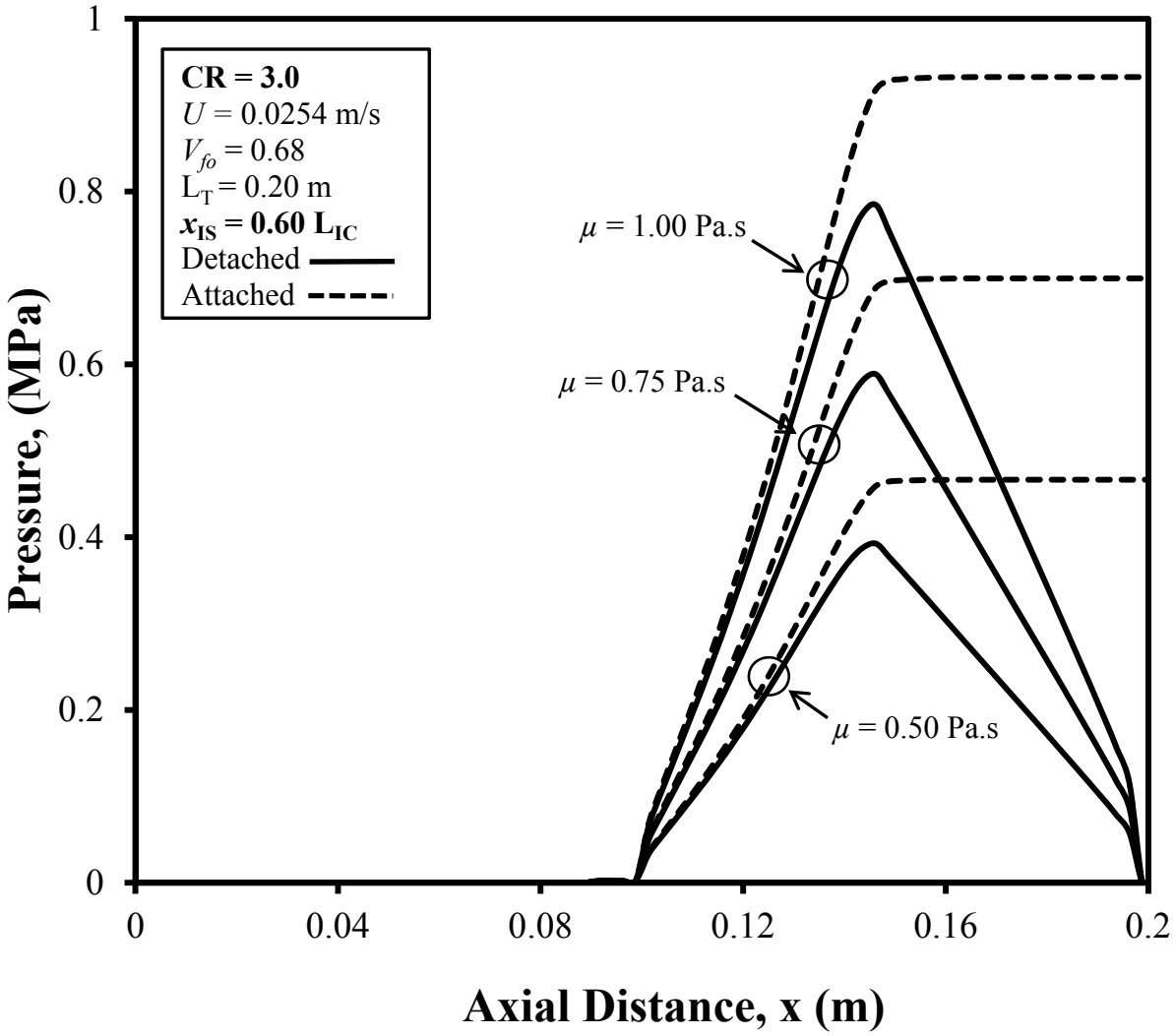

Figure 4-53. Chamber Wall Axial Pressure Profiles for Detached Injection Chamber and Attached Injection Chamber for Chamber Length of 0.20 m for CR = 3.0, (H_D = 0.0635 m, W_D = 0.00318 m).

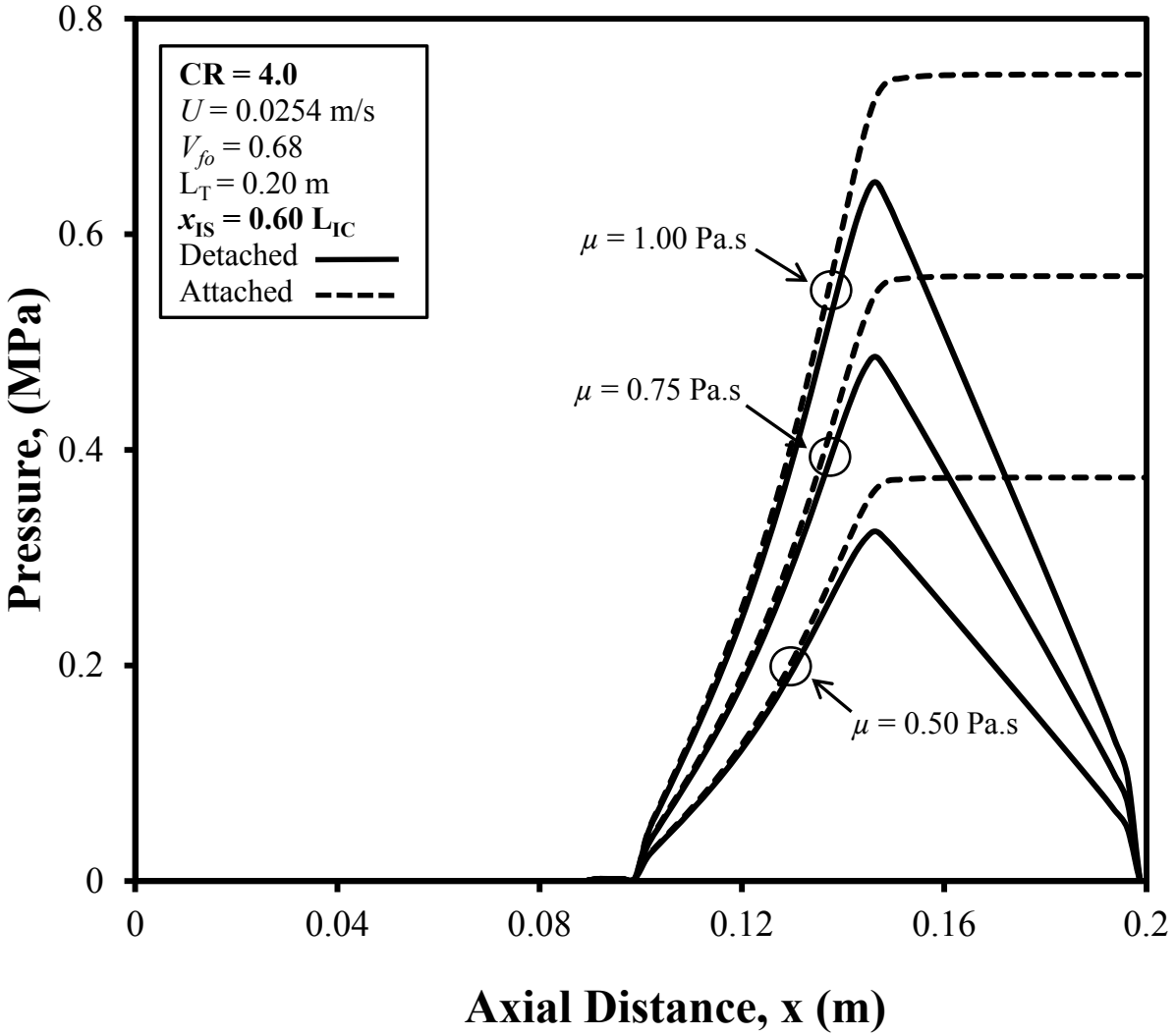

Figure 4-54. Chamber Wall Axial Pressure Profiles for Detached Injection Chamber and Attached Injection Chamber for Chamber Length of 0.20 m for CR = 4.0, (H_D = 0.0635 m, W_D = 0.00318 m).

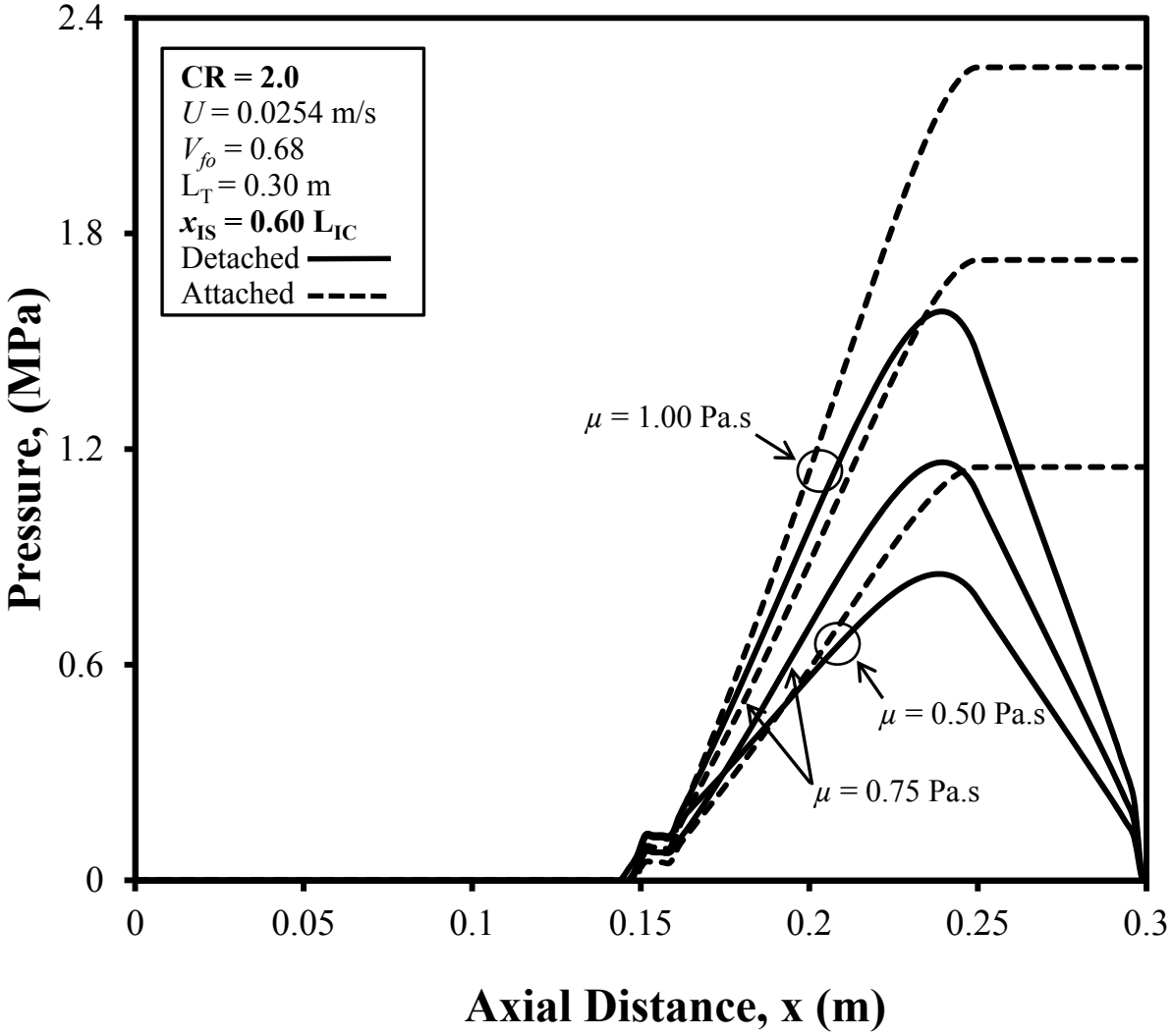

Figure 4-55. Chamber Wall Axial Pressure Profiles for Detached Injection Chamber and Attached Injection Chamber for Chamber Length of 0.30 m for CR = 2.0, (H_D = 0.0635 m, W_D = 0.00318 m).

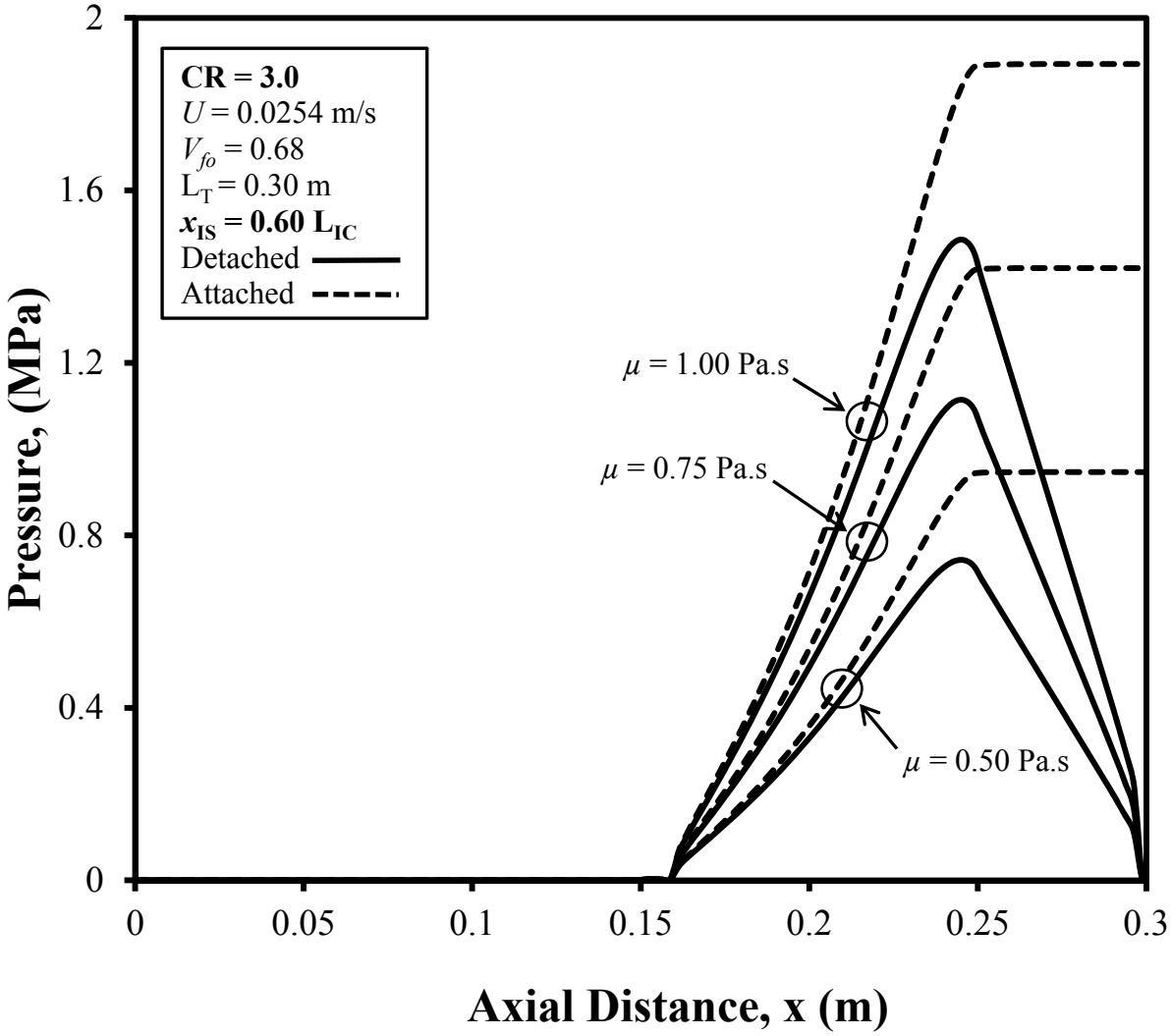

Figure 4-56. Chamber Wall Axial Pressure Profiles for Detached Injection Chamber and Attached Injection Chamber for Chamber Length of 0.30 m for CR = 3.0, (H_D = 0.0635 m, W_D = 0.00318 m).

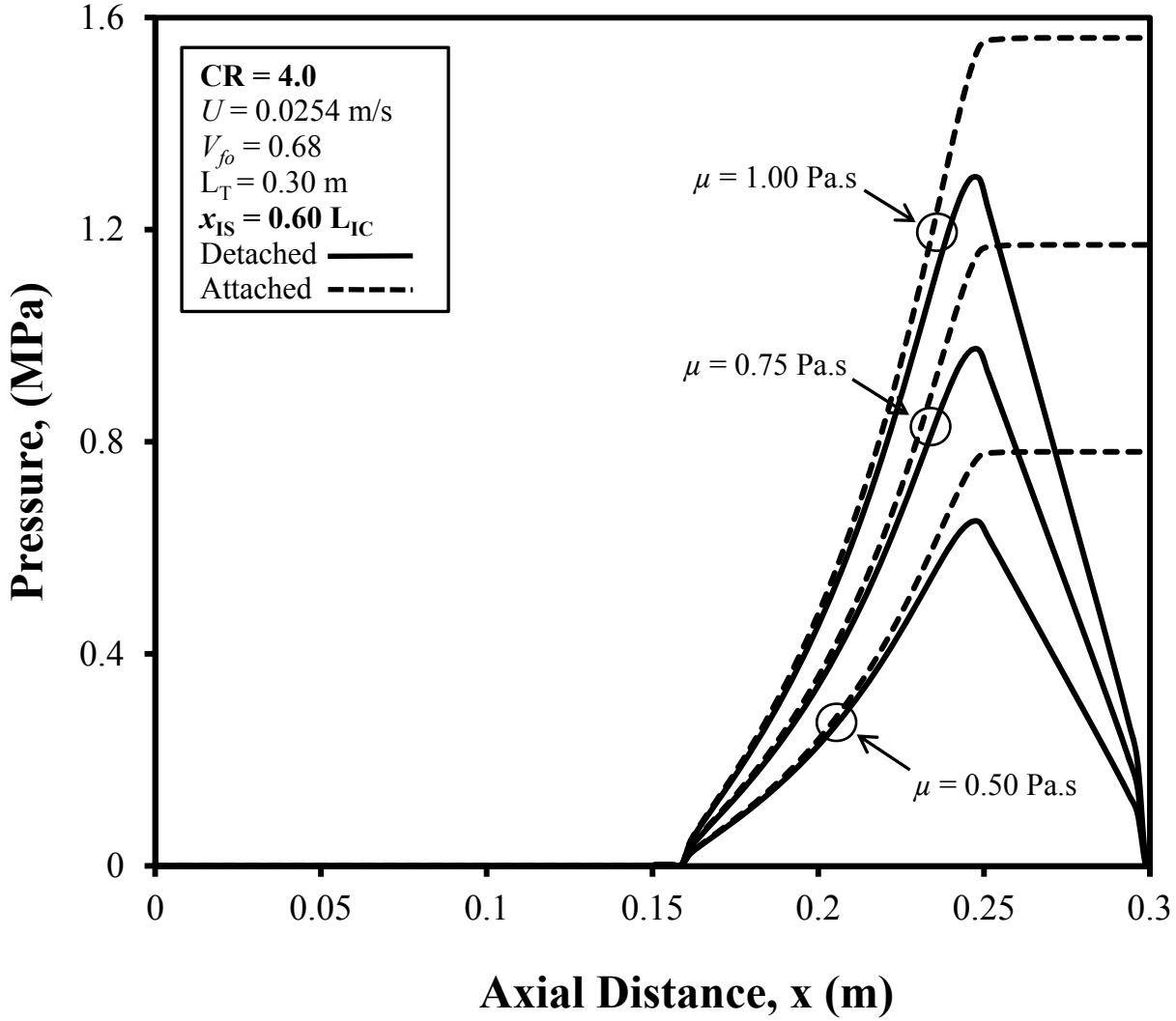

Figure 4-57. Chamber Wall Axial Pressure Profiles for Detached Injection Chamber and Attached Injection Chamber for Chamber Length of 0.30 m for CR = 4.0, (H_D = 0.0635 m, W_D = 0.00318 m).

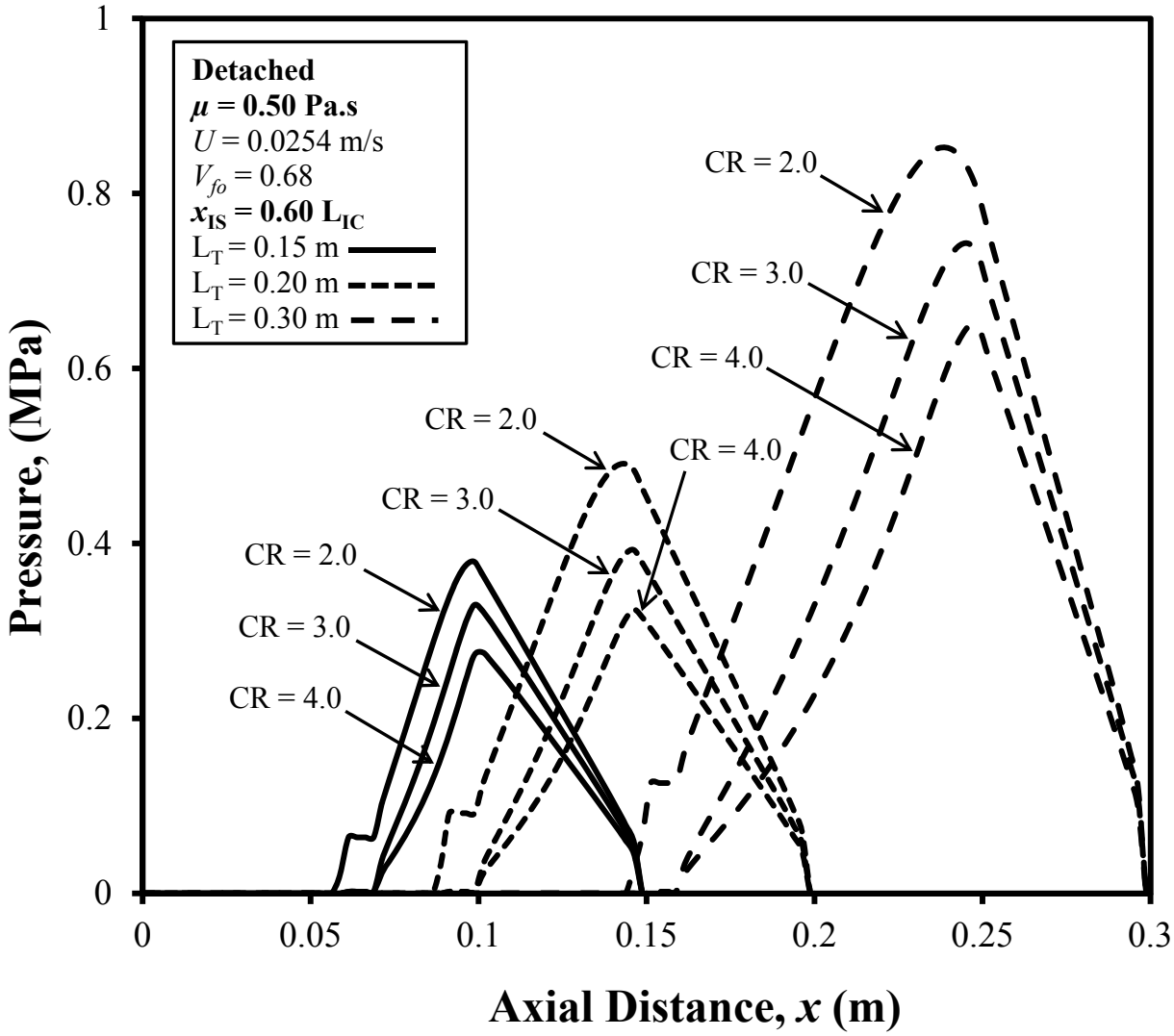

Figure 4-58(a). Chamber Wall Axial Pressure Profiles of Detached Injection Chamber for different Chamber Lengths of 0.15 m, 0.20 m and 0.30 m for V_{fo} = 0.64, (H_D = 0.0635 m, W_D = 0.00318 m).

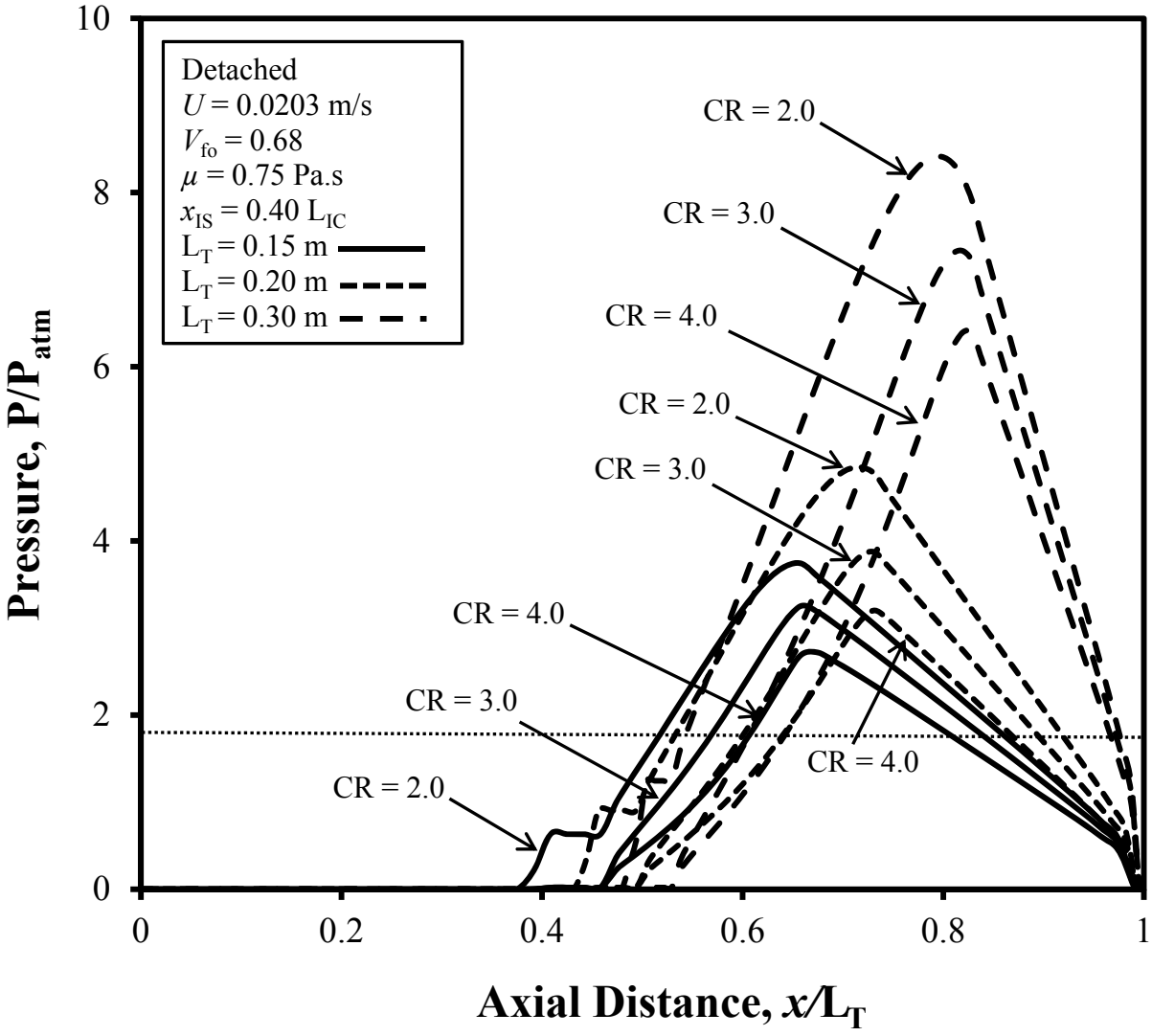

Figure 4-58(b). Chamber Wall Axial Pressure Profiles of Detached Injection Chamber for different Chamber Lengths of 0.15 m, 0.20 m and 0.30 m for V_{fo} = 0.64, (H_D = 0.0635 m, W_D = 0.00318 m) (Dimensionless Value Graph)

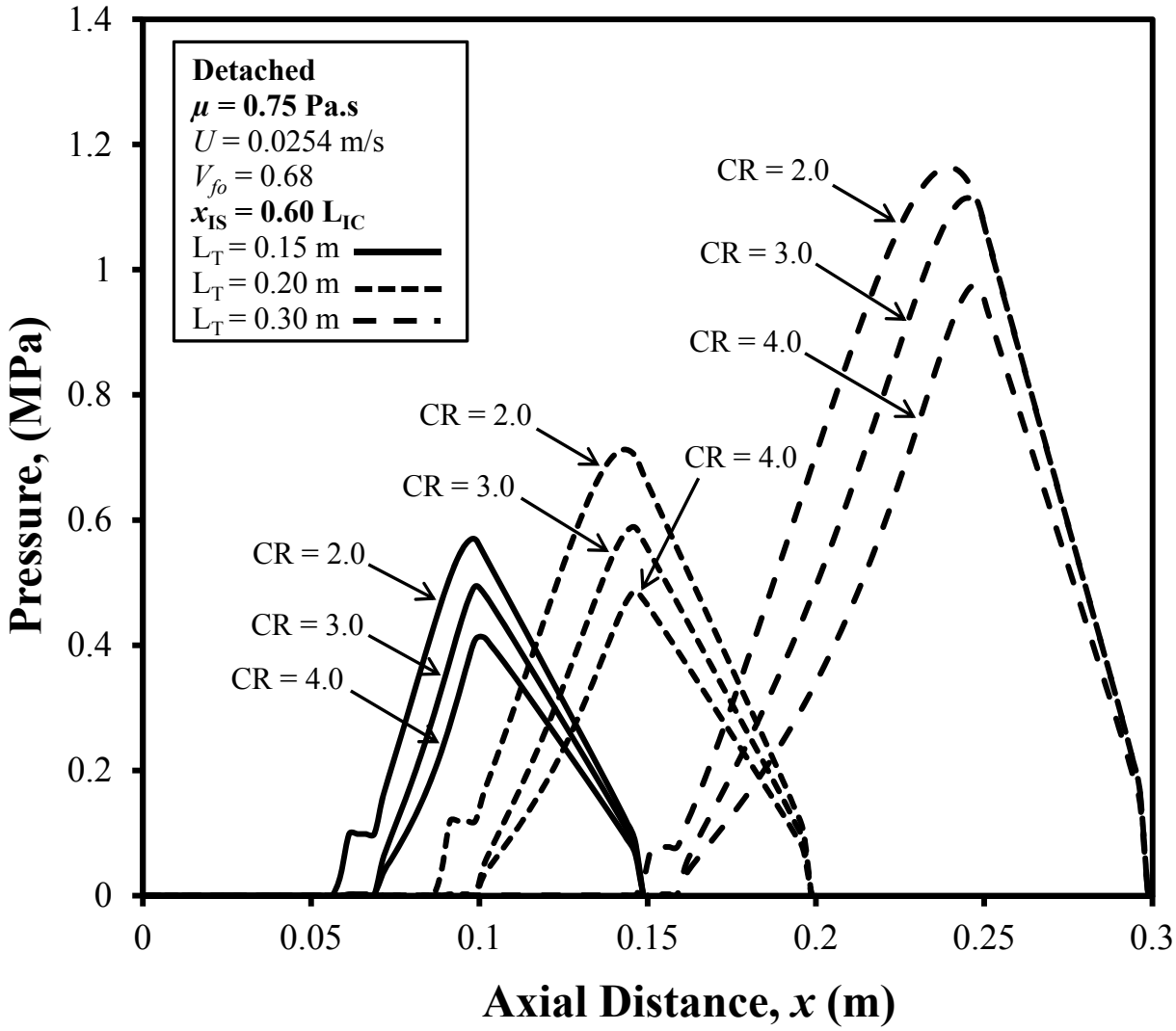

Figure 4-59. Chamber Wall Axial Pressure Profiles of Detached Injection Chamber for different Chamber Lengths of 0.15 m, 0.20 m and 0.30 m for V_{fo} = 0.68, (H_D = 0.0635 m, W_D = 0.00318 m).

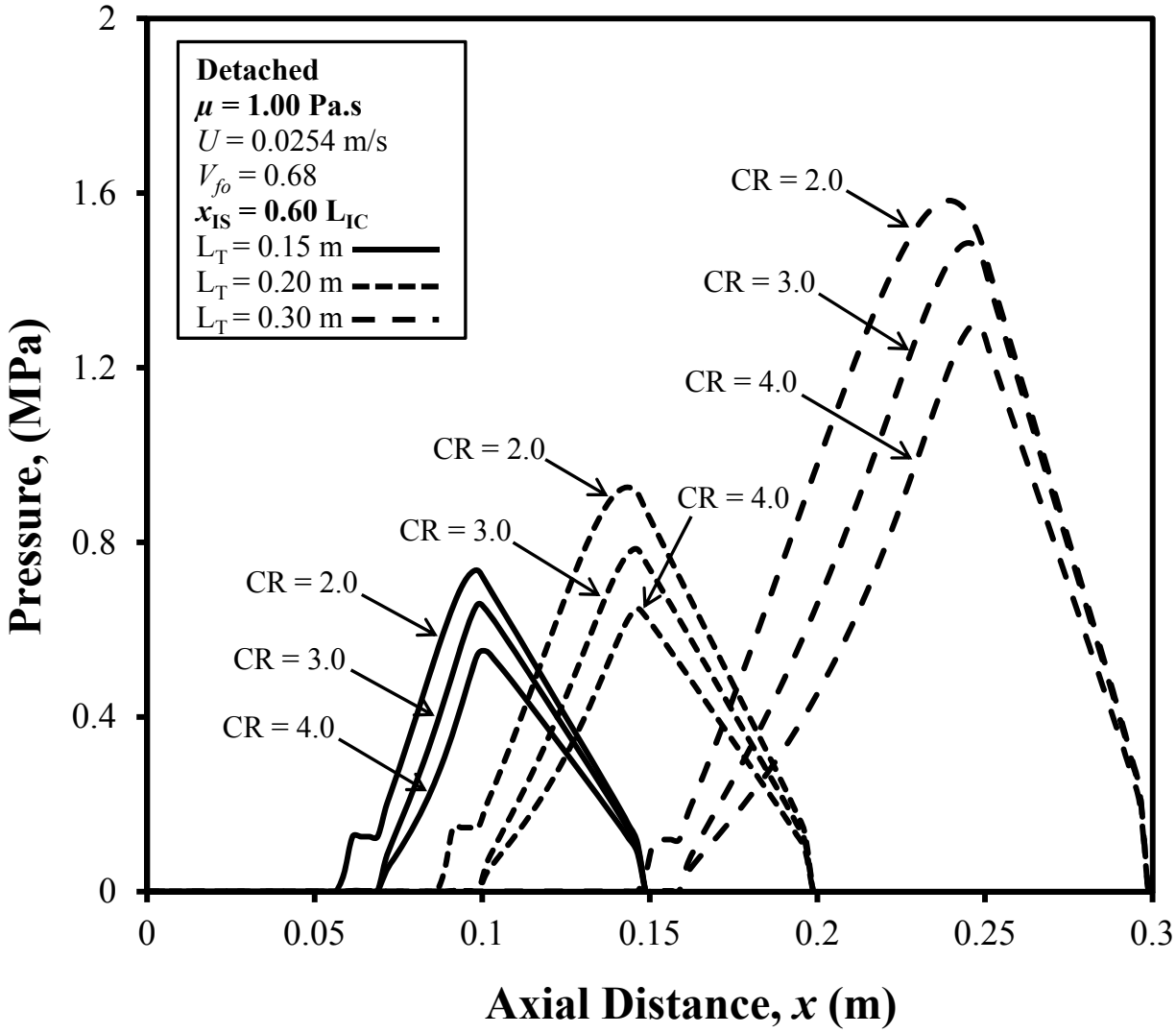

Figure 4-60. Chamber Wall Axial Pressure Profiles of Detached Injection Chamber for different Chamber Lengths of 0.15 m, 0.20 m and 0.30 m for V_{fo} = 0.72, (H_D = 0.0635 m, W_D = 0.00318 m).

CHAPTER 5

CONCLUSIONS

This work is focused on the study of the impact of processing parameters (Pull Speed, Fiber Volume Fraction, and Viscosity) on the injection pressure required for complete wet out and the corresponding maximum chamber wall pressure in the attached die and detached die configuration. For this a 3D finite volume method is applied to simulate the flow of liquid resin through the fiber reinforcement in the resin injection pultrusion manufacturing process. The objective of the present work has been to investigate attached die and detached die configuration injection pultrusion process as a function of the processing parameters and various chamber lengths. The processing parameters considered are pull speed, fiber volume fraction and viscosity with their nominal values of U = 0.0254 m/s, V_{fo} = 0.68 and μ = 0.75 Pa·s respectively. Some trial cases for CR values of 5.0 were tired which didn't showed much improvement in lowering the maximum chamber wall pressure. Thus CR values selected in the work are 2.0, 3.0 and 4.0 whereas the injection chamber lengths (L_T) considered for this study are 0.15m, 0.20 m, and 0.30 m. In this work, the practical limit criteria is set for the successful manufacturing solutions; the minimum injection pressure should be below 0.42 MPa (60 psi or about 4 atm) and corresponding maximum chamber wall pressure should be below 1.72 MPa (250 psi). With these criteria as the standard for the acceptable manufacturing solutions, the result from the simulation cases in attached die and detached die configuration is analyzed.

- Simulation results (Table 4-1 and 4-2) show that the total number of non-acceptable manufacturing solutions for the proportional axial injection slot location x_{IS} = 0.40 L_{IC} is

- 16 cases for the attached and 8 cases for the detached die configuration, and for the proportional axial injection slot location of x_{IS} = 0.60 L_{IC}, it is 8 cases for the attached and 4 cases for the detached die configuration. However the general trends of data for both axial locations are similar. This shows that location of the injection slot further downstream of the inlet of injection chamber provide the lower maximum wall pressure for more number of acceptable manufacturing solutions and thus x_{IS} = 0.60 L_{IC} in this study is the improved design measure for the location of injection slot.
- The general behavior of the maximum chamber wall pressure (e.g. Figs. 4-4, 4-5, and 4-6 for *U*) for different processing parameters with respect to injection chamber length is identical and non-linearly increasing for both attached and detached die configuration.
- For higher CR values the local fiber volume fraction at the injection slot location is lower which decreases the resistance to the resin flow into fiber and this plays significant role in the injection pressure requirement to achieve complete wet out. Thus higher injection pressure values are required for CR value of 2.0 whereas for CR value of 3.0 and 4.0, the injection pressure of 0.002 MPa gauge pressure (slightly greater than atmospheric pressure) is sufficient for complete fiber wet out and the processing parameters have no effect on the injection pressure required for complete fiber wet out.
- Figures 4-4, 4-5 and 4-6 demonstrate the pressure profile of the maximum chamber wall pressure which illustrate that it increases with the increase of pull speed and injection chamber lengths and for lower CR values. Thus, when higher pull speed is desired (0.0508 m/s in this work), a short injection chamber length of 0.15 m and high CR value of 4.0 is selected to have an acceptable pultrusion manufacturing solution.

- Fiber volume fraction of 0.64, 0.68 and 0.72 studied with other processing parameters at their nominal values show that the higher fiber volume fraction increases the maximum chamber wall pressure and acceptable manufacturing solutions is always favored by the detached die configuration with shorter injection chamber length and higher CR values. Similar observation is obtained for the study of the effect of resin viscosity.

For the special case with maximum value of processing parameters i.e. pull speed of U = 0.0508 m/s, fiber volume fraction of V_{fo} = 0.72 and resin viscosity of μ = 1.0, the acceptable manufacturing solutions for attached die configuration are obtained for $x_{IS} = 0.60L_{IC}$; CR = 4.0, L_T = 0.15 m and 0.20 m, whereas for detached die configuration, the acceptable manufacturing solutions are obtained for $x_{IS} = 0.40L_{IC}$; CR = 4.0, L_T = 0.15 m and $x_{IS} = 0.60L_{IC}$; CR = 4.0, L_T = 0.15 m and 0.20 m. This demonstrate that for even for these extreme processing parameters value shorter injection chamber length and higher CR value gives acceptable manufacturing solution and also detached die configuration has solution for both axial locations of $x_{IS} = 0.40\ L_{IC}$ and $x_{IS} = 0.60\ L_{IC}$.

Even though the study of effect of different processing parameters give the same conclusion; this work provide the valuable converging idea for the experimental work that detached die configuration with shorter injection chamber length and higher CR value provide the optimum measure for operating condition of pultrusion manufacturing process.

REFERENCES

1. Jeswani, J.L., and Roux, J.A., "Numerical Modeling of Design Parameters for Manufacturing Polyster/Glass Composites by Resin Injection Pultrusion," *Polymers and Polymer Composites,* Vol. 14, No. 7, 2006, pp. 651-669.
2. Dube, M. G., Batch, G. L., Vogel, J. H., and Mocosko, C. W., "Reaction Injection Pultrusion of Thermoplastic and Thermoset Composites," *Polymer Composites*, 1995; 16:378-85.
3. Lackey, E., Vaughan, J.G., and Roux, J.A., "Experimental Development and Evaluation of a Resin Injection System for Pultrusion," *Journal of Advanced Materials,* 1997: 29, pp. 30-37.
4. Rahatekar, S.S., and Roux, J.A., "Numerical Simulation of Pressure Variation and Resin Flow in Injection Pultrusion," *Journal of Composites Materials,* Vol. 37; 12:2003, pp. 1067-1082.
5. Roux, J.A., Sharma, D. McCarty, T.A., Vaughan, J.G., "Investigation of Dynamic Behavior in a Pultrusion Die," *Journal of Composite Materials*, Vol. 32, No. 10, July 1998, pp. 929-950.
6. Ranga, B.K., *Impact of Chamber Length on Performance of Tapered Resin Injection Pultrusion*, Masters Thesis, University of Mississippi; August 2009.
7. Srinivasagupta, D., and Kardos, J.L., "Rigorous Dynamic Model-based Economic Design of the Injected Pultrusion Process with Controllability Considerations," *Journal of Composite Materials,* Vol. 37, No. 20; 2003, pp. 1851-1888.

8. Srinivasagupta, D., Potaraju, S., Kardos, J.L., and Joseph, B., "Steady State and Dynamic Analysis of a Bench-Scale Injected Pultrusion Process," *Composites Part A: Applied Science and Manufacturing,* Vol. 34; 2003, pp. 835-846.
9. Mustafa, I., Khomami, B., and Kardos, J.L., "3-D Nonisothermal Flow Simulation Model for Injected Pultrusion Processes," *AIChE journal,* Vol. 45, No.1; 1999, pp. 151-163.
10. Li, S., Xu, L., Ding, Z., and Lee, L.J., "Experimental and Theoretical Analysis of Pulling Force in Pultrusion and Resin Injection Pultrusion (RIP) – Part I: Experimental," *Journal of Composite Materials,* Vol. 37; No.3; 2003, pp. 163-189.
11. Li, S., Xu, L., Ding, Z., and Lee, L.J., "Experimental and Theoretical Analysis of Pulling Force in Pultrusion and Resin Injection Pultrusion (RIP) – Part II: Modeling and Simulation," *Journal of Composite Materials,* Vol. 37; No.3; 2003, pp. 195-216.
12. Liu, X.L., "A Finite Element/Nodal Volume Technique for Flow Simulation of Injection Pultrusion," *Composites: Part A,* 34 (2003), pp. 649-661.
13. Liu, X.L., "Iterative and Transient Numerical Models for Flow Simulation of Injection Pultrusion," *Composite Structures:* 66; 1-4, 2003, pp. 175-181.
14. Kommu, S., Khomami, B., Kardos, J. L., "Modeling of Injection Pultrusion Processes: A Numerical Approach," *Polymer Composites*, 19: 1998; pp. 335-46.
15. Darcy, H. 1856. *Les fontaines publique de la ville de Dijon*. Paris: Dalmont.
16. Gutowski, T. G., Cai, A., Bauer, S., Boucher, D., Kingery, J., and Wineman, S., 1987*,* "Consolidation Experiments for Laminate Composites*," Journal of Composite Materials*, Vol. 21, pp. 650-669.

17. Carman, P. C. 1937, “Fluid Flow through Granular Beds,” *Trans. Int. Chem. Eng*., 5:150-166.

18. Patankar, S. 1980, *Numerical Heat Transfer and Fluid Flow*, Hemisphere Publishing Corporation, New York.

APPENDIX A

MANUAL FOR EXCEL PLOTS

Procedure on how to produce EXCEL graphs using the output file (CL AND DIE WALL PRESSURE. DAT):

1. Open the Microsoft Excel 2003 or 2007.
2. File > Open > the output file (CL AND DIE WALL PRESSURE.DAT) from the FORTRAN output file.
3. Select the chart wizard from the excel menu, select the proper graph option – XY (Scatter) and click the graph picture showing Scatter with data points connected by smooth lines without markers and select next. A dialogue box opens, select series tab and the add option, input the X values and the Y values from the output file, continue with the next button until a proper graph is obtained.
4. Make necessary changes in the graph like scale, background area, label the axes, and turn on the legend so that the graph looks brightly and in a tidy way.
5. Label the parameters (processing/design) with 14 pt. font and font format as Times New Roman throughout, X, Y axes with 18 pt. font and in bold fashion, the values of X, Y axis scale as 14 pt. font.
6. Make the orientation of the graph in Portrait style.
7. The graph should have the specifications approximately equal to Height = 6.50 inches and width = 6.50 inches.
8. Follow the same procedure for different plots with various parameters.

APPENDIX B
MANUAL FOR SURFER PLOTS

Procedure on how to produce SURFER plots using the output file (PRESSURE.DAT):

1. Open the Golden software which opens to SURFER. Double click on it, a dialogue box opens.
2. Select Grid > Data > File Name > Ok.
3. After Ok > Scattered Data Interpolation.
4. See whether the data is right or not.
5. Enter the required number of lines in X and Y as 241 and 121 respectively (For the chamber length of 0.15 m, selected no. of nodes while running the program are x-nodes is 32, y-nodes is 7 and z-nodes is 3)
6. For Gridding method, select Krigging, click options and enter the values of radius1as 0.1and radius 2 as 0.001 and scale to 210000.
7. A Grid file is created.
8. For Blanking operation, create a new worksheet, enter the required number of nodes and Save as BLN file.
9. Click Grid > Blank > Grid file from last step and in next window select the BLN file. After this step, a new Grid file is created. Use this to create Contour map in the next step.
10. Map > Contour > select appropriate Grid file (last step) and select proper options. You see a plot.
11. Map > Load base Map. Select the BLN file and say Ok. Boundary file is visible in the graphic area but with different scale.

12. To overlay both the Contour and Boundary file, go to Edit >Select all > Map > Overlay Maps, then both maps are overlayed.
13. Change Scale by going to Map > Scale X as 6.00 and y as 3.00. Uncheck the proportional XY scale.

How to darken Boundary File:

1. Select Grid > Blank > select the proper Grid file option and then the Blank file is created.
2. Map > Load Base Map > select the Blank file and say Ok.
3. Finally, we can see the Map with dark boundaries.